IN VIVO AND *IN VITRO* CHARACTERIZATION OF p66SHCA INACTIVATION: AXONAL AND NEURONAL PROTECTION IN THE CONTEXT OF MULTIPLE SCLEROSIS

By

Kimmy Ger-wen Su

A DISSERTATION

Presented to the Neuroscience Graduate Program
and the Oregon Health & Science University
School of Medicine
in partial fulfillment of
the requirements for the degree of

Doctor of Philosophy

July 2011

School of Medicine
Oregon Health & Science University

CERTIFICATE OF APPROVAL

This is to certify that the Ph.D. dissertation of
KIMMY SU
has been approved on July 28, 2011

Advisor, Dennis Bourdette, MD

Advisor, Michael Forte, PhD

Member and Chair, Philip Copenhaver, PhD

Member, Gary Banker, PhD

Member, Ruth Whitham, MD

TABLE OF CONTENTS

LIST OF FIGURES

ACKNOWLEDGEMENTS

I would like to thank my wonderful thesis committee composed of Drs. Philip Copenhaver, Gary Banker, Dennis Bourdette, Michael Forte, and Ruth Whitham for their amazing guidance these past few years. Their time, expertise, and thoughtful suggestions were invaluable to the completion of this thesis project.

In particular, I would like to thank Dr. Philip Copenhaver for being an excellent committee chair and for providing insightful recommendations for my experiments. Thank you to Dr. Gary Banker for his suggestions on my *in vitro* work and for helping me decipher the results of my mitochondrial transport experiments. Thank you to Dr. Ruth Whitham for serving as the honorary committee member of my thesis defense.

I would like to express my heartfelt gratitude to my spectacular thesis mentors Dr. Dennis Bourdette and Dr. Michael Forte, who have both been instrumental in my achievements these past few years. Thank you to Dennis for continuously providing me with wonderful opportunities essential to my training as a future physician-scientist. The incredible experiences I've had and the people I've met attending MS meetings and neurology conferences will undoubtedly be important in shaping my career. Thank you to Mike for being an amazing thesis mentor who has always welcomed me whenever I

come by his office for guidance, both professional and personal. His unwavering encouragement and enthusiasm has been extremely important to the completion of this thesis and to my development as a scientist.

I also would like to thank the members of the Bourdette, Forte, and Banker labs for their friendship and assistance these past few years, without which the completion of this thesis project would not have been possible. In particular, I thank Drs. Gail Marracci and Priya Chaudhary as well as Xiaolin Yu, Danielle Galipeau, and Brooke Morris of the Bourdette lab for their generous help with Aim 1 of this thesis project. In addition, I thank Dr. Anna Barsukova-Bell of the Bourdette and Forte labs for her invaluable help on the adult neuronal culture experiments and live-cell imaging. Thank you also to Christine Fenner for her help on my grant submissions, and to Kristen Jones, Jackie Parker, and former member Elizabeth Blachly-Dyson of the Forte lab for their wonderful company and support. Thank you to Dr. Cheng Fang and members of the Banker lab for their guidance on the mitochondrial transport studies. Finally, thank you to Dr. Stefanie Kaech-Petrie and Aurelie Snyder of the Jungers Center Advanced Light Microscopy Core for their invaluable guidance on the imaging and analysis components of my project.

Last but not least, I would like to express my sincere appreciation and love to my family and friends near and far, as close by as Portland, Seattle, and the SF Bay Area, and as far as Taiwan. They have all been pivotal to my life, and I am so thankful for their tremendous support and encouragement. Finally, a special thank you to my parents and my brother for always believing in me, and to Kory for helping me see the light at the end of this very long tunnel.

ABSTRACT

Though multiple sclerosis (MS) has traditionally been considered an inflammatory disease, recent evidence has brought neurodegeneration to the spotlight, suggesting that axonal and neuronal injury and loss are important factors in disease progression. Various mechanisms have been proposed to address the neurodegenerative component in MS, which all at some level posit cytosolic and subsequent mitochondrial Ca^{2+} overload, generation of reactive oxygen species (ROS), and ensuing mitochondrial dysfunction as precipitating factors. Previous studies have shown that mutational inhibition in mice of a mitochondrial Ca^{2+} and ROS efflux pathway, the permeability transition pore (PTP), results in resistance to the axonal degeneration that accompanies the murine model of MS, experimental autoimmune encephalomyelitis (EAE). These studies point to PTP activation as a key player in the degenerative mechanisms that occurs in EAE, and potentially MS. In an effort to elucidate the pathways leading to PTP activation and mitochondrial dysfunction in EAE, the role of a potential upstream effector was investigated. Notably, p66ShcA (p66) has recently been discovered as a redox enzyme that regulates mitochondrial ROS levels by oxidizing cytochrome C and catalyzing the reduction of oxygen to hydrogen peroxide. Oxidative insults induce p66 mitochondrial translocation and accumulation of active enzyme within the intermembrane space. Utilizing the murine disease model EAE, p66-knockout (p66-KO)

and WT mice were immunized with myelin oligodendrocyte glycoprotein (MOG) 35-55 peptide. The results demonstrated that p66-KO mice developed EAE, but had less severe clinical impairment and paralysis compared to WT mice. Histologic examination of spinal cords and optic nerves showed significant tissue and axonal protection in the p66-KO mice despite similar levels of inflammation as reported by immunohistologic studies, T-cell proliferation, and cytokine assays. Furthermore, neuronal cultures derived from p66-KO mice were more resistant to reactive oxygen and nitrogen species implicated in neurodegenerative pathways of EAE and MS. This resistance was correlated with greater preservation of mitochondrial integrity in p66-KO neurons as indicated by less altered mitochondrial morphology and mitochondrial ROS levels following oxidative insults. Interestingly, however, mitochondrial transport was in general similarly decreased in both p66-KO and WT neurons, suggesting that p66 elimination has no direct effect on transport mechanisms. Overall, these results provide additional evidence that inactivation of mediators of mitochondrial PTP opening confers axonal and neuronal protection. Hence, in addition to mitochondrial PTP- and ROS-targeted drugs, pharmacologic p66 inhibitors may represent a new approach to neuroprotection in MS therapy.

CHAPTER I:

Introduction

I. Axonal degeneration in multiple sclerosis: The mitochondrial hypothesis

Multiple sclerosis (MS) is the most common chronic inflammatory disease of the central nervous system (CNS), affecting upwards of 2 million people worldwide. Patients present with a spectrum of clinical signs and symptoms, including weakness, vision loss, fatigue, and cognitive impairment. Around 85% of patients have a relapsing-remitting (RRMS) clinical course, characterized by periods of clinical stability punctuated by subacute attacks of clinical worsening after complete or partial recovery. Many of these patients eventually transition into secondary progressive MS, during which there is continuous neurological deterioration. A minority of patients (around 10%) present with primary progressive MS, characterized by unremitting decline of neurological function. The remaining 5% of patients experience a clinical course termed progressive relapsing MS, during which there is a steady progressive neurological decline interspersed with acute attacks with or without recovery (Noseworthy et al., 2000).

Traditionally, MS has been classified as an immunological, demyelinating disease caused by autoreactive T cells directed against myelin-associated antigens such as myelin oligodendrocyte glycoprotein, proteolipoprotein, and myelin basic protein (Schmidt, 1999). Acute lesions are thought to result when activated T cells responsive to these and other potential antigens traffic to the CNS and trigger a cascade of inflammatory events. This involves activation of recruited monocytes and resident microglial cells to generate

macrophages that are key mediators of tissue injury and are the most abundant inflammatory cells found in MS lesions (Huitinga et al., 1990). These acute inflammatory lesions are often clinically silent but may result in clinical relapses depending on the severity and location of the lesion. Currently, all available FDA-approved therapies for MS are anti-inflammatory in nature and have been successful at treating RRMS, but not progressive forms of MS (De Jager and Hafler, 2007). This includes the recently FDA-approved oral drug fingolimod, which inhibits lymphocyte egression from lymph nodes (Cohen et al., 2010).

While classically thought of as a demyelinating disease, it is now recognized that MS pathology is much more complex. Technological advancements in such areas as immunohistochemistry, microscopic imaging, and magnetic resonance spectrometry have allowed for closer examination of patient brain and spinal cord tissue both post-mortem and *in* vivo (Lovas et al., 2000; Kuhlmann et al., 2002; Ingle et al., 2003; Kutzelnigg et al., 2005; Herrero-Herranz et al., 2008). From these studies, there is accumulating evidence of prominent axonal damage throughout the nervous tissue. For example, immunohistochemistry, confocal imaging, and 3-D computer reconstruction of post-mortem MS patient brains showed a significant amount of transected axons in both active and chronic active white matter lesions (Trapp et al., 1998). In addition, axonal degeneration analysis in chronic *inactive* lesions of secondary progressive MS patient spinal cords using similar methods indicated a 61% reduction in axonal density (Bjartmar et al., 2003). Likewise, analysis of normal appearing white matter (NAWM) showed decreased nerve fiber densities in patient spinal cords (Bjartmar et al., 2001). These

results in post-mortem tissue have been confirmed by *in vivo* studies utilizing magnetic resonance spectrometry (MRS). MRS is a method of live imaging in which the chemical composition of the brain can be determined through analysis of certain peaks in the resonance spectra. Of particular importance is the metabolite N-acetylaspartate (NAA), which is produced by mitochondria in neurons and is the second most abundant compound in the CNS following glutamate. Therefore, NAA levels are used to monitor neuronal integrity *in vivo* over time, and decreases in NAA have been correlated with relapses and neurological decline in MS patients (Signoretti et al., 2001; Lu et al., 2004; Benarroch, 2008). In depth analysis of NAA levels throughout patient CNS tissue has shown significant decreases in both MS white matter lesions and NAWM, thus supporting the aforementioned findings in post-mortem tissue samples (Fu et al., 1998). Furthermore, decreased levels have been found in gray matter of MS patients, suggesting that damage occurs throughout the CNS. Overall, there is now convincing evidence that widespread axonal degeneration appears early on in MS and is prominent in progressive forms of the disease. Of importance to this thesis is the recognition that axonal loss plays a critical role in the irreversible disability that occurs in MS.

The actual mechanisms involved in MS axonal injury may vary depending on the stage of disease. First, acute axonal disruption is a prominent part of active inflammatory lesions of MS (Trapp et al., 1998). Second, clinical, pathologic and magnetic resonance evidence suggests widespread axonal degeneration independent of acute inflammation, most prevalent in progressive forms of MS (Lovas et al., 2000). While it is likely that the specific mechanisms of axonal injury and degeneration differ between these two stages of

disease, there seems to be a convergence of the pathways that involves mitochondrial failure *(Figure 1)*.

There is accumulating evidence that mitochondria are key players in axonal degeneration in all stages of MS, playing crucial roles in energy metabolism and cell homeostasis. For one, NAA, the commonly used MRS marker of axonal integrity, is produced by neuronal mitochondria. Therefore, changes in NAA levels can also reflect the integrity of mitochondrial function within axons (Fu et al., 1998; Signoretti et al., 2001; Benarroch, 2008). As previously mentioned, changes in NAA levels correspond with relapses and have been shown to fall dramatically in acute inflammatory lesions and partially reverse as inflammation subsides (Fu et al., 1998; Khan et al., 2005). The initial dramatic decline in NAA undoubtedly reflects reversible mitochondrial dysfunction in axons within these acute lesions. Similar NAA decreases in chronic focal white matter lesions and NAWM also may suggest chronic mitochondrial dysfunction within axons as well as axonal loss (Bjartmar et al., 2000). In addition, evidence linking mitochondrial dysfunction to axonal degeneration has been shown by post-mortem analysis of MS patient brain tissue, including lesioned areas, NAWM, and nonlesional cortex. Structurally, electron microscopy of demyelinated spinal cord lesions show dramatically decreased numbers of mitochondria and microtubules (Dutta et al., 2006). Further analysis indicates oxidative damage of mitochondrial DNA and impaired activity of mitochondrial enzyme complexes in lesioned tissue (Lu et al., 2000), and reduced mitochondrial gene expression specific to neurons in nonlesional tissue

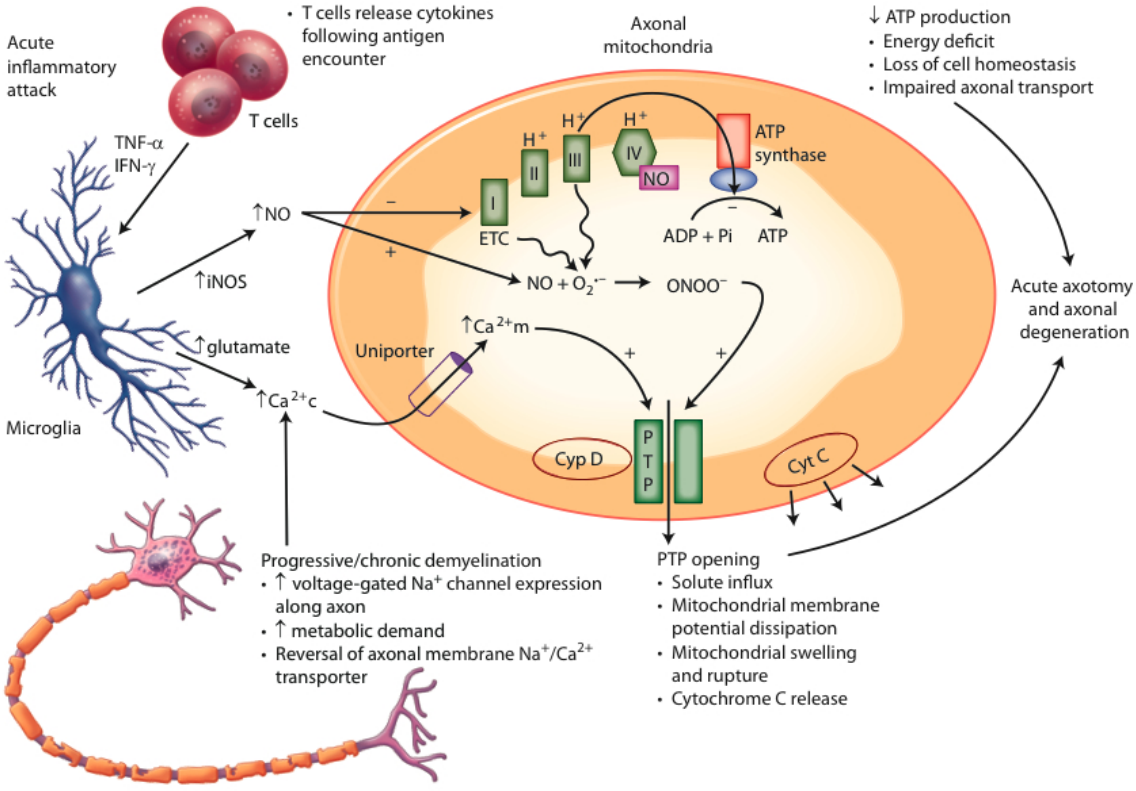

Figure 1. Schematic representation of the mitochondrial hypothesis for axonal degeneration in multiple sclerosis. ATP - adenosine triphosphate (adenosine diphosphate plus a single phosphate [ADP + Pi]); $Ca^{2+}c$ - cytoplasmic calcium; Ca^{2+} m - matrix calcium; CyPD - cyclophilin D; CytC - cytochrome C; ETC - electron transport chain; IFN-γ - interferon-γ; iNOS - inducible nitric oxide synthase; NO - nitric oxide; $O_2^{\cdot -}$ - superoxide; $ONOO^-$ - peroxynitrite; PTP - permeability transition pore; TNF-α - tumor necrosis factor-α (Su et al., 2009).

(Dutta et al., 2006). Finally, a recent paper has provided compelling evidence from *in vivo* imaging of double-transgenic mice with CFP-labeled axonal mitochondria and YFP-labeled axoplasm *(Thy1-MitoCFP × Thy1-YFP-16)* induced with experimental autoimmune encephalomyelitis (EAE), a commonly used animal model for MS (Nikic et al., 2011). In monitoring single axons in the EAE-induced animals, the group noted the presence of focal axonal degeneration (FAD) that was independent of demyelination. Importantly, they found that abnormal axonal mitochondrial morphology was the earliest ultrastructural sign of damage, preceding axon structural changes. Dysmorphic, swollen mitochondria were present at various degenerative stages in axons of EAE-induced animals, and were absent in axons of control animals. To correlate this observation to human MS, the authors subsequently analyzed patient biopsies of actively demyelinating lesions and found mitochondrial damage in axons, including those still myelinated and without apparent changes in axon morphology. Overall, these multifaceted studies provide convincing evidence that mitochondrial function may play a significant role in mechanisms of axonal degeneration in MS.

The following sections will focus on the mechanisms of mitochondrial dysfunction leading to 1) axonal disruption in acute inflammatory lesions, and 2) the chronic axonopathy and axonal degeneration in progressive MS. In particular, the acute inflammatory attacks common in RRMS will be analyzed, and the potential effects of inflammatory components such as nitric oxide and glutamate will be addressed. In addition, the mechanisms by which axons degenerate during the progressive phases independent of acute inflammation will be discussed, emphasizing Ca^{2+}, free radicals, and

opening of the permeability transition pore as key players in mitochondrial failure and subsequent axonal damage. Finally, the effect of mitochondrial dysfunction on axonal transport, specifically with regards to mitochondria motility, will be summarized.

Mitochondria: background

The mitochondrion is commonly defined as the power plant of the cell, the site at which aerobic respiration and ATP synthesis take place. A cytoplasmic organelle with double membranes, the mitochondrion is divided into two main compartments, the matrix and the intermembrane space. The outer mitochondrial membrane enclosing the organelle contains a large number of porin channels, which allow free diffusion of molecules 5000 Daltons or less. Larger proteins can enter mitochondria through the translocase of the outer membrane, which shuttles them into the intermembrane space. The intermembrane space is located between the outer and inner mitochondrial membranes; the pro-apoptotic protein cytochrome C is located here. The inner mitochondrial membrane (IMM) separates the intermembrane space from the matrix, and contains a wide range of proteins including the electron transport chain, ATP synthase, the translocase of the inner membrane, and the permeability transition pore. The electron transport chain and ATP synthase are involved in oxidative phosphorylation, which generates the mitochondrial membrane potential, the proton gradient, and of course, the ATP that is necessary for cell survival. In addition, channels regulating influx and efflux of Ca^{2+} between the cytoplasm and mitochondrial matrix are located in the IMM. High affinity Ca^{2+} uniporters mediate Ca^{2+} entry down the electrochemical gradient into the matrix, and various exporters utilizing Na^{+} and H^{+} gradients extrude Ca^{2+} back out

into the cytoplasm. Mitochondrial Ca^{2+} levels can also be regulated via the permeability transition pore (PTP), a transient pore in the IMM that opens in response to elevated levels of Ca^{2+} or reactive oxygen species (ROS), and allows solutes with molecular masses up to 1500 Daltons to enter the matrix (Bernardi et al., 2006). More about the PTP will be addressed later in the introduction.

As evident by their structural components, mitochondria are crucial to cell survival, not only by producing ATP, but also functioning to maintain ion homeostasis and to regulate apoptosis. Therefore, it is not surprising that external factors altering mitochondrial function during the acute and progressive phases of MS have a profound downstream effect on axonal degeneration.

Axonal degeneration within acute inflammatory lesions:

Nitric oxide hypothesis

During an acute inflammatory attack in MS, activated T cells initiate the pro-inflammatory cascade in response to antigens within the CNS. This response produces interferon gamma, which activates macrophages to produce elevated levels of nitric oxide (NO) by upregulating inducible nitric oxide synthase (Bogdan, 2001). The increase in NO inhibits mitochondrial respiration and reduces ATP synthesis (Brown and Borutaite, 2001).

The mechanism by which NO inhibits mitochondrial respiration involves cytochrome c oxidase, the terminal member of the electron transport chain situated in the inner mitochondrial membrane. Cytochrome c oxidase has a binding domain for O_2 and catalyzes the oxidation of cytochrome c and the reduction of O_2 to water. At elevated levels, NO can outcompete O_2 for the binding position, block electron flow, and disrupt

mitochondrial respiration (Cleeter et al., 1994; Brown and Borutaite, 2002). Since the pumping of protons from the mitochondrial matrix into the intermembrane space is coupled to the electron flow, ATP synthesis is subsequently hindered (Brown and Borutaite, 2001). Inadequate ATP production prevents crucial ATPase pumps from working properly, and the downstream effects are detrimental on cell survival.

Besides inhibiting oxidative phosphorylation, NO also can affect mitochondrial function by increasing free radical production. For one, interruption of electron transfer at cytochrome c oxidase by NO significantly increases electron leakage from the respiratory system resulting in elevated levels of superoxide (Beckman and Koppenol, 1996). Superoxide levels are usually regulated by antioxidant systems, which convert superoxide into hydrogen peroxide, and subsequently, oxygen and water. Superoxide that evades conversion can cause significant cellular damage by reacting with and inactivating lipids, proteins, DNA, and carbohydrates, as well as initiating apoptotic pathways via pathologic PTP opening. Furthermore, it can combine with NO to form highly toxic peroxynitrite ($ONOO^-$) (Beckman and Koppenol, 1996; Pacher et al., 2007), which also has a profound direct effect on mitochondrial function, increasing the peroxidation of mitochondrial membrane lipids, disrupting nearly all components of the electron transport chain, opening the PTP, and inducing cytochrome c release from the intermembrane space leading to apoptosis. Interestingly, peroxynitrite is prominent in acute inflammatory lesions, but absent from chronic non-inflammatory lesions (Cross et al., 1998). This suggests that peroxynitrite plays more of a role in axonal damage during acute inflammatory MS attacks.

Glutamate hypothesis

Excitotoxicity due to elevated glutamate release can also disrupt mitochondrial function. Glutamate is an essential excitatory neurotransmitter that acts on AMPA and NMDA receptors located on the post-synaptic membrane of neurons. Upon binding and activation of these receptors, ion channels open allowing various cations such as Na^+, K^+, and Ca^{2+} to enter the cell. Synaptic levels of glutamate are regulated by glutamate transporters present on astrocytes, oligodendrocytes, and microglia, which take up released glutamate and convert it into glutamine. Glutamine is then shuttled back to neurons and regenerated into glutamate by glutaminase (Groom et al., 2003).

Glutamate excitotoxicity occurs when there is elevated release of glutamate into the synapses, and inadequate reuptake by the transporters on supporting cells. For instance, during an active inflammatory attack in MS, large quantities of glutamate are produced by activated immune cells such as macrophages and microglia (Groom et al., 2003). There may also be a decrease in glutamate transporter expression in surrounding oligodendrocytes and astrocytes, further enhancing the severity of excitotoxicity.

Overstimulation of glutamate receptors leads to dysregulation of ionic gradients, including Ca^{2+} homeostasis. The increase in intracellular Ca^{2+} activates several enzymes including phospholipases, endonucleases, and proteases, which damage DNA, disrupt the cytoskeleton, and alter membrane lipids (Gunter et al., 2004). Elevated intracellular Ca^{2+} levels also alter mitochondrial dynamics, promoting Ca^{2+} entry into the matrix, PTP opening, and release of pro-apoptotic cytochrome c into the cytosol.

Magnetic resonance spectrometry can be used to monitor glutamate levels at various stages of MS (Srinivasan et al., 2005). Studies show that glutamate levels are elevated in acute inflammatory lesions as well as in normal appearing white matter. In comparison, glutamate levels are not elevated in chronic demyelinated regions. These findings suggest that glutamate-mediated excitotoxicity plays more of a role in acute than in chronic stages of MS.

Mitochondrial damage: the converging pathway

It is important to note that while the proposed NO and glutamate mechanisms of axonal injury are separate and distinct, they both converge onto a common pathway leading towards mitochondrial dysfunction. Both mechanisms affect the electron transport chain, ATP synthesis, ionic homeostasis, PTP opening, and release of pro-apoptotic factors. This convergence is not exclusive to the acute inflammatory attacks, and as will be discussed, is present in the progressive stages independent of acute inflammation as well, further emphasizing the importance of mitochondria in maintaining axonal integrity and survival throughout the entire MS disease course.

Axonal degeneration during progressive stages independent of acute inflammation:

Chronic demyelination promotes upregulation and reorganization of ionic channels

In the progressive stages of MS, there are fewer acute inflammatory lesions developing within the CNS, suggesting that other mechanisms are involved in axonal degeneration. At this stage in disease, commonly used anti-inflammatory medications, such as

interferon beta and glatiramer acetate, have minimal effect on delaying or inhibiting the degenerative symptoms of MS.

One of the main structural changes during progressive MS is the loss of myelin. In a normal myelinated axon, voltage-gated sodium channels are highly concentrated at the nodes of Ranvier, and the myelin sheath insulates the internodal axon so that current "jumps" from node to node. Loss of myelin greatly impairs the efficiency of action potential propagation. In response to demyelination, sodium channels become redistributed all along the axon and synthesis is upregulated, including both Nav1.6 and Nav1.2 subtypes (Craner et al., 2004). The Nav1.6 subtype, which is normally expressed at the nodes of Ranvier, tends to produce larger and more persistent currents in comparison to the Nav1.2 subtype, which is predominately expressed on premyelinated axons.

The reorganization of voltage-gated sodium channels and upregulation of channel expression along demyelinated axons leads to altered energy requirements. The demand for ATP exceeds the production capabilities of existing mitochondria, and the Na^+/K^+ ATPase pumps crucial to maintaining ionic gradients begin to fail. An excess of Na^+ ions accumulates intracellularly, and eventually reverses the Na^+/Ca^{2+} exchanger that normally moves Na^+ into the cell and Ca^{2+} from the cell (Stys et al., 1992; Dutta et al., 2006). Prolonged elevation of Ca^{2+} levels within the axoplasm can stimulate a multitude of downstream events that ultimately results in mitochondrial dysfunction and axonal damage.

Effect of elevated intracellular Ca^{2+} levels on mitochondrial function

As mentioned previously, mitochondria are composed of two membrane systems, an outer membrane that is freely permeable to most ions and an inner membrane that is more tightly regulated and surrounds the innermost mitochondrial matrix. During oxidative phosphorylation and ATP synthesis, electrons are transferred along the electron transport chain located in the inner mitochondrial membrane, which is coupled with the movement of H^+ ions from the matrix across the membrane into the intermembrane space. This ionic movement generates a transmembrane potential across the inner membrane (~-200 mV), and it is this voltage gradient that is subsequently used to synthesize ATP.

Beyond ATP synthesis, this inside-negative transmembrane potential also drives positively charged ions such as Ca^{2+} into the matrix. Consequently, mitochondria accumulate Ca^{2+} whenever local cytoplasmic levels rise above a critical set point, and then slowly release Ca^{2+} when cytoplasmic levels are restored (Krieger and Duchen, 2002).

The accumulation of Ca^{2+} ions within the mitochondrial matrix is dependent on the cytoplasmic concentration of Ca^{2+} as well as the affinity of two key mitochondrial transporters in the IMM, the inward electrogenic uniporter and the Na^+ or H^+/Ca^{2+} antiporters that extrude Ca^{2+} ions from the matrix. As Ca^{2+} ions have a higher affinity for the inward uniporter, they tend to be shuttled into the mitochondrial matrix when cytoplasmic Ca^{2+} levels are elevated (Gunter and Sheu, 2009).

Ca^{2+} accumulation in the mitochondrial matrix is physiologically relevant in the stimulation of oxidative phosphorylation. Three important rate-limiting metabolic enzymes are activated by matrix Ca^{2+}, including pyruvate dehydrogenase, alpha-

ketoglutarate, and isocitrate dehydrogenase (Gunter and Sheu, 2009). However, prolonged elevated Ca^{2+} levels can also induce opening of the PTP, leading to a cascade of events, including matrix swelling, rupture of the outer mitochondrial membrane, collapse of ATP production, and release of cytochrome c, triggering the pro-apoptotic pathway.

The permeability transition pore revisited:

The PTP, as mentioned before, is a pore in the IMM that opens when induced by mitochondrial Ca^{2+} overload or ROS. This phenomenon of permeability transition was recognized several decades ago, when it was found that isolated mitochondria *in vitro* exposed to high concentrations of Ca^{2+} became massively swollen as characterized by large decreases in light scattering, and that this swelling could be partially reversed by the addition of calcium chelators. Since this initial discovery, much effort have been made to define PTP components and dynamics, as well as to determine its physiologic relevance to human diseases.

As of now, our understanding of mitochondrial permeability transition and the PTP is still a work in progress. It has been shown by the pioneers of PTP research that the transient pore located in the IMM opens upon stimulation by elevated levels of Ca^{2+} and ROS. This, in turn, allows solutes with molecular masses up to 1500 Daltons to enter the matrix (Bernardi et al., 2006). One major consequence of PTP opening is that the IMM no longer maintains a barrier to protons, leading to dissipation of the proton motive force necessary for ATP synthesis. Furthermore, ATPases can work in reverse, hydrolyzing generated ATP leading to energy depletion that is detrimental to cell survival. Persistent PTP opening generates loss of the mitochondrial membrane potential and equilibration of

ionic gradients, which promotes matrix swelling, outer membrane rupture, and release of cytochrome c from the intermembrane space to activate cytoplasmic pro-apoptotic factors.

Interestingly, in preparations of isolated mitochondria, induction of PTP opening produces mitochondria with either normal or massively swollen morphology, and none in an intermediate state. Therefore, the magnitude of the decrease in light scattering within a mitochondria suspension reflects the number of mitochondria within a population that have undergone permeability transition, rather than a progressive increase in volume of all the mitochondria (Halestrap, 2009). The stochastic nature of permeability transition in isolated mitochondria suggests that within a population, once a mitochondrion undergoes permeability transition to a swollen state, the ensuing release of matrix Ca^{2+} and mitochondrial ROS induces surrounding mitochondria to undergo transition themselves. One can speculate that this phenomenon observed in isolated mitochondria may similarly occur *in vivo*. Within the confines of a neuron, the stimulus for PTP opening increases as more mitochondria become dysfunctional and swollen. Once the ratio of damaged to intact mitochondria reaches a certain threshold, adequate ATP levels and ionic homeostasis cannot be successfully maintained, and the neuron is eventually committed to cell death.

Again, it is important to note that both the acute and chronic pathways of axonal degeneration in MS converge on the mitochondria, and specifically, the pathological opening of the PTP. This apparent convergence in degenerative mechanisms suggests that the PTP may be an ideal therapeutic target for both relapsing-remitting and

progressive forms of MS. Given that the structure of the PTP still remains elusive, it is essential to investigate the properties of this pore in order to potentially develop neuroprotective MS treatments that regulate pore opening and prevent mitochondrial rupture and ensuing axonal damage.

Much work has been done in the recent years to investigate permeability transition and the PTP. Some of the candidate proteins include ANT (adenine nucleotide translocator), VDAC (voltage-dependent anion channel), and cyclophilin D (a peptidyl-prolyl cis-trans isomerase) (Bernardi et al., 2006). Whether these proteins are essential components of the PTP has been heavily debated for numerous years. There is convincing evidence now from genetic studies that neither VDAC nor ANT are essential for PTP formation, but some experiments suggest that ANT may still play a regulatory role (Bernardi et al., 2006).

In contrast, increasing evidence indicates that cyclophilin D (CyPD) plays a crucial regulatory role in the PTP. Various pharmacologic and genetic techniques have been used to alter CyPD activity and expression, including cyclosporin A (CsA) administration, which inhibits CyPD, and deletion of the murine *Ppif* gene, which encodes CyPD. CsA treatment has long been shown to inhibit PTP opening, and has been tested in several *ex vivo* and *in vivo* models of disease, including ischemic-reperfusion injury of the heart, and ischemic and traumatic brain injury (Griffiths and Halestrap, 1993; Friberg et al., 1998). In particular, CsA pre-treatment of insulin-induced hypoglycemic mice has been shown to significantly reduce brain damage, and ultrastructural examination suggests that the marked protection is due in part to mitochondrial preservation. Alteration of CyPD

activity by *Ppif* gene deletion (CyPD-KO) has resulted in viable animals that still can form the PTP (Baines et al., 2005; Basso et al., 2005) but have a higher mitochondrial Ca^{2+} set point for PTP activation. Consequently, the mitochondria in CyPD-KO mice are able to retain about double the amount of Ca^{2+} as mitochondria from wild-type (WT) animals before PTP activation, demonstrating that CyPD is a significant regulator of PTP opening.

Due to the altered PTP properties in CyPD-KO mice, they have been used in many studies addressing mitochondria dysfunction and disease pathology. For instance, CyPD-KO mice subjected to cardiac ischemia/reperfusion showed a 40% reduction in myocardial infarction compared to WT mice (Baines et al., 2005). Similarly, Schinzel et al. found that CyPD-KO mice were significantly protected from brain ischemia/reperfusion injury via middle cerebral artery occlusion, demonstrating a 62% reduction in brain infarct size (Schinzel et al., 2005). These findings suggest that CyPD elimination and ensuing alteration of PTP properties generates significant protection in various disease models and organ systems.

To address the mitochondrial hypothesis of axonal degeneration in MS, CyPD-KO mice were induced with experimental autoimmune encephalomyelitis (EAE) (Forte et al., 2007). EAE is a well-recognized animal model for MS, and involves immunization with fragments of myelin proteins, including myelin oligodendrocyte glycoprotein (MOG) and proteolipoprotein (PLP). In this study, C57BL/6 background CyPD-KO and WT mice were immunized with MOG 35-55 peptide to induce EAE. The immunized CyPD-KO mice developed clinical symptoms of hindlimb and forelimb weakness and paralysis, but unlike the WT mice, partially recovered. Histologic analysis of CyPD-KO spinal cords showed

significantly decreased axonal damage and loss compared to WT cords despite having similar levels of CD4+ T cells and CD11b+ macrophages/microglia. Furthermore, isolated CyPD-KO neurons were more resistant to treatment with H_2O_2 and NO, and CyPD-KO brain mitochondria were able to sequester substantially greater amounts of Ca^{2+}. These results indicate that regulation of PTP opening and mitochondria integrity has a significant effect on EAE disease progression and axonal and neuronal survival. In the broader scheme, they also suggest that pharmacologic blockers of the PTP might be beneficial in reducing or preventing axonal and neuronal degeneration in MS.

Mitochondrial dysfunction and axonal transport in MS:

The previous introductory sections have focused on mitochondrial dysfunction in MS axonal degeneration as mediated by pathologic PTP opening and cell death activation. In this next section, I take a slight tangent and introduce the effects of mitochondrial dysfunction on transport, and how this may contribute to degenerative pathways in MS.

To begin with, axonal transport is necessary for the normal function and survival of neurons, conveying newly synthesized proteins from the cell body to sites along the axon, and delivering trophic signaling complexes from synaptic terminals back to the cell body. Despite the importance of axonal transport to neuronal function and survival, little research has been done on the effects of inflammation on axonal transport and nothing is known about dysfunction of axonal transport in MS. It seems likely that mitochondrial dysfunction in MS could lead to abnormalities of axonal transport, which in turn could contribute to axonal degeneration.

Axonal transport is mediated by motor proteins that walk along microtubules, carrying membranous organelles along for the ride. Because axonal microtubules are oriented with plus ends pointing away from the cell body, members of the kinesin family of plus-end directed motors mediate anterograde transport and cytoplasmic dyneins mediate retrograde transport. The motors that drive axonal transport require ATP produced locally by mitochondria all along the axon. At the same time, motor-driven transport is required to deliver mitochondria to appropriate sites along the axon. Thus deficits in mitochondrial ATP production can disrupt axonal transport, and disruptions in transport can interfere with mitochondrial trafficking.

The number and localization of mitochondria in axons is a function of mitochondrial fission, mitochondrial fusion, and long-range bidirectional transport along the axon. These same processes occur in all cells, but neurons are likely to be particularly susceptible to dysfunctions in mitochondrial trafficking due to their extended dimensions. In support of this idea, mutations in genes that regulate mitochondrial fusion, fission, and transport are responsible for forms of spastic paraplegia, Charcot-Marie-Tooth disease and optic atrophy (Chen and Chan, 2006). Thus mitochondrial trafficking is essential for maintaining axonal integrity.

While mitochondria are present all along the axon, they are concentrated in areas with high metabolic demand, such as presynaptic terminals and in some cases, nodes of Ranvier (Hollenbeck and Saxton, 2005). Three recent studies have elucidated the molecular mechanisms by which neural activity and associated increases in cytoplasmic Ca^{2+} regulate mitochondrial transport (Saotome et al., 2008; Wang and Schwarz, 2009;

MacAskill et al., 2009). The principal motor responsible for anterograde mitochondrial transport is Kinesin-1 (Hollenbeck and Saxton, 2005). Kinesin-1 is linked to the mitochondrion by the protein Milton, which binds to the kinesin tail domain and links it to Miro, a protein in the outer mitochondrial membrane. Miro, a GTPase with two Ca^{2+} binding domains, regulates the integrity of this complex and hence the efficiency of mitochondrial transport. Ca^{2+} binding to Miro inhibits mitochondrial transport, either by causing dissociation of the complex or by inhibiting the kinesin-microtubule interaction, causing mitochondria to accumulate at sites of increased Ca^{2+} levels. This mechanism, which is essential for correctly positioning mitochondria under normal circumstances, may enhance the susceptibility of mitochondria to damage under pathological conditions, as discussed below.

During an acute inflammatory attack, increases in free radicals lead to mitochondrial damage and decreased ATP production, which would be expected to inhibit axonal transport, including the transport of mitochondria (Rintoul et al., 2006). Inflammation also activates signaling pathways that inhibit axonal transport. For example, TNF-alpha and NO inhibit the transport of mitochondria and synaptic vesicle proteins by activation of JNK kinase (Stagi et al., 2006). JNK kinase phosphorylates a serine in the kinesin-1 motor domain, which inhibits its translocation (Morfini et al., 2009). Elevated glutamate release during the acute inflammatory phase also leads to increased Ca^{2+} entry, Ca^{2+} binding to Miro, and inhibition of kinesin-mediated transport, causing mitochondria to accumulate in the affected regions. While this response may temporarily enhance the buffering of axoplasmic Ca^{2+} and increase the availability of ATP to restore ionic concentrations, it also

exposes the immobilized mitochondria to further oxidative damage, which would eventually exacerbate the depletion of ATP and its effects on axonal organelle transport.

Likewise, during the progressive phases of MS, intracellular Ca^{2+} levels are elevated by altered distribution of voltage-gated channels, increased metabolic requirements, and inability of ATPase pumps to regulate ionic gradients. Again, the elevated intracellular Ca^{2+} levels would inhibit mitochondrial transport, and retain the organelles in damaged areas. With time, the persistent elevation in Ca^{2+} levels may lead to opening of the PTP, mitochondrial rupture, and initiation of apoptotic events within the axon (Nikolaev et al., 2009). Genetic studies in mice show that mutations or deletions in specific myelin proteins lead to changes in the axonal cytoskeleton, including alterations in the phosphorylation and spacing of neurofilaments and microtubules, changes in the velocity of axonal transport, and mislocalization of mitochondria (Witt and Brady, 2000). These changes can occur even in cases where myelin structure is largely intact. Thus chronic demyelination may also disrupt the signaling between oligodendrocytes and axons that is required to maintain the axonal transport machinery.

Overall, pathophysiologic changes observed in both acute and chronic stages of MS are likely to inhibit axonal transport via disruption of ATP production and mitochondrial trafficking dynamics. Given the unique elongated structure of neurons, impaired transport is particularly detrimental to cell survival, and therefore warrants further study on its potential contribution to MS degenerative mechanisms.

Summary:

In the past, MS has largely been considered a chronic inflammatory and demyelinating disease, driving most of the research and treatment development towards targeting the immune system. As of now, disease-modifying therapies for MS are limited to various anti-inflammatory agents that reduce acute inflammatory lesions, clinical relapses and disability progression in RRMS. These anti-inflammatory agents, however, do not completely prevent axonal injury and are largely ineffective in treating progressive MS.

The recent resurgence of MS research focused on axonal degeneration mechanisms has resulted in convincing experimental evidence and potential treatment targets. As reviewed above, mitochondrial function is crucial in preserving axonal integrity in both acute inflammatory and progressive stages of MS. Therefore, therapies that protect mitochondria and enhance their functioning warrant investigation. Such therapies include sodium channels blockers to reduce axoplasmic Ca^{2+}, anti-oxidants to neutralize free radical production, and PTP inhibitors to maintain mitochondrial integrity. With continued progress in the understanding of MS and the mechanisms that drive the disease, it is hopeful that a successful treatment regimen targeting both inflammation and axonal degeneration may soon be developed.

II. p66ShcA: A potential neuroprotective target for MS?

As summarized in the previous section, there is accumulating evidence that mitochondrial dysfunction plays a significant role in MS axonal degeneration. Furthermore, in teasing out the mechanisms leading to mitochondrial dysfunction, a key player that stands out is the mitochondrial PTP. Previous studies altering pore activation have shown significant axonal protection in the MS model EAE. In particular, elimination of PTP regulatory component CyPD resulted in less severe clinical EAE and decreased axonal damage in spinal cord tissue (Forte et al., 2007).

Besides altering PTP opening by targeting pore regulatory components such at CyPD, much research is being directed towards investigating potential upstream *in vivo*

activators of the PTP. Studies have shown that Ca^{2+} and ROS are critical to PTP opening and cell death (Bernardi et al., 2006). In terms of ROS, these are potent intracellular oxidants that include hydrogen peroxide, superoxide, and hydroxyl radicals. They are commonly produced by dedicated enzymes, the NADPH oxidases, and as metabolic byproducts due to electron leaks by the electron transport chain (Esposito et al., 1999; Turrens, 2003; Bedard et al., 2007). Because of their potential damaging effects on cellular macromolecules such as nucleic acids, proteins, and lipids, ROS levels are tightly regulated by intracellular superoxide dismutases and catalases. However, various stressors can dramatically increase ROS levels leading to significant intracellular damage. This is especially true for mitochondria, which are major sites of ROS production due to aerobic respiration and oxidative phosphorylation.

Recently, yet another pathway for mitochondrial ROS production has been discovered involving the p66ShcA (p66) protein (Giorgio et al., 2005; Pinton et al., 2007; Hajnóczky and Hoek, 2007). The ShcA gene encodes two mRNA species, one specific for p66 and one, by the use of alternate translation start sites, encoding the p46 and p52 isoforms (Migliaccio et al., 1999). While all three isoforms share the same amino acid sequence at the C terminus, including phosphotyrosine-binding (PTB), Src homology 2 (SH2) and collagen homology (CH1) domains, only the p66 isoform has a unique N terminus that allows it to be serine phosphorylated and targeted to mitochondria. Consequently, in contrast to p46 and p52, p66 is not involved in the transmission of activation signals from receptor tyrosine kinases to Ras proteins (Migliaccio et al., 1997). Rather, the p66 isoform gets serine phosphorylated by protein kinase C-Beta (PKC-β) in the cytoplasm, and

following interaction with isomerase Pin1, subsequently targets to the mitochondrial intermembrane space. There, it serves as a redox enzyme by oxidizing cytochrome C, and transferring electrons to reduce oxygen into superoxide and hydrogen peroxide (Giorgio et al., 2005). This localized pool of mitochondrial ROS is proposed to mediate PTP opening and cell death activation (*Figure 2*).

Furthermore, p66 is part of a positive feed-forward signaling pathway for mitochondria-mediated cell death, serving as both a ROS sensor and amplifier. At typical cellular conditions, cytoplasmic p66 is unphosphorylated, and according to various studies in mitochondrial preparations, is sequestered in a

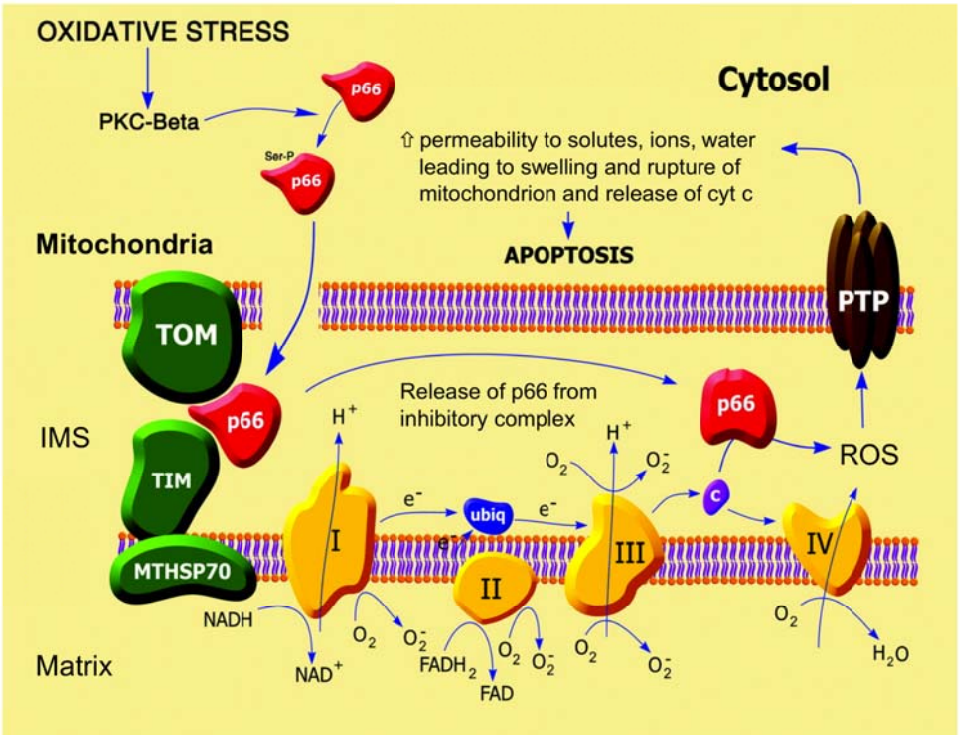

ROS stress-sensing complex that keeps p66 inactive at low to moderate stress levels. In particular, peroxiredoxin (Prx) 1 has been proposed to be part of this complex (Gertz et al., 2009). Prxs are a family of thiol-based H_2O_2-degrading enzymes, so-called peroxidases,

Figure 2: Activation and translocation of p66 into the mitochondrial intermembrane space. Serine phosphorylation of p66 leads to translocation into the intermitochondrial membrane space (IMS). There, it generates ROS that work downstream to activate PTP opening and cell death (Figure adapted from Consentino et al., 2008).

and are weak scavengers with the ability to degrade low levels of cellular H_2O_2. At these conditions, the stress-sensing complex consists of Prx1 in its dimerized, active form, and p66 in its dimerized, inactive form. However, at elevated levels of cellular stress, Prx1 function becomes overwhelmed, and the Prx1/p66 complex disassembles, freeing up p66 for activation. In addition, it has been shown that upon induction by stress factors, p66 expression increases and existing p66 becomes stabilized, further amplifying the pool of cytosolic p66 available for serine phosphorylation by stress activated PKC-β. Phosphorylated p66 translocates into the mitochondrial intermembrane space following interaction with Pin1 isomerase, and there, it serves as a ROS amplifier by generating mitochondrial ROS to induce PTP opening, which further elevates oxidative stress levels and activates mitochondria-mediated cell death.

Efforts to analyze the potential protective effects of p66 elimination have led to *in vitro* and *in vivo* studies of p66 elimination by genetic manipulation. For instance, p66-KO mouse embryonic fibroblasts (MEFs) were found to have increased resistance to H_2O_2 treatment compared to WT MEFs, and notably, this greater viability could be significantly reduced via retroviral-induced p66 expression (Migliaccio et al., 1999). Furthermore, assessment of mitochondria morphology in the stressed MEFs showed that p66-KO MEF mitochondria remained intact and elongated following H_2O_2 treatment compared to the noticeably swollen and fragmented WT MEF mitochondria (Pinton et al., 2007). In the *in vivo* setting, p66-KO mice are also more resistant to oxidative stress as indicated by their response to paraquat treatment, which induces superoxide production upon cellular intake. Treated p66-KO mice had a 40% increase in mean survival time compared to WT mice (Migliaccio et al., 1999). It is likely due to such protective effects that p66-KO mice have significantly prolonged lifespans, around 30% longer than those of WT mice. Hence, p66 has been termed the longevity gene.

In the context of human disease, p66 elimination has been shown to be protective in various disease models and organ systems. In particular, p66-KO mice maintained on a chronic 21% high fat diet had significantly decreased aortic cumulative early lesion area compared to WT mice (21% in WT; 3% in p66-KO), and immunohistochemical analysis showed less macrophage-derived foam cells and apoptotic vascular cells in the p66-KO lesions (Napoli et al., 2003). Similarly, p66-KO used in a diabetes disease model demonstrated less marked changes in renal structure and function as evidenced by significantly lower levels of proteinuria, albuminuria, glomerular sclerosis index, and

glomerular and mesangial areas, as well as decreased apoptotic cell death (Menini et al., 2006). The protective effects of p66 also extended to other diseases including ethanol-induced liver damage, in which p66-KO mice fed with an alcohol-rich diet showed reduced liver swelling, serum ALT levels and attenuated fatty changes compared to WT controls (Koch et al., 2008).

While the effects of p66 elimination have been well examined in diseases throughout the body, its role in the nervous system has not been well characterized. One of the few papers published studying p66 in neurodegenerative diseases attempted to associate Aβ peptide accumulation in Alzheimer's disease to p66 mediated apoptosis in mouse neuronal cultures and human neuroblastoma SH-SY cells (Smith et al., 2005). The authors showed that treatment of mouse neuronal cultures with Aβ peptide induced apoptosis and elevated levels of serine phosphorylated p66. In addition, p66 overexpression in SH-SY cells increased cell death and treatment with dominant negative p66ShcAS36A (serine mutated to a nonphosphorylatable alanine) repressed cell death. While interesting, the physiologic relevance of these results is questionable given the *in vitro* setting of the experiments, and further investigation in animal models will be necessary to define the role of p66 in Alzheimer's disease.

Currently, the role of p66 in neurodegenerative diseases has yet to be demonstrated *in vivo*. Given the correlation of mitochondrial dysfunction with MS pathophysiology, and the association of p66 with mitochondria-mediated cell death, it would be intriguing to study the effects of p66 elimination *in vivo* utilizing the MS model EAE. Hence, I propose the novel studies as outlined in the following section.

III. Thesis objectives and approaches

Though multiple sclerosis has traditionally been considered an inflammatory demyelinating disease, evidence now points to axonal degeneration as critical to early and late stage symptoms (Bjartmar and Trapp, 2001). Importantly, accumulation of axonal damage leads to progressive and permanent decline in neurological function, which is unresponsive to current immunosuppressive MS treatments (De Jager and Hafler, 2007). While the underlying mechanisms of axonal degeneration are uncertain, one proposed pathway involves oxidative stress and mitochondrial dysfunction.

In response to a variety of cellular stresses, the high conductance PTP can pathologically open, causing dissipation of the mitochondrial membrane potential, disruption of ATP synthesis, and activation of cell death by cytochrome c release (Bernardi et al., 2006). Though the exact structure of the PTP is still fairly elusive, studies have demonstrated that a mitochondrial matrix protein, CyPD, is a key regulatory component of the PTP (Nicolli et al., 1996). CyPD-KO mice have been generated by Ppif gene deletion (Basso et al., 2005), and the resulting resistance to PTP activation protects these mice from stressors associated with various animal models of human disease including MS model EAE. Following EAE induction, CyPD-KO mice partially regained function following paralysis and showed significant axonal protection in comparison to WT controls, suggesting that the PTP may be an important therapeutic target for MS (Forte et al., 2007).

Given these results, one can expect that additional protective therapeutic targets may lie in upstream promoters of PTP opening. Potential promoters include ROS, which are both activators and a consequence of PTP opening due to ensuing mitochondrial dysfunction (Petronilli et al., 1994; Madesh and Hajnóczky, 2001). Recently, a positive feed-forward pathway for ROS generation has been defined based on the mitochondrial action of p66 (Migliaccio et al., 1999). While other products of the ShcA gene function in the transmission of signals from receptor tyrosine kinases to Ras proteins, this isoform is specifically targeted to the mitochondrial intermembrane space upon increased cellular stress (Pinton et al., 2007). Functioning as a redox enzyme, p66 catalyzes mitochondrial ROS production by oxidizing cytochrome c and reducing oxygen to superoxide and hydrogen peroxide (Giorgio et al., 2005), thereby activating PTP opening and ensuing cell death.

Though p66 elimination has been shown to be protective in such diseases as liver damage, diabetes, and atherosclerosis, it has yet to be studied in the context of neurodegenerative diseases, including MS. Consequently, I designed the following thesis project organized around two specific aims to investigate the idea that p66 serves as a critical upstream promoter of pathologic PTP opening, mitochondrial dysfunction, and resultant axonal and neuronal degeneration in EAE, and may be a potential novel target for neuroprotective MS therapeutics.

Project aims:

Aim 1: Determine whether p66 elimination protects axons in the murine MS model EAE

a) Rationale:

Previous EAE studies on CyPD-KO mice showed significant axonal protection following EAE induction, suggesting that the PTP plays a pivotal role in axonal degeneration. Since p66 is proposed to be a critical upstream activator of PTP opening through its production of mitochondrial ROS, one would expect similar axonal protection in p66-KO mice. No studies to date have looked at these mice utilizing the MS disease model EAE.

Furthermore, the generation of p66/CyPD double knockout (DKO) mice and comparative analysis with the single knockout mice (i.e. p66-KO, CyPD-KO) may provide insight into the relationship between p66 and CyPD in mitochondria-mediated cell death pathways of EAE. As previously mentioned, both p66-KO and CyPD-KO cells and tissues share phenotypic similarities. Given that both proteins are found within the mitochondria and are localized to different compartments, it is likely that they act on the PTP at two distinct sites. Specifically, p66 interacts with cytochrome c to generate a PTP activator, ROS, in the intermembrane space, while CyPD regulates the PTP by direct association with the complex in the matrix (i.e., on opposite sides of the inner mitochondrial membrane). While many biochemical details remain to be established, notably, the nature of the core components forming the PTP, the generation and study of p66/CyPD-DKO mice will undoubtedly provide novel information and insight on the pathway outlined in Figure 2. Taking previous EAE results and the proposed pathway into consideration, if p66 is an upstream promoter of CyPD-regulated PTP opening, p66/CyPD-DKO animals should show similar levels of axonal protection in response to EAE induction as observed in each mutant alone. Consistent with this prediction, overexpression of p66 itself induces

apoptosis, likely through increased coupling with cytochrome c and increased ROS generation, which can be inhibited by CsA (Trinei et al., 2002).

Thus, the goals of this first aim was to use a series of rigorous genetic methods to 1) evaluate the role of p66 in the etiology of axonal pathology associated with EAE, and 2) to test the functional relationship between p66 and CyPD in regulating PTP activation and the ensuing axonal pathology associated with this disease model, thereby potentially defining new therapeutic targets for the treatment of MS.

b) Approaches:

The general experimental plan was based on the analysis of EAE responses in animals individually missing p66 or CyPD, and double mutants in which both proteins are absent (p66-KO; CyPD-KO; p66/CyPD-DKO; all in isogenic C57/Bl6 backgrounds). Mice of these genotypes have either been obtained from established colonies in the Forte and Giorgio labs (CyPD-KO; p66-KO) or generated using standard genetic approaches (p66/CyPD-DKO). CyPD-KO mice, generated by *Ppif* gene deletion, show no overt phenotype and no obvious changes in mitochondrial function. Similarly, p66-KO mice are fully viable without any overt phenotype or alterations in mitochondrial function. Importantly, no differences have been found in any of the known ROS scavenging systems (catalase, superoxide dismutase and GSH-peroxidases) in p66-KO or CyPD-KO cells and tissues (Blachly-Dyson and Forte, unpublished observation). Finally, using standard genetic approaches, I successfully generated a p66/CyPD-DKO colony, and have observed no overt phenotypes (unpublished results).

In terms of methodology, 10-12 week old female mice of the four genotypic groups (p66-KO, CyPD-KO, p66/CyPD-DKO, WT) were used for the EAE studies. The mice were immunized by subcutaneous injection of myelin oligodendrocyte glycoprotein (MOG) 35-55 peptide following standard EAE protocol (Forte et al., 2007). Immunized mice were scored daily for clinical EAE, including hindlimb and forelimb weakness and paralysis. Following 36 days of clinical assessment, and the mice were perfused and spinal cords and optic nerves were dissected out for further histologic analysis.

To assess for the degree of axonal damage, thoracic spinal cords and optic nerves were embedded in plastic, sectioned, and stained with toluidine blue. Photomontages of the sections were quantified manually to determine the percent damage area in the ventrolateral spinal cord white matter and in each entire optic nerve cross-section. In addition, an axonal count was performed on a sampling of ventrolateral spinal cord white matter images. Finally, electron microscopy was utilized to provide a magnified qualitative comparison of p66-KO and WT mice axon damage.

Furthermore, it was necessary to rule out potential differences in MOG immunoreactivity attributable to p66 elimination, which would hence confound the aforementioned comparative damage analysis. A series of immune response assessments was carried out to determine whether differences did exist between the p66-KO and WT groups. First, the infiltration of CD4+ T cells and CD11b+ macrophages/microglia was analyzed in collected lumbar spinal cords and optic nerves of the EAE-induced mice via immunofluorescence staining. In addition, lymph node cell cultures were prepared from EAE-induced p66-KO and WT animals for proliferation studies and cytokine assays.

Respectively, these studies assessed T cell immunoreactivity and cytokine production following MOG peptide stimulation.

c) Hypothesis:

These proposed experiments aimed to elucidate the effects of p66-mediated mitochondrial ROS production on axonal survival following EAE induction. Given that p66 is both a ROS- sensing and ROS-amplifying molecule in a feed-forward signaling pathway that induces mitochondrial dysfunction, PTP opening, and cell death activation, I hypothesized that p66 elimination would inhibit this apoptotic pathway and protect axons. In addition, assuming the relationship between p66- and CyPD-regulation of the PTP represents a linear pathway, I hypothesized that the corresponding axonal degeneration observed in p66/CyPD-DKO mice would be similar to that of p66-KO and CyPD-KO mice.

d) Results

The results of Aim 1 have been summarized in the Chapter II manuscript that follows this introductory section, focusing on the protective effects of p66 elimination following EAE induction. Work on the p66/CyPD-DKO genotype was briefly addressed in the manuscript, but is described in more detail in the supplemental Chapter III.

Aim 2: Determine whether p66 elimination increases neuronal robustness and preserves mitochondrial integrity following oxidative insults implicated in EAE and MS neurodegenerative pathways

a) Rationale:

Recent emphasis on neurodegeneration in MS research has led to the formulation of hypotheses addressing the mechanisms behind axonal damage as previously mentioned. It is proposed that acute inflammatory attacks triggered by activated T cells following exposure to myelin protein antigens induce microglia infiltration of nervous tissue and production of toxic molecules including NO and H_2O_2. Elevated levels affect cellular homeostasis and essential mechanisms governed by mitochondria, leading to disruption of the electron transport chain, inhibition of ATP synthesis, increased ROS production, and ultimately PTP opening and cell death.

To directly assess the robustness of p66-eliminated neurons to damaging agents (i.e. NO, H_2O_2) implicated in MS neurodegenerative pathways, *in vitro* neuronal culture studies are ideal given the isolated and controlled experimental setting. The following proposed *in vitro* work allowed for closer observation of neuronal changes following oxidative stress, which was not possible in the *in vivo* EAE studies of Aim 1.

b) Approaches:

Aim 2 was approached by treating p66-KO and WT neuronal cultures with various concentrations of NO and H_2O_2, and then characterizing the cells using multiple assessments. Cultures established from either adult brain cortices or post-natal day 0-2 hippocampi were utilized for these studies, and experimental manipulation occurred at day 7 *in vitro*. The first assessment compared neuronal viability in the treated cultures 24 hours later by using a standard calcein AM live cell assay and by manually counting the number of live cells under a fluorescence microscope. Subsequent assessments compared mitochondrial dynamics in the treated neurons, including changes in mitochondrial morphology, ROS production, and transport. Specifically, cultures were electroporated with mito-GFP plasmid to examine changes in mitochondrial morphology and transport following treatment. For the assessment of mitochondrial ROS, cultures were incubated with Mitosox Red, a mitochondria-specific ROS dye, following oxidative insults.

Finally, to further define the relationship between p66 and CyPD in mitochondria-mediated cell death pathways of EAE as described in Aim 1, neuronal cultures were prepared from single and double knockout mice (p66-KO, CyPD-KO, p66/CyPD-DKO) and cell viability was assessed following treatment.

c) Hypothesis

The experiments for this aim were designed to investigate the effects of p66 elimination in neurons following treatment with various agents implicated in EAE and MS neurodegenerative pathways. The proposed *in vitro* studies complement the *in vivo* EAE studies described in Aim 1, with the added benefit of being a more specific and controlled

examination of neuronal changes in response to treatment. In terms of the neuronal viability assay, it has been previously shown that CyPD-KO neurons have greater viability in comparison to WT neurons following treatment with NO and H_2O_2, suggesting that altering PTP regulation increases cellular protection (Baines et al., 2005; Schinzel et al., 2005; Forte et al., 2007). Based on these results and the hypothesized role of p66 in mitochondria and PTP pathways, I anticipated that similar increased survival percentages would be seen in the p66-KO neurons. In addition, assuming the relationship between p66- and CyPD-regulation of the PTP represents a linear pathway, I hypothesized that the corresponding cell viability observed in p66/CyPD-DKO mice would be similar to that of p66-KO and CyPD-KO mice. For the assessment of mitochondrial dynamics following treatment, I anticipated significant preservation of mitochondrial structure and function in the p66-KO neurons as demonstrated by mitochondrial morphology and transport. Interestingly, a recent study demonstrated that changes in mitochondrial morphology preceded observable axonal damage in live imaging studies of EAE-induced mice (Nikic et al., 2011). These results suggest that mitochondrial structure and function are likely affected by neurodegenerative mechanisms of EAE, and by inference, MS, and therefore maintaining mitochondria integrity is essential to axonal preservation. For the assessment of ROS levels in p66-KO and WT cultures following treatment with agents implicated in MS neurodegeneration, I hypothesized that the p66-KO neurons would have lower cellular ROS levels given that p66 is both a ROS sensor and amplifier in a feed-forward signaling pathway mediating ROS production, mitochondrial dysfunction, PTP opening, and cell death activation.

d) Results:

The results for Aim 2 are presented in Chapter IV of this thesis, addressing the enhanced robustness and preservation of mitochondrial integrity in the p66-KO neurons as hypothesized. Work on the p66/CyPD-DKO genotype was briefly addressed in supplemental Chapter III.

Summary

The novel *in vivo* and *in vitro* experiments of my thesis aimed to advance current understanding of MS neurodegenerative pathways that generate progressive, irreversible disability in patients. The obvious lack of neuroprotective MS drugs highlights the need to examine underlying mechanisms leading to axonal and neuronal damage, which I have discussed in detail in this introduction. Ultimately, the overarching goal of my research is to identify potential drug targets for the development of neuroprotective MS treatments.

D. References

Baines CP, Kaiser RA, Purcell NH, Blair NS, Osinska H, Hambleton MA, Brunskill EW, Sayen MR, Gottlieb RA, Dorn GW, Robbins J, Molkentin JD (2005) Loss of cyclophilin D reveals a critical role for mitochondrial permeability transition in cell death. Nature 434:658-662.

Basso E, Fante L, Fowlkes J, Petronilli V, Forte MA, Bernardi P (2005) Properties of the Permeability Transition Pore in Mitochondria Devoid of Cyclophilin D. Journal of Biological Chemistry 280:18558-18561.

Beckman JS, Koppenol WH (1996) Nitric oxide, superoxide, and peroxynitrite: the good, the bad, and ugly. American Journal of Physiology - Cell Physiology 271:C1424-C1437.

Bedard K, Lardy B, Krause K-H (2007) NOX family NADPH oxidases: Not just in mammals. Biochimie 89:1107-1112.

Benarroch EE (2008) N-Acetylaspartate and N-acetylaspartylglutamate. Neurology 70:1353-1357.

Bernardi P, Krauskopf A, Basso E, Petronilli V, Blalchy-Dyson E, Di Lisa F, Forte MA (2006) The mitochondrial permeability transition from in vitro artifact to disease target. FEBS Journal 273:2077-2099.

Bjartmar C, Kinkel RP, Kidd G, Rudick RA, Trapp BD (2001) Axonal loss in normal-appearing white matter in a patient with acute MS. Neurology 57:1248-1252.

Bjartmar C, Wujek JR, Trapp BD (2003) Axonal loss in the pathology of MS: consequences for understanding the progressive phase of the disease. Journal of the neurological sciences 206:165-171.

Bjartmar C, Kidd G, Mörk S, Rudick R, Trapp BD (2000) Neurological disability correlates with spinal cord axonal loss and reduced N-acetyl aspartate in chronic multiple sclerosis patients. Annals of Neurology 48:893-901.

Bjartmar C, Trapp BD (2001) Axonal and neuronal degeneration in multiple sclerosis: mechanisms and functional consequences. Current Opinion in Neurology 14: 271–278.

Bogdan C (2001) Nitric oxide and the immune response. Nat Immunol 2:907-916.

Brown GC, Borutaite V (2001) Nitric Oxide, Mitochondria, and Cell Death. IUBMB Life 52:189-195.

Brown GC, Borutaite V (2002) Nitric oxide inhibition of mitochondrial respiration and its role in cell death. Free Radical Biology and Medicine 33:1440-1450.

Chen H, Chan DC (2006) Critical dependence of neurons on mitochondrial dynamics. Current Opinion in Cell Biology 18:453-459.

Cleeter MWJ, Cooper JM, Darley-Usmar VM, Moncada S, Schapira AHV (1994) Reversible inhibition of cytochrome c oxidase, the terminal enzyme of the mitochondrial respiratory chain, by nitric oxide: Implications for neurodegenerative diseases. FEBS Letters 345:50-54.

Cohen JA, Barkhof F, Comi G, Hartung H-P, Khatri BO, Montalban X, Pelletier J, Capra R, Gallo P, Izquierdo G, Tiel-Wilck K, Vera A de, Jin J, Stites T, Wu S, Aradhye S, Kappos L (2010) Oral Fingolimod or Intramuscular Interferon for Relapsing Multiple Sclerosis. New England Journal of Medicine 362:402-415.

Cosentino F, Francia P, Camici GG, Pelicci PG, Volpe M, Lüscher TF (2008) Final Common Molecular Pathways of Aging and Cardiovascular Disease. Arteriosclerosis, Thrombosis, and Vascular Biology 28:622-628.

Craner MJ, Newcombe J, Black JA, Hartle C, Cuzner ML, Waxman SG (2004) Molecular changes in neurons in multiple sclerosis: Altered axonal expression of Nav1.2 and Nav1.6 sodium channels and Na+/Ca2+ exchanger. Proceedings of the National Academy of Sciences of the United States of America 101:8168-8173.

Cross AH, Manning PT, Keeling RM, Schmidt RE, Misko TP (1998) Peroxynitrite formation within the central nervous system in active multiple sclerosis. Journal of neuroimmunology 88:45-56.

De Jager PL, Hafler DA (2007) New therapeutic approaches for multiple sclerosis. Annual Review of Medicine 58:417-432.

Dutta R, McDonough J, Yin X, Peterson J, Chang A, Torres T, Gudz T, Macklin WB, Lewis DA, Fox RJ, Rudick R, Mirnics K, Trapp BD (2006) Mitochondrial dysfunction as a cause of axonal degeneration in multiple sclerosis patients. Annals of Neurology 59:478-489.

Esposito LA, Melov S, Panov A, Cottrell BA, Wallace DC (1999) Mitochondrial disease in mouse results in increased oxidative stress. Proceedings of the National Academy of Sciences 96:4820-4825.

Forte M, Gold BG, Marracci G, Chaudhary P, Basso E, Johnsen D, Yu X, Fowlkes J, Bernardi P, Bourdette D (2007) Cyclophilin D inactivation protects axons in experimental autoimmune encephalomyelitis, an animal model of multiple sclerosis. Proceedings of the National Academy of Sciences 104:7558-7563.

Friberg H, Ferrand-Drake M, Bengtsson F, Halestrap AP, Wieloch T (1998) Cyclosporin A, But Not FK 506, Protects Mitochondria and Neurons against Hypoglycemic Damage and Implicates the Mitochondrial Permeability Transition in Cell Death. The Journal of Neuroscience 18:5151-5159.

Fu L, Matthews PM, De Stefano N, Worsley KJ, Narayanan S, Francis GS, Antel JP, Wolfson C, Arnold DL (1998) Imaging axonal damage of normal-appearing white matter in multiple sclerosis. Brain 121:103-113.

Gertz M, Fischer F, Leipelt M, Wolters D, Steegborn C (2009) Identification of Peroxiredoxin 1 as a novel interaction partner for the lifespan regulator protein p66Shc. Aging 1:254-265.

Giorgio M, Migliaccio E, Orsini F, Paolucci D, Moroni M, Contursi C, Pelliccia G, Luzi L, Minucci S, Marcaccio M, Pinton P, Rizzuto R, Bernardi P, Paolucci F, Pelicci PG (2005) Electron Transfer between Cytochrome c and p66Shc Generates Reactive Oxygen Species that Trigger Mitochondrial Apoptosis. Cell 122:221-233.

Griffiths EJ, Halestrap AP (1993) Protection by Cyclosporin A of Ischemia/Reperfusion-Induced Damage in Isolated Rat Hearts. Journal of Molecular and Cellular Cardiology 25:1461-1469.

Groom AJ, Smith T, Turski L (2003) Multiple Sclerosis and Glutamate. Annals of the New York Academy of Sciences 993:229-275.

Gunter TE, Sheu SS (2009) Characteristics and possible functions of mitochondrial Ca2+ transport mechanisms. Biochimica et Biophysica Acta (BBA) - Bioenergetics 1787:1291-1308.

Gunter TE, Yule DI, Gunter KK, Eliseev RA, Salter JD (2004) Calcium and mitochondria. FEBS Letters 567:96-102.

Hajnóczky G, Hoek JB (2007) Mitochondrial Longevity Pathways. Science 315:607-609.

Halestrap AP (2009) What is the mitochondrial permeability transition pore? Journal of Molecular and Cellular Cardiology 46:821-831.

Herrero-Herranz E, Pardo LA, Gold R, Linker RA (2008) Pattern of axonal injury in murine myelin oligodendrocyte glycoprotein induced experimental autoimmune encephalomyelitis: Implications for multiple sclerosis. Neurobiology of Disease 30:162-173.

Hollenbeck PJ, Saxton WM (2005) The axonal transport of mitochondria. Journal of Cell Science 118:5411-5419.

Huitinga I, van Rooijen N, de Groot CJ, Uitdehaag BM, Dijkstra CD (1990) Suppression of experimental allergic encephalomyelitis in Lewis rats after elimination of macrophages. The Journal of Experimental Medicine 172:1025-1033.

Ingle GT, Stevenson VL, Miller DH, Thompson AJ (2003) Primary progressive multiple sclerosis: a 5-year clinical and MR study. Brain 126:2528-2536.

Khan O, Shen Y, Caon C, Bao F, Ching W, Reznar M, Buccheister A, Hu J, Latif Z, Tselis A, Lisak R (2005) Axonal metabolic recovery and potential neuroprotective effect of glatiramer acetate in relapsing-remitting multiple sclerosis. Multiple Sclerosis 11:646-651.

Koch OR, Fusco S, Ranieri SC, Maulucci G, Palozza P, Larocca LM, Cravero AAM, Farre SM, De Spirito M, Galeotti T, Pani G (2008) Role of the life span determinant P66shcA in ethanol-induced liver damage. Lab Invest 88:750-760.

Krieger C, Duchen MR (2002) Mitochondria, Ca2+ and neurodegenerative disease. European Journal of Pharmacology 447:177-188.

Kuhlmann T, Lingfeld G, Bitsch A, Schuchardt J, Brück W (2002) Acute axonal damage in multiple sclerosis is most extensive in early disease stages and decreases over time. Brain 125:2202-2212.

Kutzelnigg A, Lucchinetti CF, Stadelmann C, Brück W, Rauschka H, Bergmann M, Schmidbauer M, Parisi JE, Lassmann H (2005) Cortical demyelination and diffuse white matter injury in multiple sclerosis. Brain 128:2705-2712.

Lovas G, Szilágyi N, Majtényi K, Palkovits M, Komoly S (2000) Axonal changes in chronic demyelinated cervical spinal cord plaques. Brain 123:308-317.

Lu F, Selak M, O'Connor J, Croul S, Lorenzana C, Butunoi C, Kalman B (2000) Oxidative damage to mitochondrial DNA and activity of mitochondrial enzymes in chronic active lesions of multiple sclerosis. Journal of the neurological sciences 177:95-103.

Lu Z-H, Chakraborty G, Ledeen RW, Yahya D, Wu G (2004) N-Acetylaspartate synthase is bimodally expressed in microsomes and mitochondria of brain. Molecular Brain Research 122:71-78.

MacAskill AF, Rinholm JE, Twelvetrees AE, Arancibia-Carcamo IL, Muir J, Fransson A, Aspenstrom P, Attwell D, Kittler JT (2009) Miro1 Is a Calcium Sensor for Glutamate Receptor-Dependent Localization of Mitochondria at Synapses. Neuron 61:541-555.

Madesh M, Hajnóczky G (2001) VDAC-dependent permeabilization of the outer mitochondrial membrane by superoxide induces rapid and massive cytochrome c release. The Journal of Cell Biology 155:1003-1016.

Menini S, Amadio L, Oddi G, Ricci C, Pesce C, Pugliese F, Giorgio M, Migliaccio E, Pelicci P, Iacobini C, Pugliese G (2006) Deletion of p66Shc Longevity Gene Protects Against Experimental Diabetic Glomerulopathy by Preventing Diabetes-Induced Oxidative Stress. Diabetes 55:1642-1650.

Migliaccio E, Giorgio M, Mele S, Pelicci G, Reboldi P, Pandolfi PP, Lanfrancone L, Pelicci PG (1999) The p66shc adaptor protein controls oxidative stress response and life span in mammals. Nature 402:309-313.

Migliaccio E, Mele S, Salcini AE, Pelicci G, Lai KM, Superti-Furga G, Pawson T, Di Fiore PP, Lanfrancone L, Pelicci PG (1997) Opposite effects of the p52shc/p46shc and p66shc splicing isoforms on the EGF receptor-MAP kinase-fos signalling pathway. EMBO J 16:706-716.

Morfini GA, You Y-M, Pollema SL, Kaminska A, Liu K, Yoshioka K, Bjorkblom B, Coffey ET, Bagnato C, Han D, Huang C-F, Banker G, Pigino G, Brady ST (2009) Pathogenic huntingtin inhibits fast axonal transport by activating JNK3 and phosphorylating kinesin. Nat Neurosci 12:864-871.

Napoli C, Martin-Padura I, Nigris F de, Giorgio M, Mansueto G, Somma P, Condorelli M, Sica G, De Rosa G, Pelicci P (2003) Deletion of the p66Shc longevity gene reduces systemic and tissue oxidative stress, vascular cell apoptosis, and early atherogenesis in mice fed a high-fat diet. Proceedings of the National Academy of Sciences 100:2112-2116.

Nicolli A, Basso E, Petronilli V, Wenger RM, Bernardi P (1996) Interactions of Cyclophilin with the Mitochondrial Inner Membrane and Regulation of the Permeability Transition Pore, a Cyclosporin A-sensitive Channel. Journal of Biological Chemistry 271:2185-2192.

Nikic I, Merkler D, Sorbara C, Brinkoetter M, Kreutzfeldt M, Bareyre FM, Bruck W, Bishop D, Misgeld T, Kerschensteiner M (2011) A reversible form of axon damage in experimental autoimmune encephalomyelitis and multiple sclerosis. Nat Med 17:495-499.

Nikolaev A, McLaughlin T, O/□Leary DDM, Tessier-Lavigne M (2009) APP binds DR6 to trigger axon pruning and neuron death via distinct caspases. Nature 457:981-989.

Noseworthy JH, Lucchinetti C, Rodriguez M, Weinshenker BG (2000) Multiple Sclerosis. New England Journal of Medicine 343:938-952.

Pacher P, Beckman JS, Liaudet L (2007) Nitric Oxide and Peroxynitrite in Health and Disease. Physiological Reviews 87:315-424.

Petronilli V, Nicolli A, Costantini P, Colonna R, Bernardi P (1994) Regulation of the permeability transition pore, a voltage-dependent mitochondrial channel inhibited by cyclosporin A. Biochimica et Biophysica Acta (BBA) - Bioenergetics 1187:255-259.

Pinton P, Rimessi A, Marchi S, Orsini F, Migliaccio E, Giorgio M, Contursi C, Minucci S, Mantovani F, Wieckowski MR, Del Sal G, Pelicci PG, Rizzuto R (2007) Protein Kinase C ß and Prolyl Isomerase 1 Regulate Mitochondrial Effects of the Life-Span Determinant p66Shc. Science 315:659-663.

Rintoul GL, Bennett VJ, Papaconstandinou NA, Reynolds IJ (2006) Nitric oxide inhibits mitochondrial movement in forebrain neurons associated with disruption of mitochondrial membrane potential. Journal of Neurochemistry 97:800-806.

Saotome M, Safiulina D, Szabadkai G, Das S, Fransson Å, Aspenstrom P, Rizzuto R, Hajnóczky G (2008) Bidirectional Ca2+-dependent control of mitochondrial dynamics by the Miro GTPase. Proceedings of the National Academy of Sciences 105:20728-20733.

Schinzel AC, Takeuchi O, Huang Z, Fisher JK, Zhou Z, Rubens J, Hetz C, Danial NN, Moskowitz MA, Korsmeyer SJ (2005) Cyclophilin D is a component of mitochondrial permeability transition and mediates neuronal cell death after focal cerebral ischemia.

Proceedings of the National Academy of Sciences of the United States of America 102:12005-12010.

Schmidt S (1999) Candidate autoantigens in multiple sclerosis. Multiple Sclerosis 5:147-160.

Signoretti S, Marmarou A, Tavazzi B, Lazzarino G, Beaumont A, Vagnozzi R (2001) N-Acetylaspartate Reduction as a Measure of Injury Severity and Mitochondrial Dysfunction Following Diffuse Traumatic Brain Injury. Journal of Neurotrauma 18:977-991.

Smith WW, Norton DD, Gorospe M, Jiang H, Nemoto S, Holbrook NJ, Finkel T, Kusiak JW (2005) Phosphorylation of p66Shc and forkhead proteins mediates Aβ toxicity. The Journal of Cell Biology 169:331-339.

Srinivasan R, Sailasuta N, Hurd R, Nelson S, Pelletier D (2005) Evidence of elevated glutamate in multiple sclerosis using magnetic resonance spectroscopy at 3 T. Brain 128:1016-1025.

Stagi M, Gorlovoy P, Larionov S, Takahashi K, Neumann H (2006) Unloading kinesin transported cargoes from the tubulin track via the inflammatory c-Jun N-terminal kinase pathway. The FASEB Journal 20:2573-2575.

Stys PK, Waxman SG, Ransom BR (1992) Ionic mechanisms of anoxic injury in mammalian CNS white matter: role of Na+ channels and Na(+)-Ca2+ exchanger. The Journal of Neuroscience 12:430-439.

Su K, Banker G, Bourdette D, Forte M (2009) Axonal degeneration in multiple sclerosis: The mitochondrial hypothesis. Current Neurology and Neuroscience Reports 9:411-417.

Trapp BD, Peterson J, Ransohoff RM, Rudick R, Mörk S, Bö L (1998) Axonal Transection in the Lesions of Multiple Sclerosis. New England Journal of Medicine 338:278-285.

Trinei M, Giorgio M, Cicalese A, Barozzi S, Ventura A, Migliaccio E, et al. (2001) A p53-p66Shc signalling pathway controls intracellular redox status, levels of oxidation-damaged DNA and oxidative stress-induced apoptosis. Oncogene 21:3872-3878.

Turrens JF (2003) Mitochondrial formation of reactive oxygen species. The Journal of Physiology 552:335-344.

Wang X, Schwarz TL (2009) The Mechanism of Ca2+-Dependent Regulation of Kinesin-Mediated Mitochondrial Motility. Cell 136:163-174.

Witt A, Brady ST (2000) Unwrapping new layers of complexity in axon/glial relationships. Glia 29:112-117.

CHAPTER II

(Submitted as a manuscript for publication in the European Journal of Neuroscience)

p66ShcA inactivation provides axonal and neuronal protection in a murine model of multiple sclerosis

I. **Abstract**

Although multiple sclerosis (MS) has traditionally been considered an inflammatory disease, recent evidence has brought neurodegeneration into the spotlight, suggesting that accumulated damage and loss of axons is critical to disease progression and associated irreversible disability. Proposed mechanisms of axonal degeneration in MS posit cytosolic and subsequent mitochondrial Ca^{2+} overload, accumulation of pathologic reactive oxygen species (ROS), and mitochondrial dysfunction leading to cell death. In this context, the role of protein p66ShcA (p66) may be significant. The ShcA isoform is uniquely targeted to the mitochondrial intermembrane space in response to elevated oxidative stress, and serves as a redox enzyme amplifying ROS generation in a positive feed-forward loop that eventually mediates cell death by activation of the mitochondrial permeability transition pore (PTP). Consequently, we tested the hypothesis that genetic inactivation of p66 would reduce axonal injury in a murine model of MS, experimental autoimmune encephalomyelitis (EAE). As predicted, the p66-KO mice developed typical signs of EAE, but had less severe clinical impairment and paralysis compared to WT mice. Histologic examination of spinal cords and optic nerves showed significant axonal protection in the p66-KO tissue despite similar levels of inflammation. Furthermore, cultured p66-KO neurons treated with agents implicated in MS neurodegenerative

pathways showed greater viability compared to WT neurons. These results confirm the critical role of ROS-mediated mitochondrial dysfunction in the axonal loss that accompanies EAE and identify p66 as a new pharmacologic target for MS neuroprotective therapeutics.

II. Introduction

Multiple sclerosis (MS) is the most common chronic inflammatory disease of the central nervous system (CNS) affecting more than 2 million people worldwide (Noseworthy et al., 2000). Pathologic immune responses have long been viewed as the primary mediator of MS, leading to the development of anti-inflammatory drugs moderately successful in treating relapsing-remitting forms of the disease (Lublin, 2005). Unfortunately, these drugs have minimal impact on neurodegeneration that is now believed to contribute to the permanent disability associated with progressive forms of MS. Effective treatment for progressive MS will likely require neuroprotective therapies targeting the underlying mechanisms of axonal degeneration.

Growing evidence suggests that MS neurodegeneration revolves around mitochondrial dysfunction (Dutta et al., 2006; Mahad et al., 2008). Various pathways leading to such dysfunction have been proposed, which all at some level postulate pathologic opening of the permeability transition pore (PTP) located in the inner mitochondrial membrane (Su et al., 2009). Specifically, mitochondrial Ca^{2+} overload and pathologic ROS generation opens the PTP, and persistent opening can initiate detrimental disruption of mitochondrial structure and function and induce cell death (Bernardi et al., 2006). Accordingly, we, and others, have suggested that PTP activation

potentially mediates neurodegeneration in MS and other neurologic diseases (Rasola and Bernardi, 2007; Forte et al., 2007).

While the structure of the PTP is poorly understood, there is solid evidence that the mitochondrial matrix protein cyclophilin D (CyPD) plays a crucial regulatory role for the pore (Baines et al., 2005; Basso et al., 2005). CyPD inhibition by pharmacologic and genetic techniques is protective in disease models of ischemic and traumatic brain injury as well as various human neurodegenerative conditions (Schinzel et al., 2005). In particular, CyPD inhibition was shown to be neuroprotective in the murine MS model experimental autoimmune encephalomyelitis (EAE) (Forte et al., 2007). CyPD-knockout (CyPD-KO) mice showed significant clinical improvement following the development of paralysis unlike the wild type (WT) mice. Furthermore, there was decreased axonal damage and loss in the CyPD-KO spinal cords despite similar levels of inflammatory cells compared to the WT mice. These results support the hypothesis that modulation of PTP opening may protect axons from injury in EAE.

Additional physiologic triggers of PTP opening include ROS exposure, and accordingly, the ShcA isoform p66 has been proposed as a potential upstream pore modulator (Migliaccio et al., 1999). In the presence of pathologic ROS levels, p66 is uniquely targeted to the mitochondrial intermembrane space by protein kinase Cβ (PKCβ)-mediated serine phosphorylation (Pinton et al., 2007). There, it serves as a redox enzyme by oxidizing cytochrome c and reducing oxygen to form ROS including superoxide and hydrogen peroxide (Giorgio et al., 2005). This source of mitochondrial ROS constitutes a positive feed-forward loop that is thought to induce pathologic PTP

opening leading to mitochondrial dysfunction and eventual cell death. Several groups have shown that p66 inhibition confers protection to oxidative stress in various experimental contexts and disease models (Migliaccio et al., 1999; Camici et al., 2007). Based on this information, we tested the hypothesis that p66-KO mice would demonstrate axonal preservation following EAE induction.

III. Materials and methods

Animals

p66-KO, CyPD-KO, p66/CyPD double knockout (p66/CyPD-DKO) mice and WT controls were maintained as homozygotes in a C57BL/6 background (Migliaccio et al., 1999). All experimental procedures were conducted following NIH guidelines under an Institutional Animal Care and Use Committee-approved protocol from the Oregon Health & Science University.

Western blots of nervous tissue and neurons

Expression of p66 was examined in lysates prepared from brain cortices and hippocampal neurons. Lysates were immunoprecipitated with anti-Shc antibody (BD Biosciences, San Jose, CA) on precleared protein G beads, and examined by immunoblot analysis using the BG8 monoclonal anti-p66Shc antibody (Orsini et al., 2004). Membranes were stripped and re-probed to detect beta-tubulin as a protein loading control.

EAE immunization and clinical scoring

Isogenic 10-12 week-old female mice (Taconic Farms, Germantown, NY) were immunized by subcutaneous injection with myelin oligodendrocyte glycoprotein (MOG) 35-55 peptide (200 μg) in complete Freund's adjuvant containing *M. tuberculosis* (400 μg) per mouse. Pertussis toxin was administered intraperitoneally following immunization (75 ng/mouse) and again 48 hours later (200 ng/mouse). Mice were scored daily for EAE by using a 9-point scale [0, no paralysis; 1, limp tail with minimal hind limb weakness (easily flipped onto their backs with a twist of the tail but able to easily right themselves); 2, mild hind limb weakness (difficulty righting themselves after being flipped on their back); 3, moderate hind limb weakness (able to walk with no difficulty but unable to right themselves after being flipped on their backs); 4, moderately severe hind limb weakness (difficulty walking upright); 5, severe hind limb weakness (unable to walk upright but still able to move hindlimbs); 6, complete hind limb paralysis (no voluntary leg movement); 7, hind limb paralysis with mild forelimb weakness (walks with chest close to the ground); 8, hind limb paralysis with moderate forelimb weakness (unable to lift chest off the ground but can move around cages with difficulty); and 9, hind paralysis with severe forelimb weakness (unable to place forelimbs under chest and unable to move around cage)] (Marracci et al., 2002; Forte et al., 2007). Scoring was performed blinded to genotype. After 36 days of clinical assessment, the mice were deeply anesthetized with isoflurane, heparinized, and perfused with ice-cold 4% paraformaldehyde. Spinal cords and optic nerves were dissected out the following day for processing, sectioning, and analysis (see details below). For the representative p66-KO and WT experiment reported in the results, 8

p66-KO mice and 18 WT mice were immunized and analyzed for clinical EAE. All mice with EAE were perfused for further histologic analyses along with 3 naïve mice per genotype. For the single and double mutant comparative experiment, 7 p66-KO, 15 CyPD-KO, and 8 p66/CyPD-DKO mice were immunized and assessed along with 3 naïve mice per genotype.

Quantitative morphologic analysis of percent white matter tissue damage

Thoracic spinal cord white matter

Thoracic spinal cord blocks were immersed in 5% glutaraldehyde for 3 days and post-fixed with 1% osmium tetroxide. Semithin sections (0.5 μm) were stained with toluidine blue and photographed at 20X magnification to create photomontages of the spinal cord cross-sections. One cross-section photomontage was generated per mouse. Quantification of the percentage of white matter tissue damage in the ventrolateral region was determined by manually marking the photomontages (digitally magnified on monitor to 40X) utilizing Image J software. Total ventrolateral area was determined by circling the entire ventrolateral region of the thoracic spinal cord cross section. Marked damage included areas devoid of axons or areas containing swollen axons, degenerating axons, demyelinated axons, irregularly myelinated axons, myelin ovoids, or microcysts. The percentage of area damaged in the ventrolateral region for each thoracic section was determined using the following formula: (total marked damaged area)/(total ventrolateral area) x 100. All analyses were done blinded to genotype.

Optic nerve

Optic nerves were immersed in 5% glutaraldehyde overnight and post-fixed with 1% osmium tetroxide. Semithin sections (0.5 μm) were stained with toluidine blue and photographed at 100X magnification to create photomontages of the optic nerve cross-sections. One cross-section photomontage was generated for each mouse. The percentage of area damaged was quantified by manually marking the photomontages at 100X utilizing Image J software. The total cross-sectional area was determined by outlining the entire optic nerve, and damage was manually marked based on the same criteria described for the spinal cord white matter. The percentage of area damaged for each optic nerve section was determined by the following formula: (total marked damaged area)/(total cross-sectional area) x 100. All analyses were done blinded to genotype.

Axonal count of thoracic spinal cord ventrolateral white matter

For each plastic-embedded, toluidine blue-stained spinal cord section, a total of 8 images (4 on either side of the cord midline) were taken of the ventrolateral white matter at 20X magnification. The area of each image was 344 x 258 μM^2. Utilizing Metamorph software (Molecular Devices, CA), each image was first thresholded to maximize the number of axon cross-sections highlighted. Next, the integrated morphometry analysis measurement parameters of area, shape factor, and elliptical form factor were applied to the thresholded regions to generate an initial axon count for the image. False positive axons and highlighted damaged axons were manually subtracted from this initial axon count to determine the final axon count for the image. All analyses were done blinded to genotype.

Electron microscopy

Ultrathin plastic embedded thoracic spinal cord and optic nerve sections (70 nm) were collected on copper grids and stained with uranyl acetate and lead citrate. Stained sections were examined at 4800x and 9300x using a JEOL or an FEI Tecnai 12 electron microscope, and images were captured using a digital camera (Advanced Microscopy Techniques (AMT) Corporation, Danvers, MA, USA). All analyses were done blinded to genotype.

Analysis of immune cell infiltration

Lumbar spinal cord

Spinal cord blocks were embedded in 3% agarose and sectioned (50μm) using a Leica Vibratome (Leica Microsystems, Nussloch, Germany). Three sections from each lumbar spinal cord region were randomly selected for antibody staining. Sections were permeabilized, washed, and blocked (0.5% fish skin gelatin/3% BSA in PBS), and then incubated with primary antibody at 4°C overnight. Primary anti-CD4 antibody (PharMingen, San Diego, CA) was used to identify T cells, and anti-CD11b (Leinco Technologies, St. Louis, MO) was used as a microglial/macrophage marker. The following day, the sections were washed and incubated in secondary Alexa Fluor 488 conjugated donkey anti-rat IgG (Invitrogen, Carlsbad, CA) at room temperature for 1.5 hours. Following a final wash, the sections were mounted on slides in Prolong Gold Antifade, and imaged using a laser scanning Zeiss LSM710 confocal microscope (LSM-710, Carl Zeiss, Göttingen, Germany). Four images of each lumbar section (dorsal,

ventral, and two lateral regions) were photographed at 40X. Two sections were photographed per mouse. Data analyses were performed using Metamorph software (Molecular Devices, CA). The amount of fluorescence per image was determined by generating the percent threshold area, and the average background fluorescence was accounted for by analyzing the negative controls, which included sections from naïve and EAE-induced mice incubated with primary antibody only, secondary antibody only, or neither antibody. All analyses were done blinded to genotype.

Optic nerves

Optic nerves were sectioned, stained and mounted in the same manner as the lumbar spinal cords. Entire stained sections were imaged at 40x by confocal microscopy. Quantification of CD4 and CD11b fluorescence per section was carried out by determining the threshold percentage for a standard area of about 20,000 μM^2. All analyses were done blinded to genotype.

Proliferation and cytokine studies

WT and p66-KO 10-12 week old female mice were immunized with MOG 35-55 peptide as described above to induce EAE. At ten days post-immunization, the mice were euthanized by CO_2 inhalation and inguinal lymph nodes (LN) were harvested to establish cell cultures following previously described methods (Marracci et al. 2002). LN

cultures were incubated with IL-2, MOG 35-55 peptide (25μg/mL) or media. The data reported reflects two independent experiments (n of 5 mice/genotype per experiment).

Cytokine assay

After 48 hours of incubation at 37°C, LN culture supernatants were collected and frozen at -80°C until used for cytokine assays. The Luminex Bio-Plex mouse cytokine assay kit (Bio-Rad, Hercules, CA) was used to analyze the following cytokines per manufacturer's protocol: IL-2, IL-4, IL-6, IL-10, IL-17, IFN-gamma, and TNF-alpha.

Proliferation assay

After 48 hours of incubation at 37°C, LN cells were labeled with [^{3}H] thymidine and returned to the incubator for 18 hours. The cells were then harvested onto glass fiber filtermats and assessed for uptake of the labeled thymidine by liquid scintillation per manufacturer's protocol (Perkin Elmer-Wallac, Waltham, MA).

In vitro neuronal culture studies

Cortical neurons were obtained from dissected brains of WT and p66-KO animals as previously outlined (Barsukova et al., 2011). Immunocytochemical analysis indicated that the majority of cells in these adult preparations (>70%) were neurons with characteristic morphology. The cells were counted, resuspended in culture medium [B27/Neurobasal A medium/0.5 mM glutamine (Invitrogen, Carlsbad, CA) supplemented with 50 mg/L gentamicin (Sigma, St. Louis, MO)] and seeded at high density into 24 well plates pre-coated overnight with 10 μg/mL poly-d-lysine (Sigma, St. Louis, MO). The neuronal cultures were maintained for one week before experimental manipulation.

Prior to treatment with either diethylenetriamine/nitric oxide adduct (DETA-NO) or H_2O_2 (Sigma, St. Louis, MO), the cells were washed with Neurobasal A medium/0.5 mM glutamine. Half of the 24 wells were designated control wells and treated with Neurobasal A medium/0.5 mM glutamine. The other half were designated treatment wells and treated with either 500 µM DETA-NO or 200 µM H_2O_2. Following a treatment period of 15 minutes in a 37 °C incubator, the cells were washed twice in Neurobasal A medium/0.5 mM glutamine and returned to the incubator in fresh culture medium. Neuronal viability was assessed 24 hours later by incubating the cells in Calcein AM (AnaSpec, San Jose, CA) and manually counting live neurons based on morphologic appearance and presence of green fluorescent dye at 20X with a fluorescence inverted microscope. Four random areas were counted per well, for a total of 48 random areas counted per treatment or control group per plate. The cell viability percentage was calculated per plate as follows: live cell count in treatment group/live cell count in control group x 100. All analyses were done blinded to genotype.

Statistics

All statistical comparisons between the p66-KO and WT groups were calculated using the nonparametric Mann-Whitney U test. Statistical comparison among p66-KO, CyPD-KO, and p66/CyPD-DKO mice was calculated using the one-way ANOVA for 3 independent samples. Statistical significance was defined as $p<0.05$.

IV. Results

p66 expression in WT and p66-KO nervous tissue and neurons

Three protein isoforms, p46, p52, and p66, are generated from the mammalian *ShcA* locus and share common phosphotyrosine-binding (PTB), Src homology 2 (SH2) and collagen homology (CH1) domains (Migliaccio et al., 1999). The p46 and p52 isoforms participate in the transduction of signals from activated tyrosine kinases at the plasma membrane. In comparison, the p66 isoform contains a N-terminal extension that includes unique CH2 and cytochrome c-binding domains as well as an atypical mitochondrial targeting sequence. Consequently, up to 40% of p66 is localized to mitochondria (Orsini et al., 2004; Nemoto et al., 2006). Cellular ROS exposure results in the stimulation of p66 expression and the stabilization of existing p66. Newly formed p66 is phosphorylated by PKCβ in the cytosol, which allows for conformational modification by the prolyl isomerase PIN1 (Pinton et al., 2007). Modified p66 is then translocated into the mitochondrial intermembrane space to supplement existing levels of mitochondrial p66. Following dephosphorylation within the intermembrane space, p66 functions as a redox enzyme interacting with cytochrome c to amplify ROS levels that generate a positive feed-forward loop (Giorgio et al., 2005; Gertz and Steegborn, 2010a).

Since the mammalian *ShcA* gene encodes two mRNA species via alternate translation start sites specific for p66 and p46/p52, it has been possible to generate mice exclusively missing p66 while retaining expression of the two other isoforms. While p66 expression has already been demonstrated in neuronal cell lines from different mammalian species (Smith et al., 2005; Giorgio et al., unpublished), we initially

confirmed p66 expression and elimination in the nervous tissue and neurons of the animals used in the present study. Immunoblot analyses of lysates prepared from p66-KO and WT mouse brain cortices and hippocampal neurons (*Figure 1*) demonstrated p66 expression in lysates prepared from WT animals and the absence of p66 in lysates prepared from p66-KO animals.

p66 elimination protects axons in EAE

Our previous work on CyPD-KO mice showed significant axonal protection following EAE induction (Forte et al., 2007), suggesting that regulation of the PTP and mitochondria-directed cell death may be key to preventing degenerative pathways. If p66 lies upstream of PTP activation and thereby mediates cell death via mitochondrial ROS generation, one would expect the elimination of p66 to confer similar protection in mice with EAE. To test this hypothesis, we assessed clinical severity and extent of axonal damage following EAE induction in p66-KO mice compared to WT mice. Subsequent to immunization with MOG 35-55 peptide, both WT and p66-KO mice developed clinical signs of EAE. However, the p66-KO mice exhibited less severe clinical disease compared to the WT mice. Throughout the entire 36-day observation period, the p66-KO mice had consistently lower mean EAE scores compared to the WT mice. Furthermore, at the end of this period, the p66-KO mice had significantly lower mean EAE scores (p66-KO 2.2$\pm$0.6, WT 3.6$\pm$0.5; *z= 1.80556; p=0.035*), reflecting the consistent trend of reduced clinical impairment *(Figure 2)*.

Following the 36-day observation period, spinal cords and optic nerves were collected for histologic analyses, including the quantification of tissue damage. EAE-

induced tissue damage in C57BL/6 mice typically manifests as degenerating axons and reduced axonal density and is particularly prominent in the ventrolateral spinal cord white matter. Accordingly, we assessed tissue integrity in plastic-embedded thoracic spinal cord sections stained with toluidine blue. Analysis of ventrolateral thoracic spinal cord white matter showed significantly less damage in the p66-KO mice compared to the WT mice. The WT mice had a mean damaged area of 21.9±2.3%, exhibiting prominent pathological changes including swollen axons, degenerating axons, demyelinated axons, irregularly myelinated axons, myelin ovoids, microcysts, and areas devoid of axons. By comparison, the p66-KO mice showed significantly less damage with a mean damaged area of 12.7±2.6%, indicating a 42% reduction in ventrolateral white matter damage (*z= 2.38889; p=0.008*) *(Figure 3A-C)*.

To further analyze the effects of p66 elimination on axonal integrity, an axonal count was performed in a sampling of images taken of toluidine blue-stained thoracic spinal cord sections. Unlike the results reported above, which assessed total tissue damage within the entire ventrolateral region including degenerating axons, demyelinated axons, and areas devoid of axons, this analysis focused on counting the number of intact axons within a sample area of the white matter region. The results indicated that within each sampled image (344 μm x 258 μm), the average axon count was 4719.89±158 for the p66-KO mice compared to 4352.84±99 for the WT mice. This difference was found to be statistically significant (*z=1.74471; p=0.041*), suggesting that p66 elimination preserves white matter in mice with EAE by limiting the extent of generalized tissue damage as well as preserving the number of intact axons.

Given the proposed connection between mitochondrial p66-generated ROS and PTP activation, we also assessed the stability of spinal cord axons by the approaches outlined above in p66/CyPD double mutant mice lacking both p66 and CyPD. We found no significant differences in their clinical presentation of EAE ($F_{2,30}$= *0.4873; p=0.62*) and in the amount of ventrolateral damage in the double mutants as compared to either single mutant. The p66-KO mice had a mean of 13.2±2.9% damage in the spinal cord, compared to 15.7±1.2% for the CyPD-KO mice, and 11.8±1.5% for the p66/CyPD-DKO mice ($F_{2,27}$*=1.52; p=0.237*).

In addition, most C57BL/6 mice with EAE also have inflammation and axonal degeneration in their optic nerves similar to optic neuritis seen in patients with MS (Chaudhary et al., 2011). Optic nerves stained with toluidine blue were assessed for axonal injury and were found to be protected in the p66-KO mice in a similar manner to that shown in the spinal cords. There was a significant 38% reduction in damage observed in the optic nerves of p66-KO mice as compared to WT mice (p66-KO 23.4±3.1%, WT 37.5±3.6%; *z=2.79625*; *p=0.0026)* (*Figure 3D-F).*

Finally, to capture a magnified depiction of the axonal protection observed in the thoracic spinal cords and optic nerves, electron microscopy was performed on ultra-thin plastic toluidine blue-stained tissue sections. As shown in Figure 4, there was a striking contrast in axonal morphology between the p66-KO and WT sections. In particular, the WT sections had multiple axons with noticeably abnormal structural characteristics including myelin ovoids without discernible axons and large swollen axons containing

membranous debris. Similar structural abnormalities were found in the electron microscopic analysis of optic nerve sections.

Overall, the results from our multidimensional analysis of axonal integrity in p66-KO and WT mice with EAE indicate significant neuroprotection associated with p66 elimination. Tissue and axonal preservation was apparent in CNS regions relevant to MS pathology, including the optic nerves that are commonly symptomatic and damaged in MS patients. These findings are consistent with the hypothesis that p66 operates upstream of PTP activation in MS degenerative disease processes.

EAE immune cell infiltration is similar in WT and p66-KO mice

The development of EAE in the C57BL/6 mouse background is dependent on the activation of CD4+ T cells and CD11b+ macrophages/microglia in the CNS following MOG 35-55 peptide immunization. Therefore, it is possible that the reduction in axonal damage observed in the p66-KO mice might have reflected a dampened immune response to the MOG-induced EAE. To investigate this possibility, the infiltration of immune cells within the spinal cord and optic nerve tissue was assessed.

Lumbar spinal cord sections were immunostained for inflammatory cells using anti-CD4 and anti-CD11b to identify T cells and microglia/macrophages, respectively. As expected, elevated CD4 and CD11b immunofluorescence levels were observed in both p66-KO and WT mice compared to naïve non-immunized controls of both genotypes. Analysis of fluorescence levels by percent threshold area showed no statistically significant difference in CD4 staining between p66-KO and WT mice (p66-KO

1.006±0.087%, WT 1.043±0.094; z=1.44656; p=0.074). In addition, CD11b staining was similar between p66-KO and WT mice with EAE (p66-KO 9.348±0.800%, WT 8.656±0.490%; z=0.411164; p=0.340) *(Figure 5A-D).*

Immune cell infiltration was also assessed in optic nerves by CD4 and CD11b staining. Similar to the results in the lumbar spinal cords, the optic nerves of p66-KO and WT mice had elevated CD4+ T cell and CD11b+ macrophage/microglia infiltration compared to the naïve non-immunized controls of both genotypes. Importantly, as in lumbar spinal cords, no significant difference was observed in immune cell staining between the p66-KO and WT mice for neither CD4 (p66-KO 1.043±0.139%, WT 0.921±0.102%; %; z = 0.810163; p=0.209) nor CD11b (p66-KO 21.760±1.346%, WT 20.685±1.268%; z = 0.634243; p=0.263) *(Figure 5E-H).*

Overall, a comparable inflammatory response in the two genotypes was shown in the spinal cord and optic nerve sections. This suggests that the axonal protection observed in the p66-KO mice was not primarily due to a reduced immune response to the MOG peptide immunization subsequent to the elimination of p66.

p66-KO and WT T-cells proliferate similarly in response to MOG 35-55 peptide

To further compare the immune response between the p66-KO and WT mice, particularly during the early phases of EAE, T cell proliferation studies were carried out on mice immunized with MOG 35-55 peptide 10 days following induction of EAE using the standard protocol. The results indicated no significant difference in proliferative responses between the p66-KO and WT groups, which exhibited similar stimulation

indexes (stimulated/unstimulated) for the positive control IL-2 (p66-KO 18.14±0.02, WT 18.04±3.97; z=0.960769; p=0.168) and MOG 35-55 peptide (p66-KO 4.65±1.61, WT 4.35±3.28; z=0; p=0.500) (*Figure 6*). The comparable T cell proliferation between the p66-KO and WT lymph node cultures confirms a similar response to the EAE immunization as shown by immunohistochemical staining for CD4+ T-cells (*Figure 5*). Moreover, these results suggest that immunoreactivity and infiltration capacity is unaltered between the early (day 10) and late stages (day 36) of EAE. These results further indicate that the neuroprotection shown in the p66-KO mice is not attributable to significant differences in T-cell responses to MOG 35-55 peptide.

Activated p66-KO and WT T-cells produce similar cytokine levels

A final comparative analysis of cytokine levels produced by p66-KO and WT lymph node cultures stimulated with MOG 35-55 peptide indicated no significant differences, further supporting the aforementioned results of similar immunoreactivity during the EAE induction period. Specifically, measured levels of proinflammatory Th1 (TNF-alpha, IFN-gamma), Th2 (IL-4, IL-10), and Th17 (IL-17) cytokine levels were not found to be significantly different between the two genotypes *(Table 1a-c).* Overall, the cytokine levels detected following MOG 35-55 activation of lymph node cultures from immunized mice provided further confirmation that T-cell immunoreactivity was similar between the p66-KO and WT mice at an early stage of EAE.

Isolated p66-KO neurons are protected in the presence of agents implicated in MS neurodegenerative pathways

Pathologic levels of reactive oxygen and nitrogen species are proposed to mediate mitochondrial dysfunction and ensuing axonal damage in EAE and MS neurodegenerative pathways (Su et al., 2009). Accordingly, we examined the potential protective effects of p66 elimination in neurons by utilizing a controlled *in vitro* neuronal culture system and treatment application of either 500μM DETA-NO or 200 μM H_2O_2. Our results showed that p66-KO cortical neuronal cultures had significantly greater resistance to both treatments compared to the WT neuronal cultures *(Figure 7)*. The results are consistent with the hypothesis that the axonal protection observed in p66-KO mice with EAE is due to enhanced protection from inflammatory mediators of axonal damage via modulated mitochondrial ROS production.

V. Discussion

In this report, we demonstrated that induction of EAE in p66-KO mice resulted in less severe clinical disease compared to WT mice. While the clinical protection may not be as robust as our previous studies in CyPD-KO mice (Forte et al., 2007), it is important to note that clinical EAE is largely reflective of the inflammatory response to MOG peptide immunization rather than the extent of axonal damage (Wujek JR et al., 2002). Similarly, in MS, early clinical signs include increased weakness, paralysis, visual impairment, and other disabilities, which are more often due to an active inflammatory attack on the nervous system (Steinman L, 2001). Therefore, histologic analysis of spinal cord and optic nerve tissue from mice with EAE is a better gauge of the potential neuroprotective effects incurred by p66-KO mice. Our results demonstrated a significant reduction in axonal degeneration from both spinal cord and optic nerve

tissue. Increased viability *in vitro* of p66-KO neuronal cultures following incubation with EAE- and MS-associated neurodegenerative agents (i.e., NO, H_2O_2) further confirmed the protective effects acquired by loss of p66. In addition, we demonstrated that axonal protection was not attributable to altered MOG 35-55 peptide immunoreactivity and reduced CNS inflammation following EAE induction. Given that p66 is a mediator of PTP opening and cell death via mitochondrial ROS generation, these findings provide further support for our hypothesis that PTP activation is critical to axonal degeneration in EAE, and by implication, MS (Forte et al., 2007). Our results establish the importance of p66 in mediating axonal injury in EAE and are the first to examine the role of p66 and the significance of its absence in a murine model of a human neurologic disorder.

The experiments reported here focus on the p66 ShcA isoform as part of a signaling network that contributes to stress responses, lifespan regulation, and aging through its role of ROS generation within the mitochondrial intermembrane space. Various studies, primarily those using isolated mitochondrial preparations, have supported a model in which a "ROS stress-sensing complex" keeps p66 inactive as long as stress levels remain moderate (Gertz and Steegborn, 2010b). However, under conditions of increased cellular stress as accompanies ischemia and many neurological diseases, including MS, p66 has been proposed to function in a positive feed-forward loop by oxidizing cytochrome c and reducing oxygen to form ROS, which then trigger the initiation of mitochondrial dysfunction and PTP-dependent cell death. Consequently, our results are consistent with the concept that the PTP may constitute the immediate downstream target of mitochondrial p66 action in cell death pathways, and similarly are consistent

with the recent demonstration that superoxide may be one of the key triggers for PTP opening *in situ* (Wang et al., 2008). Furthermore, p66-KO mice have been shown to be resistant to cell death resulting from a number of stresses (ex: UV, ROS) and notably exhibit a 30% increase in lifespan (Migliaccio et al., 1999).

The impact of p66 action on mitochondria-mediated cell death and neurodegenerative mechanisms likely goes beyond MS and extends to other neurodegenerative conditions such as stroke, Alzheimer's disease (AD), and amyotrophic lateral sclerosis (ALS). Evidence suggests that these diseases progress in part due to deleterious effects on mitochondrial function, including disruption of the electron transport chain, excessive ROS production, altered mitochondrial homeostasis, and pathologic PTP opening (Lin and Beal, 2006; Su et al., 2009). In particular, CyPD-KO mice demonstrate that repression of PTP activation confers protection in ALS (Martin et al., 2009), AD (Du et al., 2008), and stroke (Schinzel et al., 2005) as well as MS. Furthermore, amyloid β-peptide modulation of p66 serine phosphorylation and apoptosis in SH-SY5Y human neuroblastoma and other neuronal cell lines suggests that p66 may play a significant role in AD neurodegeneration (Smith et al., 2005).

Our work emphasizes the importance of identifying pharmacologic targets that can modulate the mitochondrial PTP, such as CyPD, and in this study, p66, for the development of neuroprotective treatments for MS and potentially other neurodegenerative diseases. Currently, mitochondria-directed therapies are still in their infancy, largely limited to *in vitro* and *in vivo* animal studies to test their properties and efficacy, although a few are now being investigated in human clinical trials. They span a

wide range of mitochondria-specific targets including the electron transport chain, ATP synthase, mitochondrial ROS, and the PTP (Camara et al., 2009; Moreira et al., 2010). The effectiveness of these mitochondria-targeted drugs in treating MS will depend on multiple factors, including the ability of the drug to accumulate within the CNS and to achieve therapeutic levels within mitochondria. Unlike many other organ systems, CNS drug delivery can be difficult due to the restrictive blood brain barrier. Cyclosporin A and its non-immunosuppressive derivatives, for instance, are highly effective in blocking the PTP, but are limited in their effectiveness as neuroprotectants due to poor CNS penetration (Begley et al., 1990). Therefore, drug modification and utilization of barrier-permeable delivery vehicles may need to be taken into consideration. In addition, drug accumulation within the mitochondria will be crucial to drug design and potential effectiveness.

In summary, we have provided novel evidence pinpointing p66 as a neuroprotective target in the MS disease model EAE. As we gain a better understanding of this redox enzyme and its role as a mitochondria-targeted signaling molecule mediating cell death, it may prove to be an ideal drug target in the development of neuroprotective treatments not only for MS, but for other neurodegenerative diseases as well.

VI. References:

Baines CP, Kaiser RA, Purcell NH, Blair NS, Osinska H, Hambleton MA, Brunskill EW, Sayen MR, Gottlieb RA, Dorn GW, Robbins J, Molkentin JD (2005) Loss of cyclophilin D reveals a critical role for mitochondrial permeability transition in cell death. Nature 434:658-662.

Barsukova A, Komarov A, Hajnóczky G, Bernardi P, Bourdette D, Forte M (2011) Activation of the mitochondrial permeability transition pore modulates Ca2+ responses to physiological stimuli in adult neurons. European Journal of Neuroscience 33:831-842.

Basso E, Fante L, Fowlkes J, Petronilli V, Forte MA, Bernardi P (2005) Properties of the Permeability Transition Pore in Mitochondria Devoid of Cyclophilin D. Journal of Biological Chemistry 280:18558-18561.

Begley DJ, Squires LK, Zloković BV, Mitrović DM, Hughes CCW, Revest PA, Greenwood J (1990) Permeability of the Blood-Brain Barrier to the Immunosuppressive Cyclic Peptide Cyclosporin A. Journal of Neurochemistry 55:1222-1230.

Bernardi P, Krauskopf A, Basso E, Petronilli V, Blalchy-Dyson E, Di Lisa F, Forte MA (2006) The mitochondrial permeability transition from in vitro artifact to disease target. FEBS Journal 273:2077-2099.

Camara AKS, Lesnefsky EJ, Stowe DF (2009) Potential Therapeutic Benefits of Strategies Directed to Mitochondria. Antioxidants & Redox Signaling 13:279-347.

Camici GG, Schiavoni M, Francia P, Bachschmid M, Martin-Padura I, Hersberger M, Tanner FC, Pelicci P, Volpe M, Anversa P, Lüscher TF, Cosentino F (2007) Genetic deletion of p66Shc adaptor protein prevents hyperglycemia-induced endothelial dysfunction and oxidative stress. Proceedings of the National Academy of Sciences 104:5217-5222.

Carpi A, Menabò R, Kaludercic N, Pelicci P, Di Lisa F, Giorgio M (2009) The cardioprotective effects elicited by p66Shc ablation demonstrate the crucial role of mitochondrial ROS formation in ischemia/reperfusion injury. Biochimica et Biophysica Acta (BBA) - Bioenergetics 1787:774-780.

Du H, Guo L, Fang F, Chen D, A Sosunov A, M McKhann G, Yan Y, Wang C, Zhang H, Molkentin JD, Gunn-Moore FJ, Vonsattel JP, Arancio O, Chen JX, Yan SD (2008) Cyclophilin D deficiency attenuates mitochondrial and neuronal perturbation and ameliorates learning and memory in Alzheimer s disease. Nature Medicine 14:1097-1105.

Dutta R, McDonough J, Yin X, Peterson J, Chang A, Torres T, Gudz T, Macklin WB, Lewis DA, Fox RJ, Rudick R, Mirnics K, Trapp BD (2006) Mitochondrial dysfunction as a cause of axonal degeneration in multiple sclerosis patients. Annals of Neurology 59:478-489.

Forte M, Gold BG, Marracci G, Chaudhary P, Basso E, Johnsen D, Yu X, Fowlkes J, Bernardi P, Bourdette D (2007) Cyclophilin D inactivation protects axons in experimental autoimmune encephalomyelitis, an animal model of multiple sclerosis. Proceedings of the National Academy of Sciences 104:7558-7563.

Gertz M, Steegborn C (2010)(a) The Lifespan-Regulator p66Shc in Mitochondria: Redox Enzyme or Redox Sensor? Antioxidants & Redox Signaling 13:1417-1428.

Gertz M, Steegborn C (2010)(b) The mitochondrial apoptosis pathway and p66Shc: A regulatory redox enzyme or an adapter protein snuggling around? Cell Cycle 9:4425-4426.

Giorgio M, Migliaccio E, Orsini F, Paolucci D, Moroni M, Contursi C, Pelliccia G, Luzi L, Minucci S, Marcaccio M, Pinton P, Rizzuto R, Bernardi P, Paolucci F, Pelicci PG (2005) Electron Transfer between Cytochrome c and p66Shc Generates Reactive Oxygen Species that Trigger Mitochondrial Apoptosis. Cell 122:221-233.

Lin MT, Beal MF (2006) Mitochondrial dysfunction and oxidative stress in neurodegenerative diseases. Nature 443:787-795.

Lublin F (2005) History of modern multiple sclerosis therapy. Journal of Neurology 252:iii3-iii9.

Mahad D, Ziabreva I, Lassmann H, Turnbull D (2008) Mitochondrial defects in acute multiple sclerosis lesions. Brain 131:1722-1735.

Martin LJ, Gertz B, Pan Y, Price AC, Molkentin JD, Chang Q (2009) The mitochondrial permeability transition pore in motor neurons: Involvement in the pathobiology of ALS mice. Experimental Neurology 218:333-346.

Marracci GH, Jones RE, McKeon GP, Bourdette DN (2002) Alpha lipoic acid inhibits T cell migration into the spinal cord and suppresses and treats experimental autoimmune encephalomyelitis. J Neuroimmunol 131:104-114.

Migliaccio E, Giorgio M, Mele S, Pelicci G, Reboldi P, Pandolfi PP, Lanfrancone L, Pelicci PG (1999) The p66shc adaptor protein controls oxidative stress response and life span in mammals. Nature 402:309-313.

Moreira PI, Zhu X, Wang X, Lee HG, Nunomura A, Petersen RB, Perry G, Smith MA (2010) Mitochondria: A therapeutic target in neurodegeneration. Biochimica et Biophysica Acta (BBA) - Molecular Basis of Disease 1802:212-220.

Nemoto S, Combs CA, French S, Ahn B-H, Fergusson MM, Balaban RS, Finkel T (2006) The Mammalian Longevity-associated Gene Product p66shc Regulates Mitochondrial Metabolism. Journal of Biological Chemistry 281:10555-10560.

Noseworthy JH, Lucchinetti C, Rodriguez M, Weinshenker BG (2000) Multiple Sclerosis. New England Journal of Medicine 343:938-952.

Orsini F, Migliaccio E, Moroni M, Contursi C, Raker VA, Piccini D, Martin-Padura I, Pelliccia G, Trinei M, Bono M, Puri C, Tacchetti C, Ferrini M, Mannucci R, Nicoletti I, Lanfrancone L, Giorgio M, Pelicci P (2004) The life span determinant p66Shc localizes to mitochondria where it associates with mtHsp70 and regulates trans-membrane potential. Journal of Biological Chemistry 279:25689-25695.

Pinton P, Rimessi A, Marchi S, Orsini F, Migliaccio E, Giorgio M, Contursi C, Minucci S, Mantovani F, Wieckowski MR, Del Sal G, Pelicci PG, Rizzuto R (2007) Protein Kinase C ß and Prolyl Isomerase 1 Regulate Mitochondrial Effects of the Life-Span Determinant p66Shc. Science 315:659-663.

Rasola A, Bernardi P (2007) The mitochondrial permeability transition pore and its involvement in cell death and in disease pathogenesis. Apoptosis 12:815-833.

Schinzel AC, Takeuchi O, Huang Z, Fisher JK, Zhou Z, Rubens J, Hetz C, Danial NN, Moskowitz MA, Korsmeyer SJ (2005) Cyclophilin D is a component of mitochondrial permeability transition and mediates neuronal cell death after focal cerebral ischemia. Proceedings of the National Academy of Sciences of the United States of America 102:12005-12010.

Smith WW, Norton DD, Gorospe M, Jiang H, Nemoto S, Holbrook NJ, Finkel T, Kusiak JW (2005) Phosphorylation of p66Shc and forkhead proteins mediates Aβ toxicity. The Journal of Cell Biology 169:331-339.

Steinman L (2001) Multiple sclerosis: a two-stage disease. Nat Immunol 2:762-764.

Su B, Wang X, Zheng L, Perry G, Smith MA, Zhu X (2010) Abnormal mitochondrial dynamics and neurodegenerative diseases. Biochimica et Biophysica Acta (BBA) - Molecular Basis of Disease 1802:135-142.

Su K, Banker G, Bourdette D, Forte M (2009) Axonal degeneration in multiple sclerosis: The mitochondrial hypothesis. Current Neurology and Neuroscience Reports 9:411-417.

Wang W et al. (2008) Superoxide Flashes in Single Mitochondria. Cell 134:279-290.

Wujek JR, Bjartmar C, Richer E, Ransohoff RM, Yu M, Tuohy VK, Trapp BD (2002) Axon loss in the spinal cord determines permanent neurological disability in an animal model of multiple sclerosis. J. Neuropathol. Exp Neurol 61:23-32.

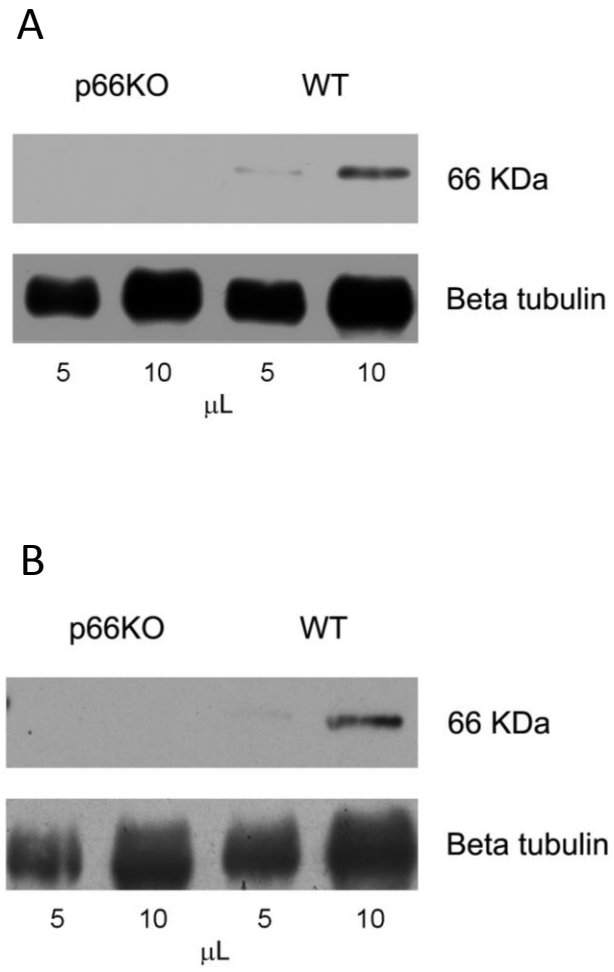

Figure 1: Analysis of p66 expression and elimination in WT and p66-KO nervous tissue and neurons. Lysates prepared from p66-KO and WT mice were immunoprecipitated with anti-Shc antibody on precleared protein G beads. Immunoprecipitates were examined by immunoblot analysis probing with the anti-Shc BG8 antibody. Immunoblots were re-probed with beta tubulin as a protein loading control. Blot analysis showed p66 expression in WT brain cortical lysates and elimination in those prepared from p66-KO mice (A). Similar results were shown in hippocampal neuronal lysates (B).

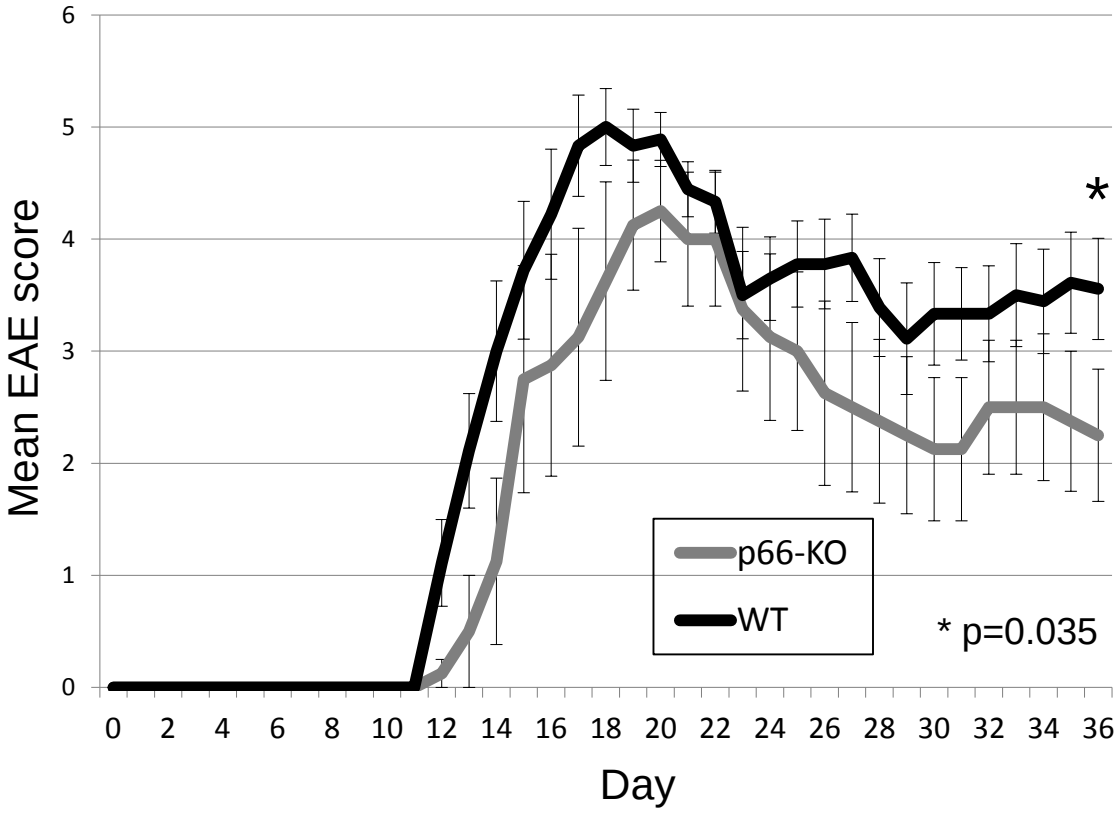

Figure 2. p66-KO mice showed less severe clinical EAE compared to WT mice.

Immunized p66-KO and WT mice were scored daily for clinical signs of weakness and paralysis over a 36-day observation period. Throughout the entire clinical course, mean p66-KO scores were less than the WT scores. At the end of the 36 days, the p66-KO mice had significantly lower scores compared to the WT mice, reflecting the overall trend of reduced clinical impairment.

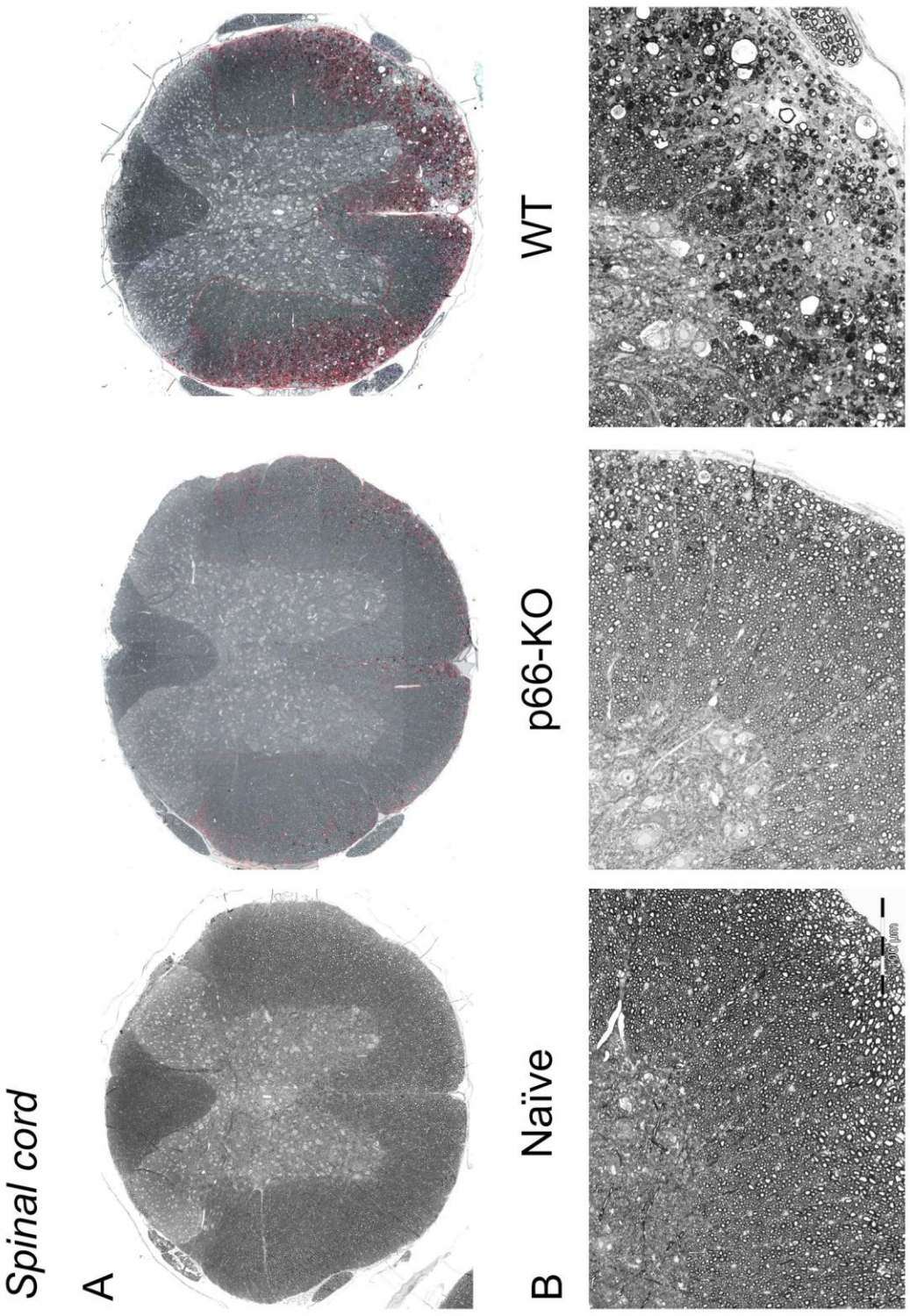
Spinal cord
A
B
WT
p66-KO
Naïve

C

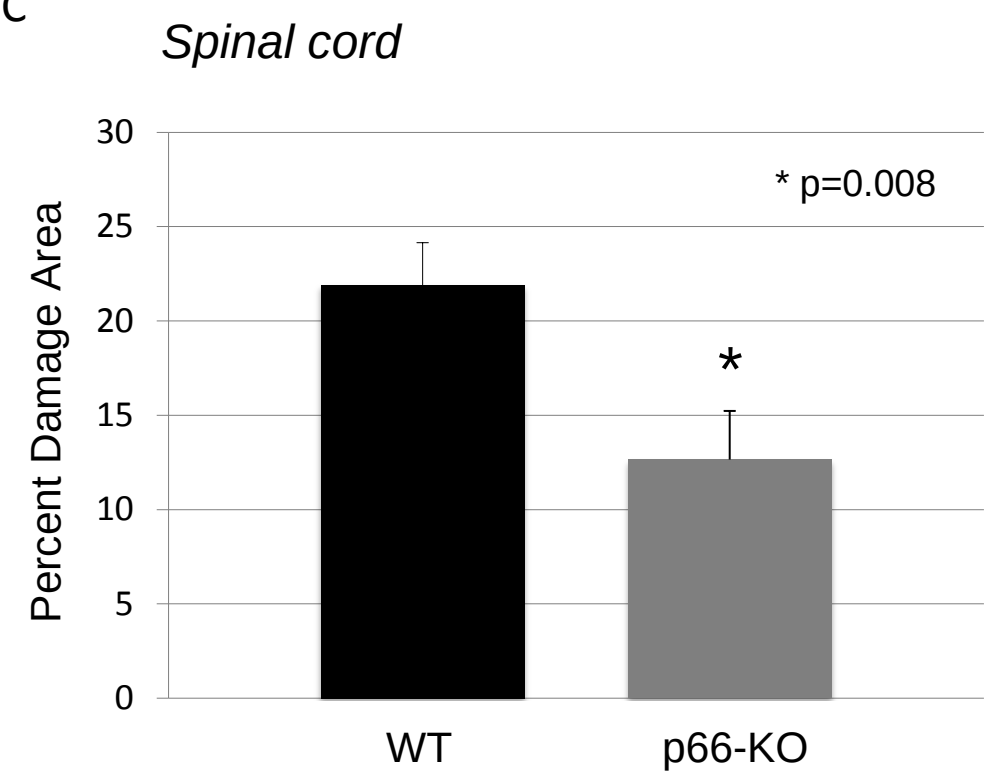
Spinal cord
Percent Damage Area
30
25
20
15
10
5
0
* p=0.008
*
WT
p66-KO

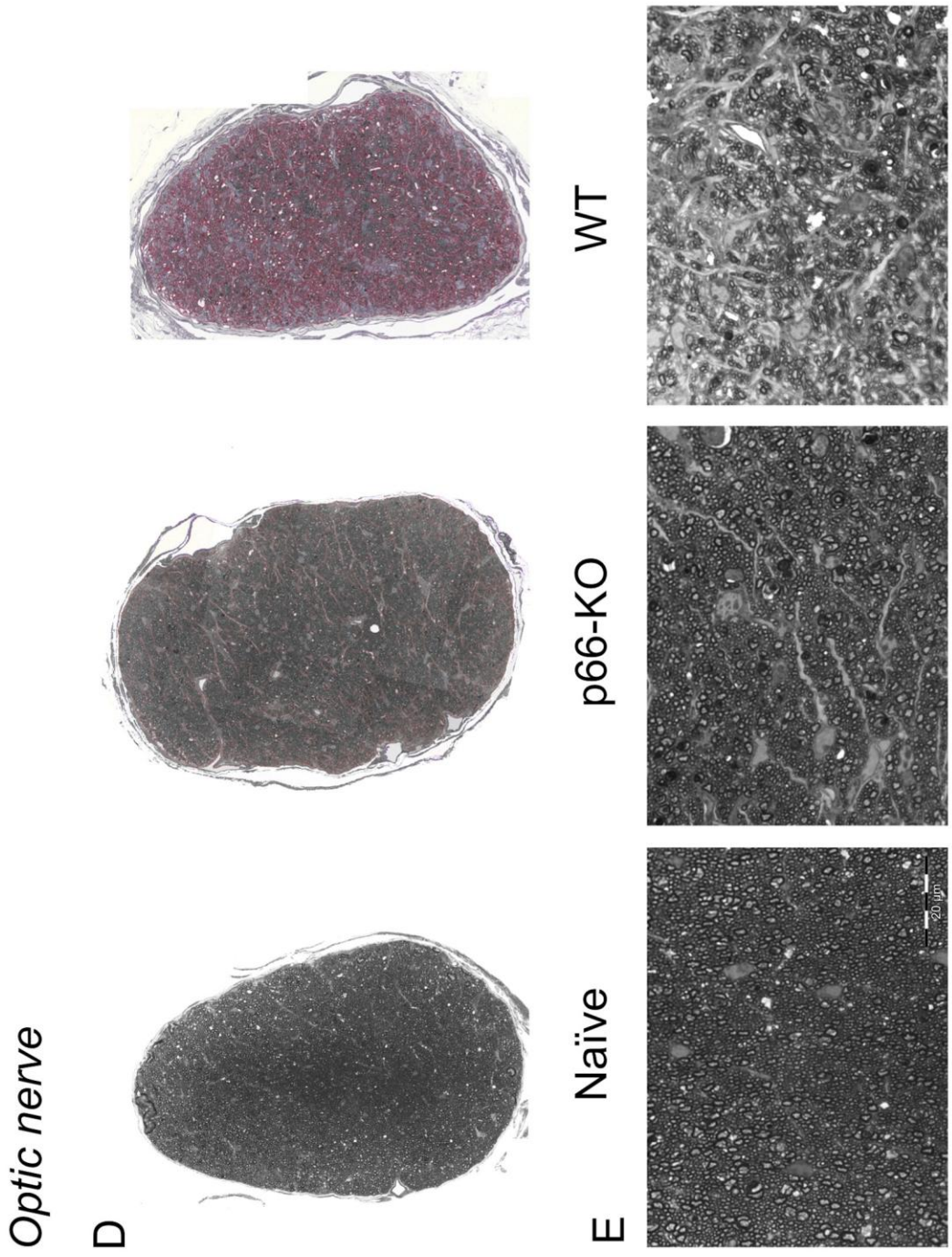
Optic nerve
D
E
Naïve
p66-KO
WT
20 µm

F

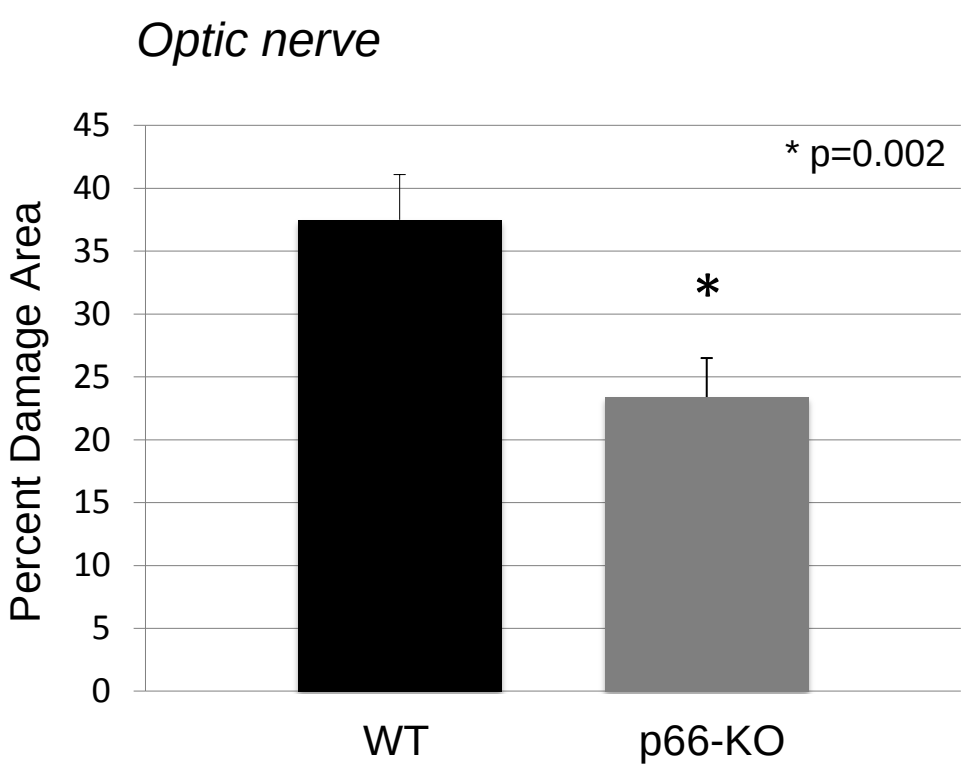
Optic nerve
Percent Damage Area
45
40
35
30
25
20
15
10
5
0
* p=0.002
*
WT
p66-KO

Figure 3. p66-KO mice showed less axonal damage than WT mice following EAE induction. A) Lower power view of plastic-embedded toluidine-blue stained thoracic spinal cord sections from representative naïve (left), p66-KO (middle), and WT (right) mice 36 days following EAE induction. Red indicates circled areas of damage. B) Higher power view of sections. Note the greater preservation of axonal integrity in the p66-KO mice compared to WT mice. C) p66-KO mice showed a significant 42% reduction in ventrolateral white matter damage compared to WT mice. D) Lower power view of plastic-embedded toluidine-blue stained optic nerve sections from representative naïve (left), p66-KO (middle), and WT (right) mice 36 days following EAE induction. Red indicates circled areas of damage. E) Higher power view of sections. Note the greater preservation of axonal integrity in the p66-KO mice compared to WT mice. F) p66-KO mice showed a significant 38% reduction in optic nerve damage compared to WT mice.

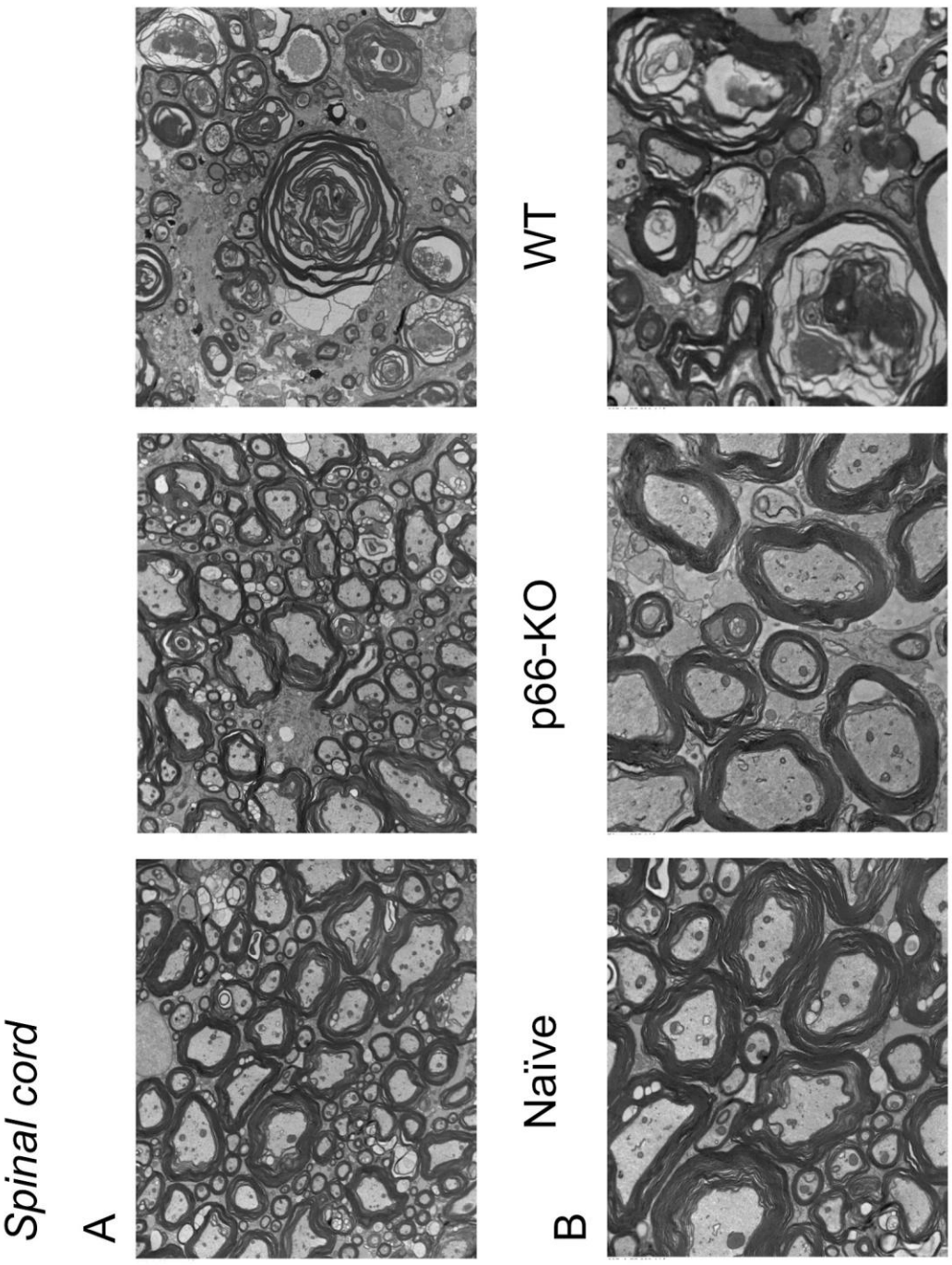
Spinal cord
A
B
Naïve
p66-KO
WT

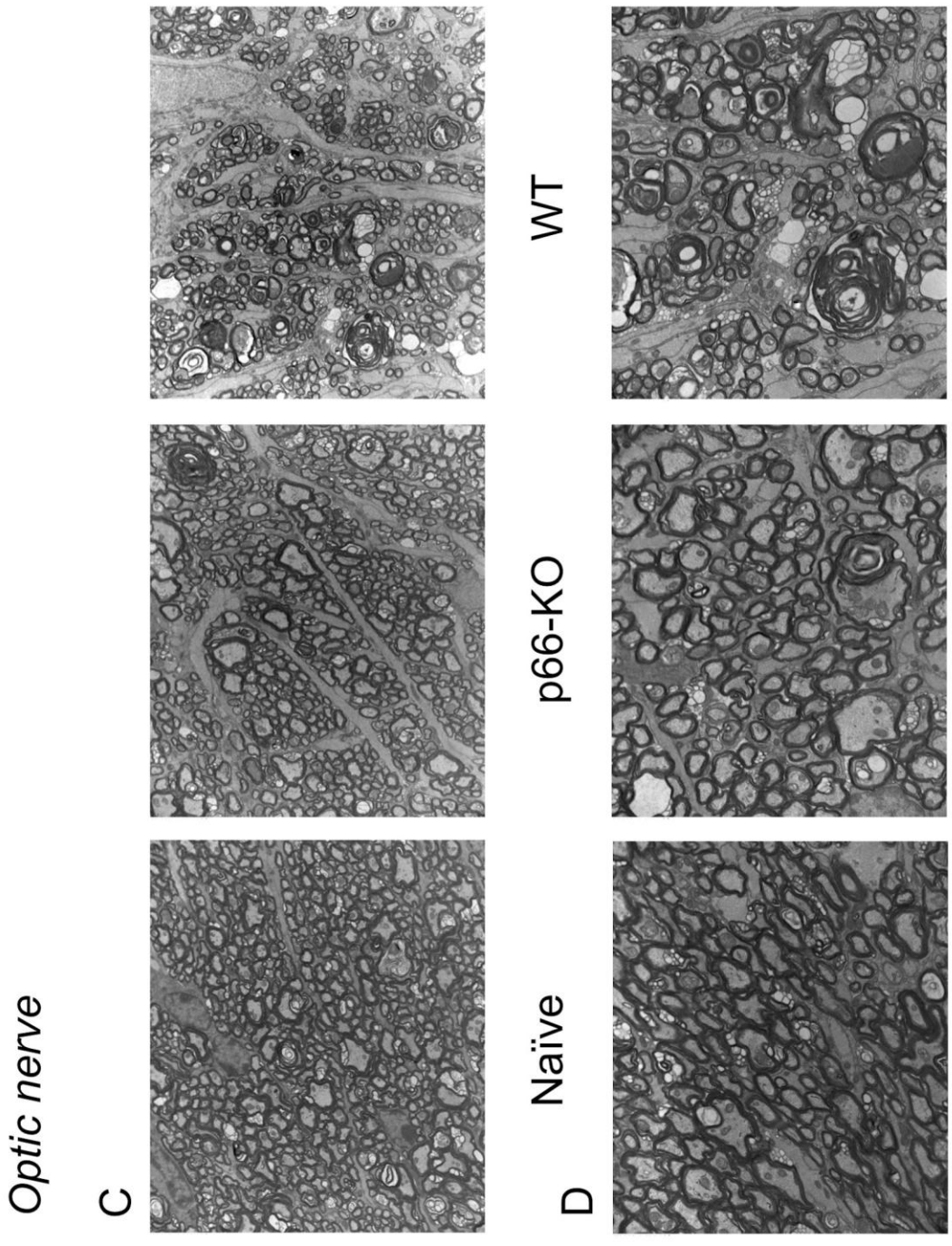
Optic nerve
C
D
Naïve
p66-KO
WT

Figure 4. Electron microscopy of p66-KO and WT nervous tissue illustrates axonal protection associated with p66 elimination. Electron microscopy images of naïve (left), p66-KO (middle), and WT (right) ultrathin sections from plastic embedded thoracic spinal cords (A,B) and optic nerves (C,D) imaged at 4800X (A,C) and 9300X (B,D). Greater axonal preservation was observed in the p66-KO images in comparison to the WT images.

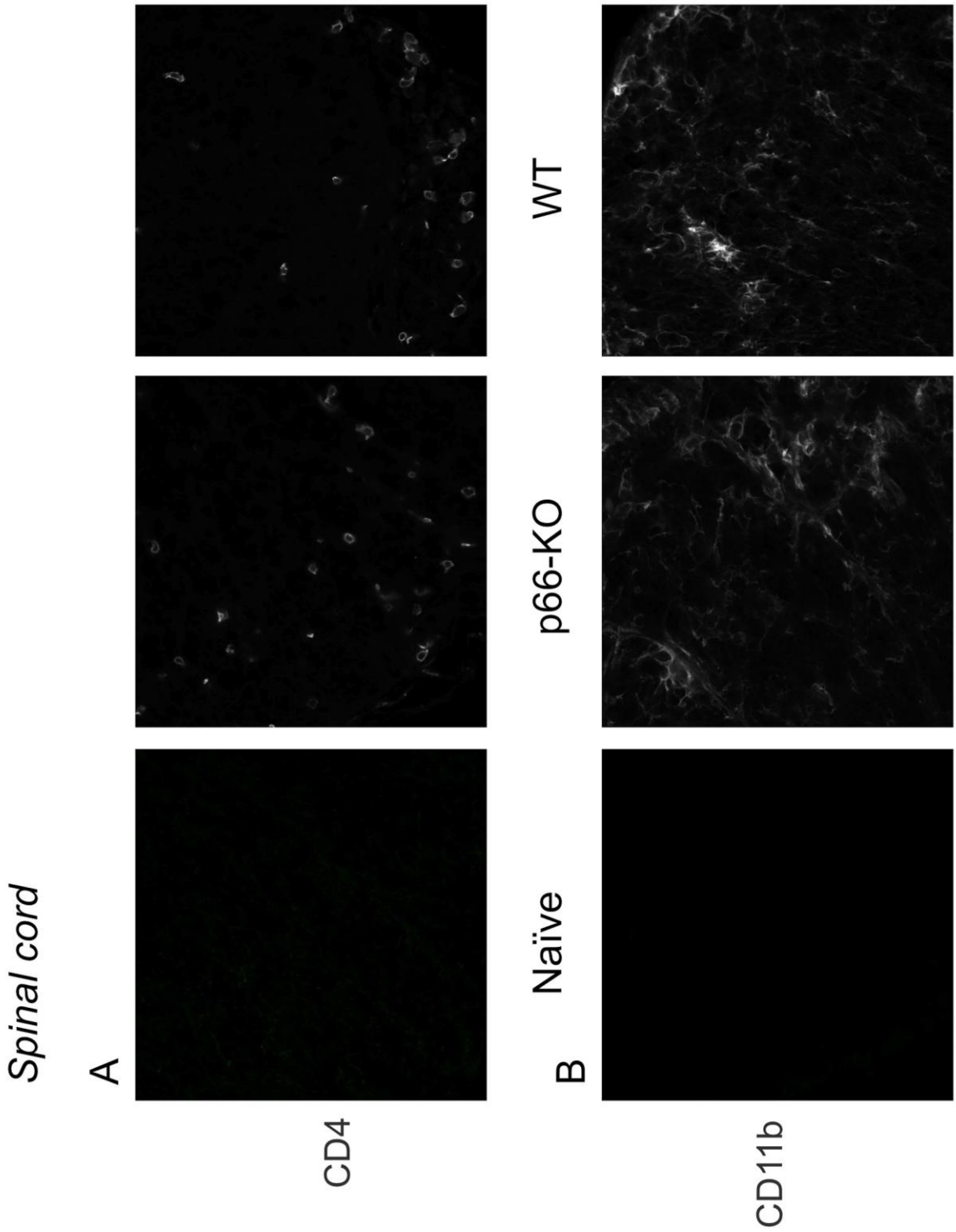
Spinal cord
A
B
Naïve
p66-KO
WT
CD4
CD11b

C

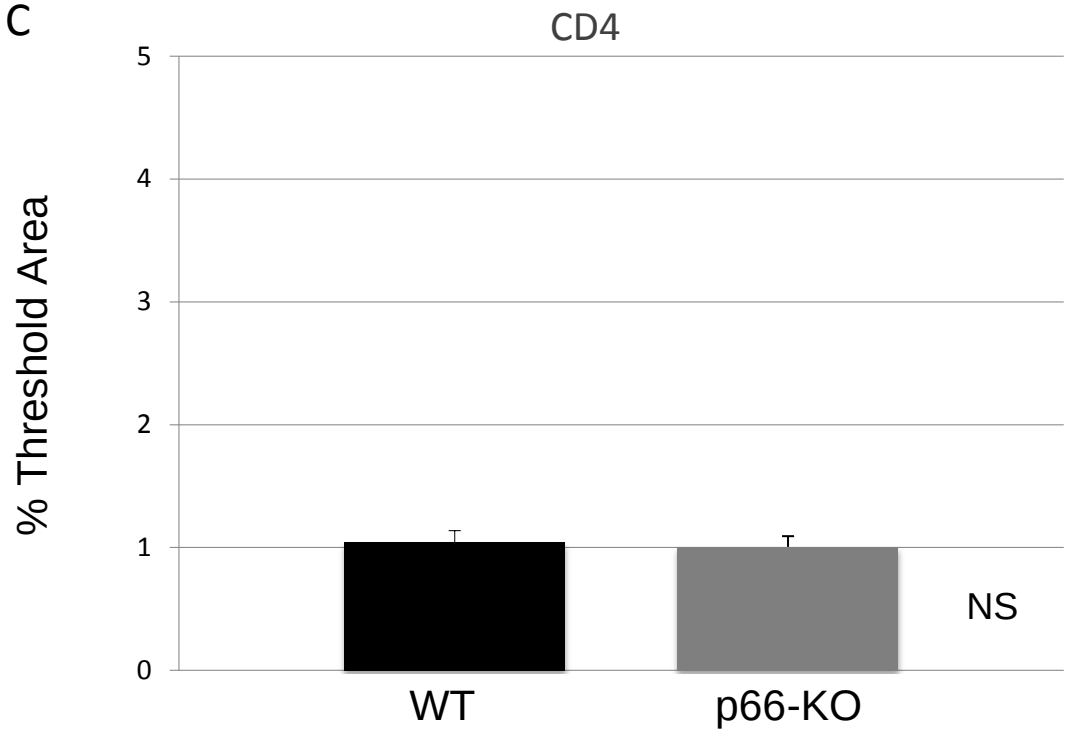
CD4
% Threshold Area
5
4
3
2
1
0
NS
WT
p66-KO

D

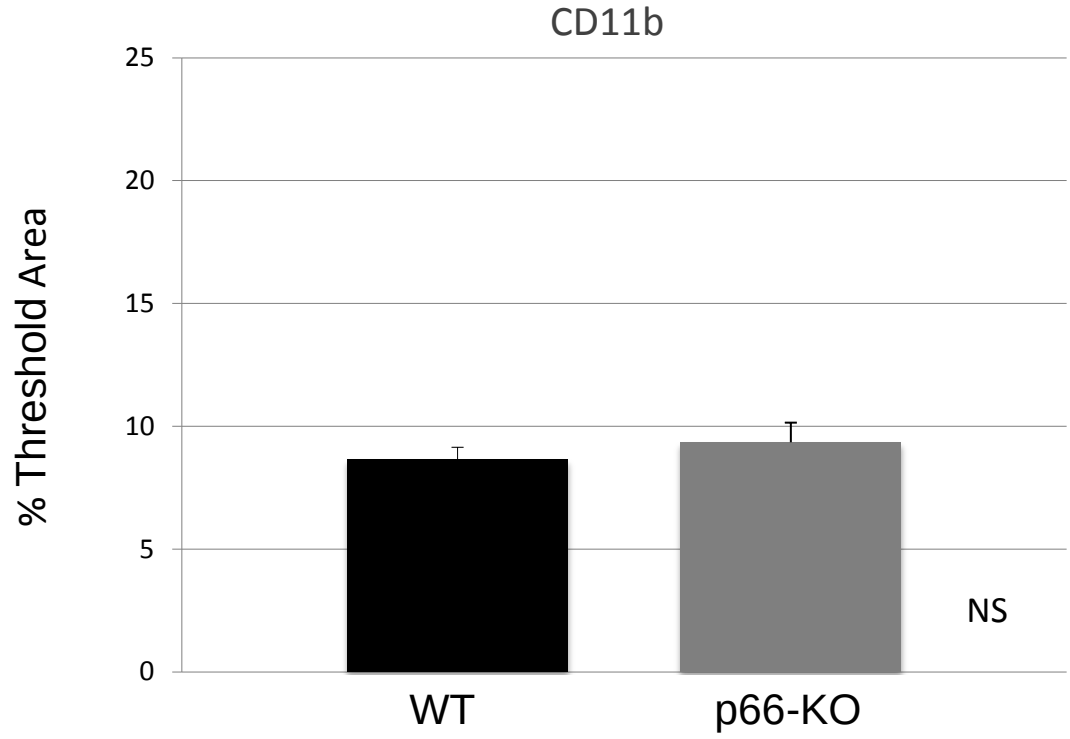
CD11b
% Threshold Area
25
20
15
10
5
0
NS
WT
p66-KO

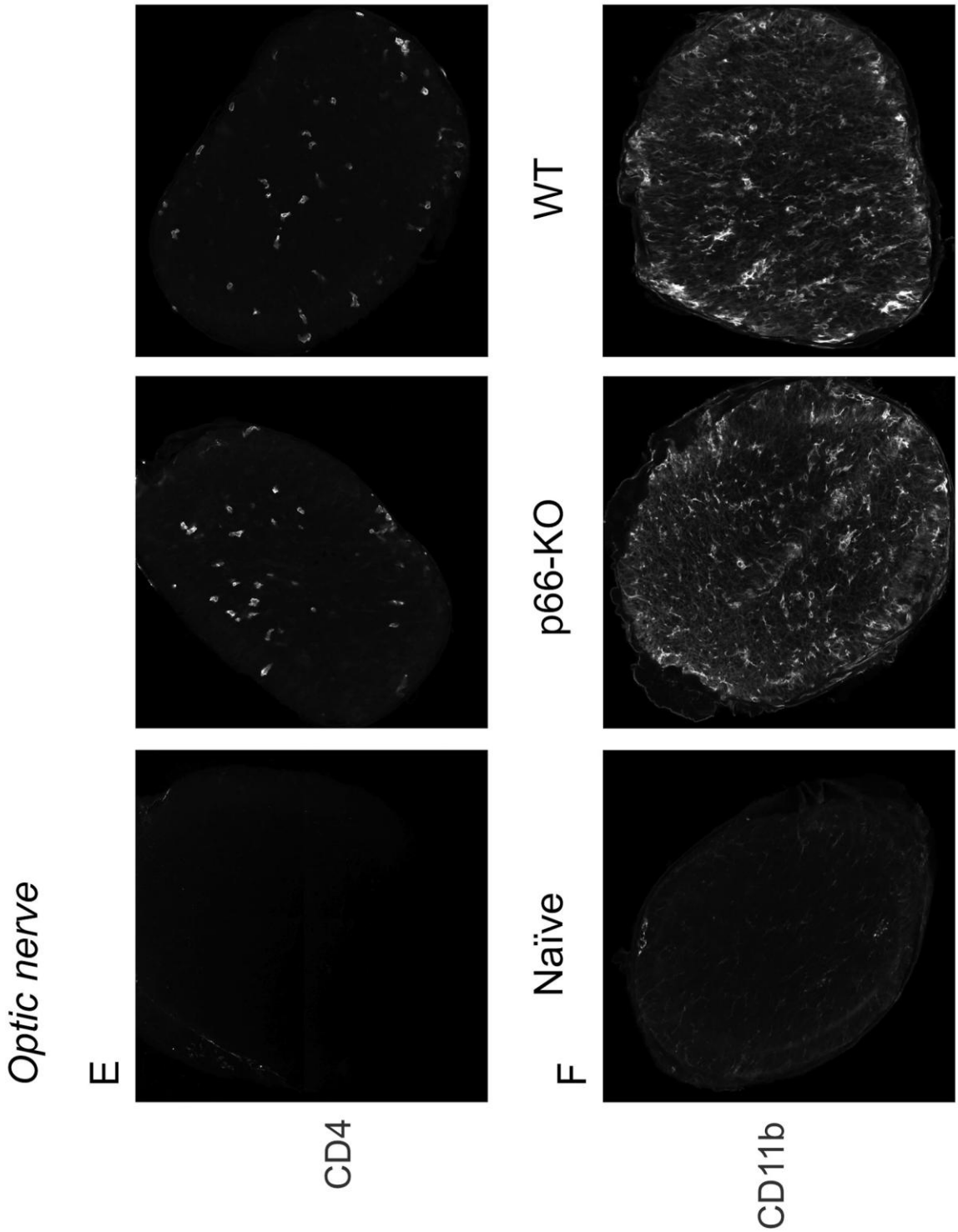
Optic nerve
E
F
Naïve
p66-KO
WT
CD4
CD11b

G

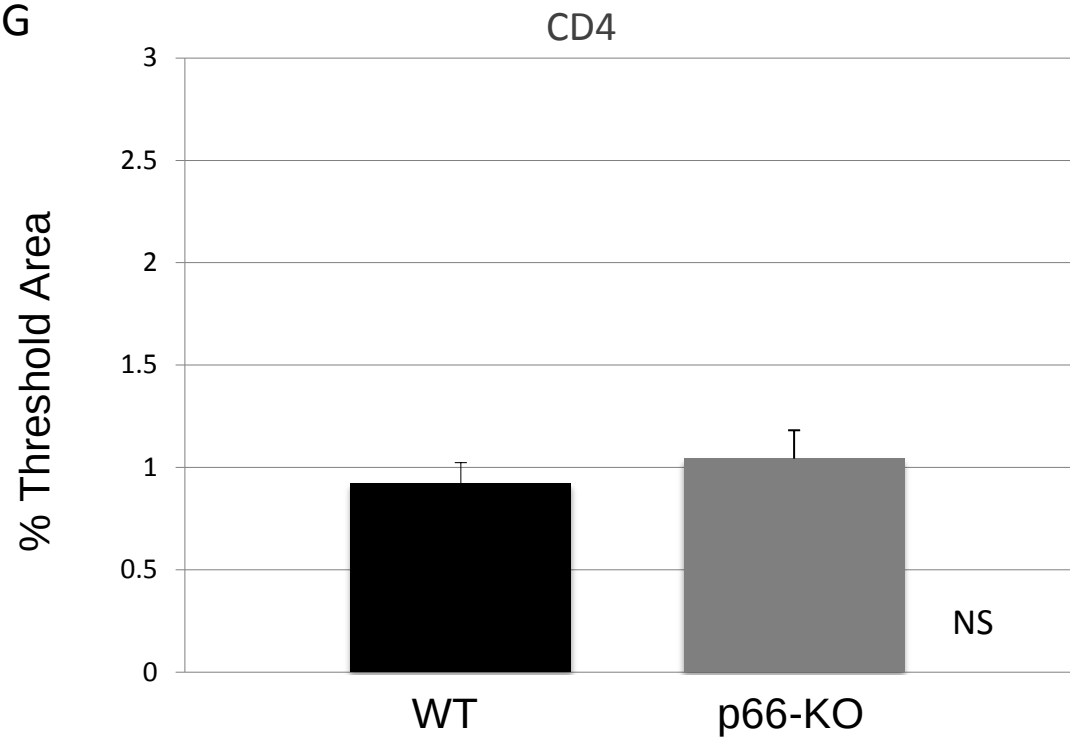
CD4
% Threshold Area
3
2.5
2
1.5
1
0.5
0
NS
WT
p66-KO

H

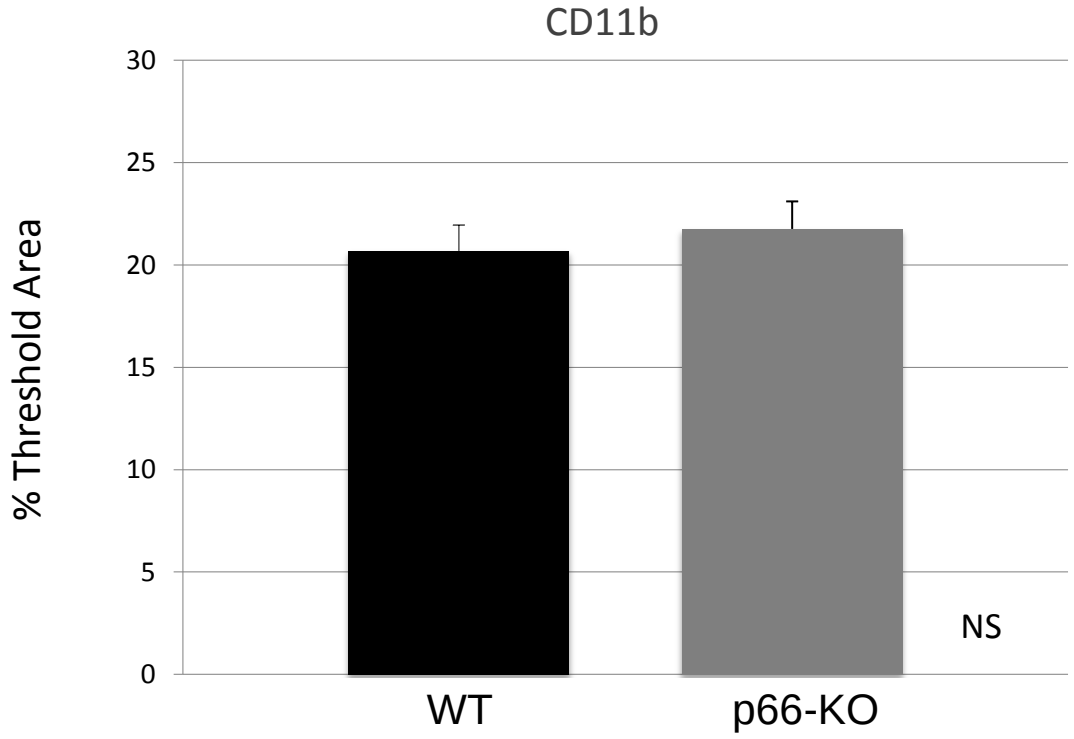
CD11b
% Threshold Area
30
25
20
15
10
5
0
NS
WT
p66-KO

Figure 5. p66-KO nervous tissue showed similar levels of immune cell infiltration compared to WT tissue following EAE induction. Naïve (left), p66-KO (middle), and WT (right) lumbar spinal cord sections 36 days following EAE induction were stained for T cells with CD4 antibody (A) and for macrophages/microglia with CD11b antibody (B). Quantification of immune cell infiltration showed no significant difference between the p66-KO and WT groups (C,D). Naïve (left), p66-KO (middle), and WT (right) optic nerve sections 36 days following EAE induction were stained for T cells with CD4 antibody (E) and for macrophages/microglia with CD11b antibody (F). Quantification of immune cell infiltration showed no significant difference between the p66-KO and WT groups (G,H). NS = difference not significant ($p>0.05$).

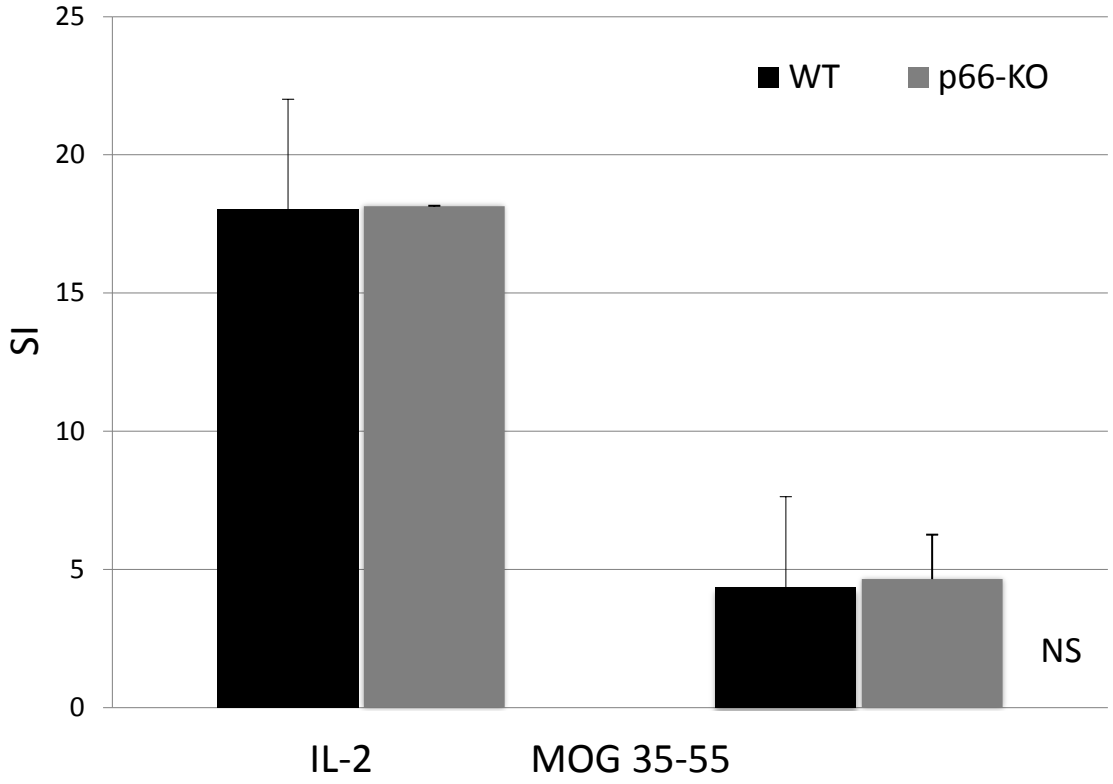

Figure 6. T cell proliferation studies showed no significant differences between p66-KO and WT mice in MOG immunoreactivity. Using standard EAE protocol, p66-KO and WT mice were immunized with MOG 35-55 peptide. Ten days post-immunization, lymph nodes were collected for proliferation studies. Lymph node cultures treated with positive control IL-2 and MOG 35-55 peptide (25μg/mL) showed no significant differences in proliferative responses between the p66-KO and WT groups. SI = Stimulation index; NS = difference not significant ($p>0.05$).

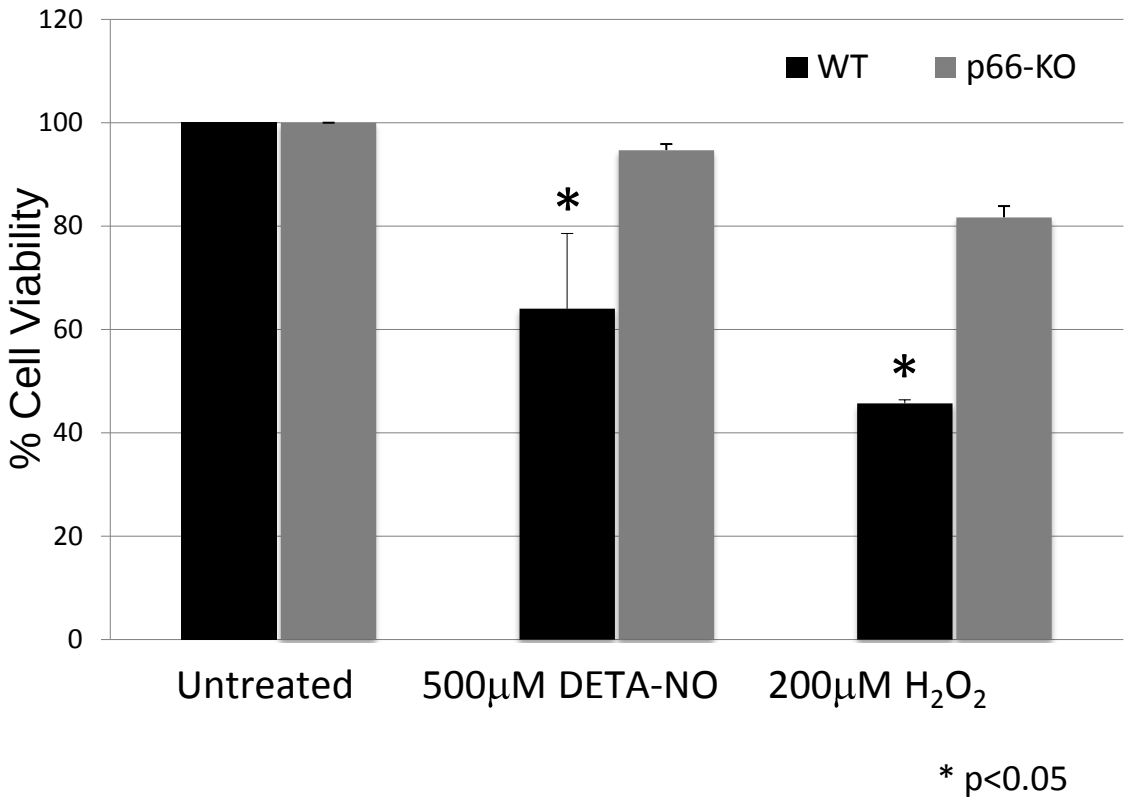

Figure 7. p66-KO neurons showed greater protection following treatment with oxidative insults implicated in EAE and MS neurodegenerative pathways. p66-KO neurons had a significantly greater cell viability percentage compared to WT neurons when treated for 15 minutes with either A) 500μM of DETA-NO or B) 200 μM H_2O_2. Cell counts were obtained 24 hours post treatment. A) DETA-NO treated p66-KO neurons had a mean cell viability of 94.7±1.2% compared to 64.0±14.6% for the WT neurons (p=0.04). B) H_2O_2 treated p66-KO neurons had a mean cell viability of 81.7±2.2% compared to 45.7±0.7% for the WT neurons (p=0.02). (n per treatment/genotype = 3 cultures/; 4 plates/culture)

a) Th1 cytokines

	Media (pg/mL)		25 μg MOG (pg/mL)	
TNF-alpha	**p66-KO:** 266.0±101.2	**WT:** 272.3±64.4	**p66-KO:** 465.0139.7	**WT:** 414.085.6
	z=0.245; p=0.403		*z=0.735; p=0.231*	
IFN-gamma	**p66-KO:** 376.0316.7	**WT:** 429.5193.0	**p66-KO:** 11033.42625.1	**WT:** 15348.22564.0
	z=0.735; p=0.231		*z=0.735; p=0.231*	

b) Th2 cytokines

	Media (pg/mL)		25 μg MOG (pg/mL)	
IL-4	**p66-KO:** 7.6±7.2	**WT:** 9.5±5.7	**p66-KO:** 21.6±24.4	**WT:** 19.6±16.2
	z=0.775; p=0.219		*z=0.490; p=0.312*	
IL-10	**p66-KO:** 50.4±47.6	**WT:** 43.3±41.5	**p66-KO:** 110.73±96.04	**WT:** 89.2±69.9
	z=0.577; p=0.282		*z=0.577; p=0.282*	

c) Th17 cytokines

	Media (pg/mL)		25 μg MOG (pg/mL)	
IL-17	**p66-KO:** 3237.6±2232.6	**WT:** 4574.2±1121.2	**p66-KO:** 13198.6±4260.0	**WT:** 14555.5±4526.3
	z=0.000; p=0.500		*z=1.443; p=0.074*	

Table 1. Cytokine studies showed no significant differences between p66-KO and WT mice with EAE. Using standard EAE protocol, p66-KO and WT mice were immunized with MOG 35-55 peptide. Ten days post-immunization, lymph nodes were collected for cytokine studies. Lymph node cultures treated with control media and MOG 35-55 (25μg/mL) peptide for 48 hours, and cell culture supernatants were collected for analysis using the Luminex Bio-Plex mouse cytokine assay kit. Results showed no significant differences between the p66-KO and WT groups for Th1 (a), Th2 (b), or Th17 (c) cytokine levels.

CHAPTER III:

in vivo and *in vitro* characterization of p66/CyPD double knockout mice and neurons

I. Introduction

As previously discussed, pathologic PTP opening leading to mitochondrial dysfunction and cell death activation has been proposed as a mechanistic pathway of neurodegeneration in MS. Furthermore, both CyPD and p66 have been proposed as mediators of PTP opening as a result of multiple studies addressing protein elimination via genetic and/or pharmacologic methods. For instance, CyPD has been shown to regulate PTP opening as demonstrated by the ability of CyPD eliminated (CyPD-KO) or inhibited (CsA treatment) mitochondria to sequester significantly more Ca^{2+} prior to permeability transition (Forte et al., 2007). Similarly, p66 elimination has been proposed to affect the activation of a positive feed-forward signaling pathway in which p66 serves as both an oxidative stress sensor and amplifier (Gertz and Steegborn, 2010). Elimination of this key signaling molecule alters the pathway of stress-induced phosphorylation, translocation, and ROS production within the mitochondrial intermembrane space, and ensuing pathologic PTP opening and cell death (Giorgio et al., 2005). Thus, CyPD functions as a direct regulator of PTP opening, and p66 functions as an upstream inducer via mitochondrial ROS production. This suggests that p66 is linearly upstream of CyPD in the proposed pathway of PTP-mediated cell death in EAE, and by extension, MS.

II. Methods

To test the relationship between CyPD and p66 in the context of EAE, a colony of p66/CyPD double knockout (DKO) mice was generated by standard genetic approaches. The mice were fully viable and exhibited no overt phenotype. The double mutant mice, along with single mutant CyPD-KO and p66-KO mice, were induced with EAE by MOG peptide immunization as previously described, and scored for clinical signs of weakness and paralysis for a period of 36 days. Following the observation period, the mice were perfused, and spinal cords were dissected out for further histologic analysis. Thoracic spinal cord blocks were embedded in plastic, sectioned and stained with toluidine blue. Photomontages of the spinal cord cross-sections were imaged at 20X via light microscopy, and areas of damage were manually circled to determine the percentage of area damaged in the ventrolateral white matter. All analyses were done blinded to genotype.

In addition, to more closely compare the single and double knockout neurons in a controlled environment, neuronal cultures were prepared and analyzed in the same manner as described in Chapter II. Briefly, cortical neuronal cultures were prepared from dissected brains of p66-KO, CyPD-KO, and p66/CyPD-DKO animals as previously outlined (Barsukova et al., 2011). Week old cultures were treated with 200 μM H_2O_2, 500 μM DETA-NO, or control medium. Following a 15-minute treatment period at 37 °C, the cultures were washed twice and returned to the incubator in fresh medium. Neuronal viability was assessed 24 hours later by incubating the cells in Calcein AM and manually counting live neurons based on morphologic appearance and presence of

green fluorescent dye at 20X with a fluorescence inverted microscope. All analyses were done blinded to genotype.

III. Results

The results of this comparative study demonstrated no significant differences between the p66-KO, CyPD-KO, and p66/CyPD-DKO genotypes in the context of EAE. Specifically, in terms of clinical EAE, the single and double knockout mice had similar EAE courses and severity in clinical weakness and paralysis following MOG peptide immunization. For each genotype, the mean cumulative EAE score was calculated by summing daily scores over the 36-day period. Overall, the p66-KO group averaged 112.3±5.3 points, the CyPD-KO group averaged 101.0±11.0 points, and the p66/CyPD DKO group averaged 113±10.3 points (*Figure 1A*). The differences between the groups were not statistically significant as determined by one-way ANOVA for 3 independent samples ($F_{2,30}=0.49$; $p=0.617$).

Furthermore, quantification of axonal and tissue damage in the spinal cords following EAE induction showed no significant differences between the single and double knockout mice as hypothesized. Thoracic spinal cord blocks that were plastic embedded, sectioned, and stained with toluidine blue showed a comparable extent of damage in the ventrolateral white matter. As reported in Chapter II, the p66-KO mice had a mean of 13.2±2.9% damage in the spinal cord, compared to 15.7±1.2% for the CyPD-KO mice, and 11.8±1.5% for the p66/CyPD-DKO mice ($F_{2,27}=1.52$; $p=0.237$) (*Figure 1B*).

Finally, single and double mutant neuronal cultures prepared from adult brain cortices showed no significant differences in cell viability following treatment with either DETA-NO or H_2O_2 (*Figure 1C*). Cell viability percentages for cultures treated with 500 μM DETA-NO were similar between the genotypes (p66-KO 94.8±1.2%, CyPD-KO 95.8±0.3, p66/CyPD-DKO 94.9±0.4; $F_{2,3}=0.53, p=0.635$). This was true also for cultures treated with 200 μM H_2O_2 (p66-KO 81.7± 2.2%, CyPD-KO 79.0±1.0, p66/CyPD-DKO 81.1±1.3; $F_{2,3}= 0.59, p=0.596$).

IV. Discussion

The aim of this comparative study was to define the relationship between p66 and CyPD in mitochondrial PTP-mediated cell death pathways. The reported similarities in EAE clinical courses and spinal cord damage between the single and double knockout mice suggest a linear relationship between p66 and CyPD, in which p66 is an upstream promoter of PTP opening as regulated by CyPD. Furthermore, the comparable results in the *in vitro* viability studies support this linear relationship as well.

Although the phenotype of p66/CyPD-DKO mice may reflect the relationship between p66 and CyPD, further confirmatory studies will be necessary given that epistatic relationships are hard to establish in mammalian systems due to increased complexity. Such studies may include the creation of transgenic lines in which p66 and CyPD are overexpressed, resulting in "gain-of-function" (GOF) phenotypes. If p66 is indeed upstream of CyPD as proposed, p66-GOF phenotypes would be suppressed in CyPD-KO animals, and CyPD-GOF phenotypes would be unaffected in p66-KO animals.

Nevertheless, the preliminary findings reported here do suggest that the relationship between p66 and CyPD may be a linear one.

V. References

Barsukova A, Komarov A, Hajnóczky G, Bernardi P, Bourdette D, Forte M (2011) Activation of the mitochondrial permeability transition pore modulates Ca2+ responses to physiological stimuli in adult neurons. European Journal of Neuroscience 33:831-842.

Forte M, Gold BG, Marracci G, Chaudhary P, Basso E, Johnsen D, Yu X, Fowlkes J, Bernardi P, Bourdette D (2007) Cyclophilin D inactivation protects axons in experimental autoimmune encephalomyelitis, an animal model of multiple sclerosis. Proceedings of the National Academy of Sciences 104:7558-7563.

Gertz M, Steegborn C (2010) The Lifespan-Regulator p66Shc in Mitochondria: Redox Enzyme or Redox Sensor? Antioxidants & Redox Signaling 13:1417-1428.

Giorgio M, Migliaccio E, Orsini F, Paolucci D, Moroni M, Contursi C, Pelliccia G, Luzi L, Minucci S, Marcaccio M, Pinton P, Rizzuto R, Bernardi P, Paolucci F, Pelicci PG (2005) Electron Transfer between Cytochrome c and p66Shc Generates Reactive Oxygen Species that Trigger Mitochondrial Apoptosis. Cell 122:221-233.

A

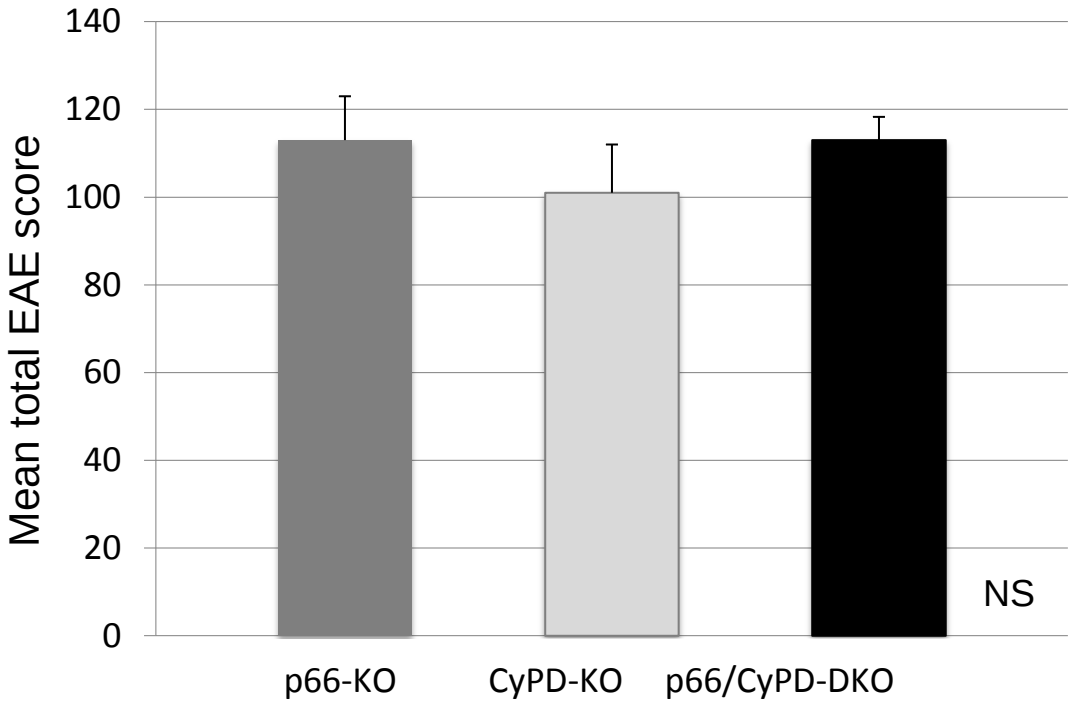
Mean total EAE score
140
120
100
80
60
40
20
0
NS
p66-KO
CyPD-KO
p66/CyPD-DKO

B

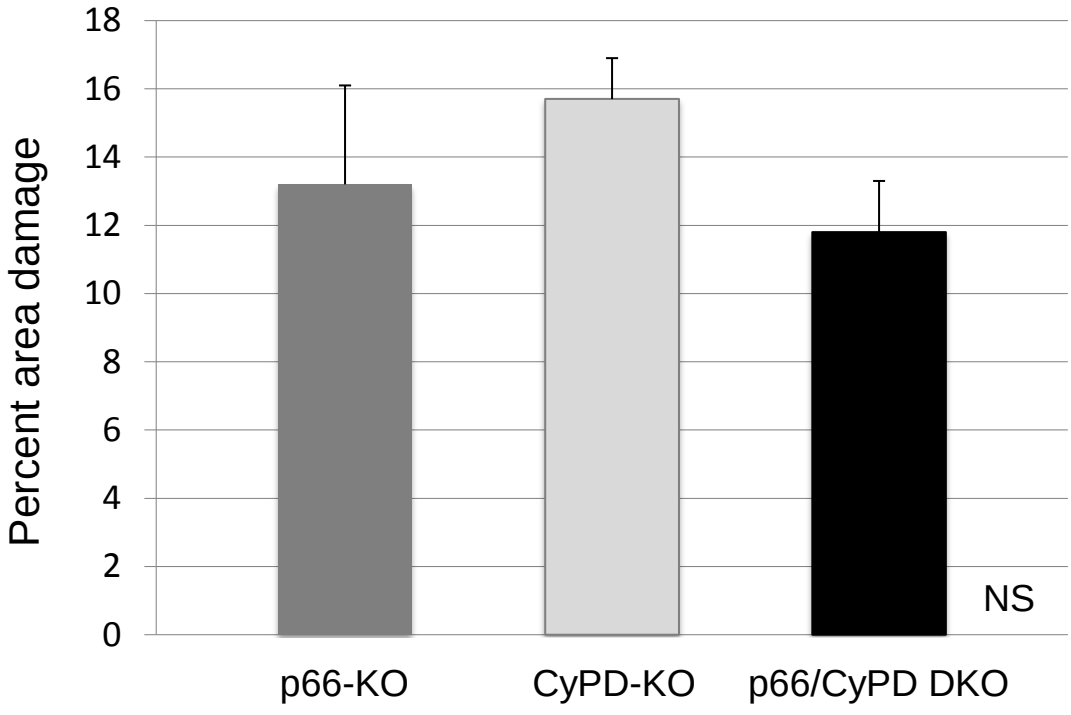
Percent area damage
18
16
14
12
10
8
6
4
2
0
NS
p66-KO
CyPD-KO
p66/CyPD DKO

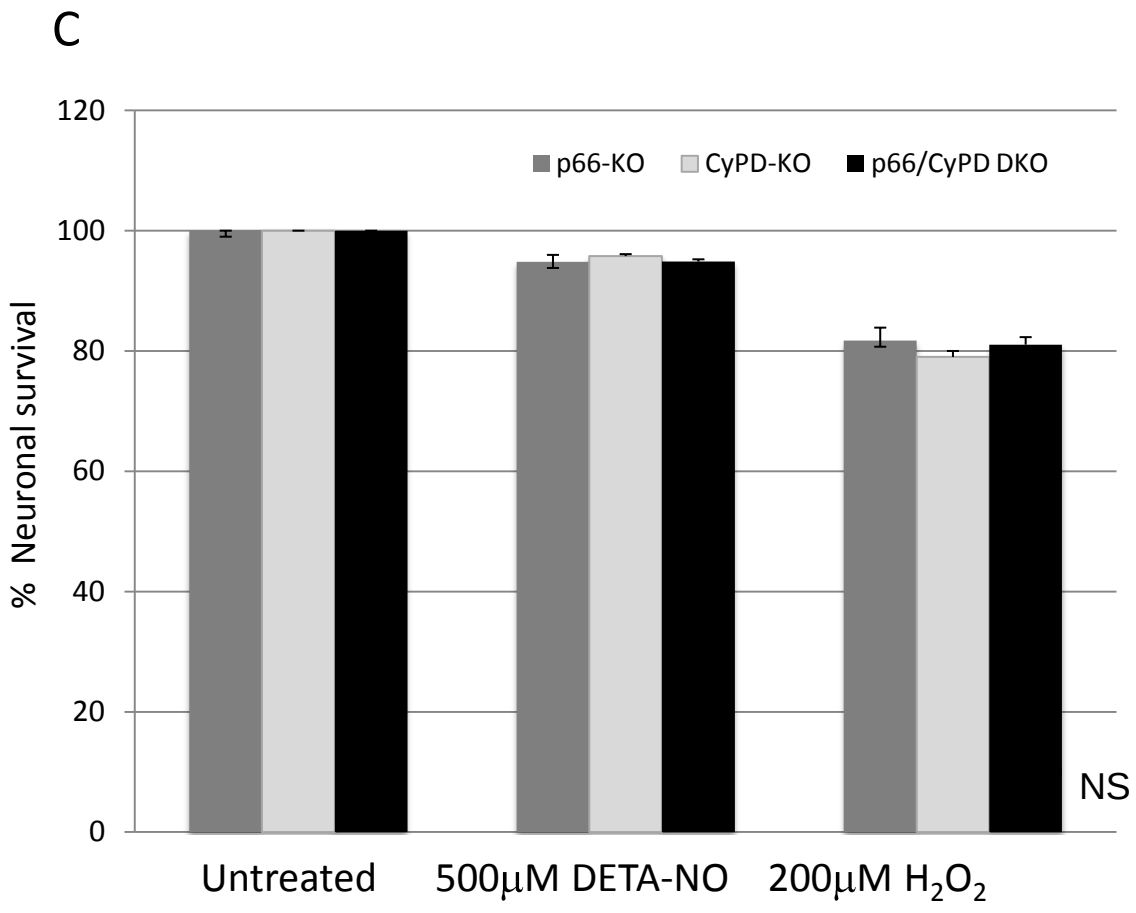

Figure 1 . Single and double knockout mice: similar in vivo and in vitro phenotypes. Comparative analysis of single knockout (p66-KO, CyPD-KO) and double knockout (p66/CyPD-DKO) mice showed no significant differences in both *in vivo* and *in vitro* experiments. The *in vivo* EAE studies showed similar results for both genotypes in clinical EAE (A) and in histologic analysis of spinal cord damage (B) (n = 7 p66-KO; 15 CyPD-KO; 8 p66/CyPD-DKO). The *in vitro* cell viability experiments also showed similar results (D) between the single and double knockout neuronal cultures. (n per treatment/genotype = 3 cultures/; 4 plates/culture) NS = difference not significant ($p>0.05$).

CHAPTER IV:

p66 inactivation incurs greater neuronal robustness and preservation of mitochondrial integrity in axons

I. Abstract

Mitochondria are essential to the life and death of neurons, functioning as energy providers, regulators of ion homeostasis, and mediators of apoptotic pathways. Accordingly, mitochondrial dysfunction has been indicated in several neurodegenerative diseases, including Alzheimer's disease, Huntington's disease, amyotrophic lateral sclerosis, and more recently, multiple sclerosis (MS). Recent evidence points to the permeability transition pore (PTP) as a key player in mitochondrial dysfunction, in which pathologic opening leads to mitochondrial swelling, rupture, release of cytochrome c, and cell death activation. Known inducers of PTP opening include reactive oxygen species (ROS), and interestingly, inactivation of a mitochondria-targeted redox enzyme p66ShcA (p66) has been shown to be neuroprotective in the context of the murine MS model experimental autoimmune encephalomyelitis (EAE). To further characterize the neuroprotective effects associated p66 elimination, p66-KO neurons were analyzed *in vitro* following treatment with oxidative stressors implicated in neurodegenerative pathways of EAE and MS. Specifically, p66-KO and WT neurons were treated with nitric oxide (NO) and hydrogen peroxide and assessed for cell viability and changes in mitochondrial properties, including morphology, ROS production, and transport. The results showed that p66-KO neurons had greater survival following treatment with oxidative stressors, and correspondingly, had less mitochondrial changes compared to

WT neurons in terms of morphology and ROS production, though mitochondrial transport was not protected. Overall, these findings highlight the importance of developing mitochondria-targeted therapeutics for neurodegenerative disorders such as MS, and emphasize p66, mitochondrial ROS, and the PTP as key targets for maintaining mitochondrial and neuronal integrity.

II. Introduction

Mitochondria are dynamic and versatile organelles commonly referred to as the "powerhouses" of the cell. In addition to ATP synthesis, they also serve to maintain ion homeostasis and regulate apoptotic pathways. Given their involvement in key cellular functions, persistent mitochondrial dysfunction can be detrimental.

Interestingly, mitochondrial dysfunction has become associated with human diseases, including neurodegenerative disorders. The unique structure and function of neurons make them particularly susceptible to the effects of damaged mitochondria. Unlike most other cells, neurons have long processes that extend far from the cell body, and therefore are dependent upon transport along microtubules to move mitochondria and vesicles containing materials anterogradely and retrogradely between the cell body and the synapse. This transport is energy-dependent and requires large amounts of ATP to fuel the kinesin and dynein motors. In addition, neurons are electrically excitable cells that transmit action potentials, which are generated and propagated by the ionic flow of cations and anions such as Na^+, K^+, Ca^{2+}, and Cl^-. Hence, ATP-powered pumps are required for maintenance of ionic gradients across cellular membranes. As described, the metabolic demand of neurons is extraordinary high, and even though the CNS only

accounts for 2% of the body's weight, it consumes around 20% of oxygen at rest (Silver and Erecińska, 1998). Therefore, the inability to generate adequate ATP levels due to altered mitochondrial function can severely hinder the functioning capacity of neurons.

Dysregulation of these key mitochondrial functions can lead to the generation of pathologic levels of reactive oxygen species (ROS). ROS are produced in mitochondria as a consequence of oxidative phosphorylation via the delivery of electrons to O_2 along the electron transport chain. Under normal circumstances, ROS levels are regulated by mitochondrial enzymes including superoxide dismutases, catalases, lactoperoxidases, glutathione peroxidases, and peroxiredoxins. However, neurodegenerative mechanisms that disrupt mitochondrial dysfunction can induce elevated ROS production and accumulation, further damaging not only the mitochondria themselves, but also contributing to cellular distress.

Common neurodegenerative disorders such as Alzheimer's disease, Parkinson's disease, and amyotrophic lateral sclerosis (ALS) have shown evidence of mitochondrial dysfunction contributing to disease mechanisms. For instance, treatment of hippocampal neurons with low concentrations of neurotoxic Aβ 25-35 peptide significantly affected fast transport of mitochondria (Rui et al., 2006). Furthermore, analysis of hippocampal tissue from Alzheimer's patients showed a reduction of key mitochondrial fission and fusion proteins in neuronal processes and an accumulation in the neuron soma, suggesting that altered mitochondrial distribution may be associated with disease pathophysiology (Wang et al., 2009). Likewise, in Parkinson's disease, it has been shown that disease-related mutations affect mitochondrial properties. In

particular, hereditary early-onset Parkinson's disease has been linked to altered expression of parkin and PINK1 proteins, which are both targeted from the cytoplasm into damaged, depolarized mitochondria to mediate mitophagy (Narendra et al., 2010). In addition, parkin and PINK1 have been demonstrated to alter transport and distribution of mitochondria (Bueler, 2009). Similarly, it was recently shown in a non-hereditary Parkinson's disease model utilizing 1-methyl-4-phenylpyridinium ion (MPP^+) that mitochondrial transport was altered in dopamine neurons, notably decreasing anterograde and increasing retrograde trafficking (Kim-Han et al., 2011). In familial ALS, as mimicked by the Cu/Zn superoxide dismutase-1 (SOD-1) mutant mouse model, anterograde mitochondrial transport was significantly reduced, and mitochondria were found to be increasingly dispersed in the axons (De Vos et al., 2007). Mitochondrial energy metabolism in the brain and spinal cord was impaired in these mutant mice, and there was a decrease in calcium-loading capacity of mitochondria prior to disease onset and motor symptoms (Mattiazzi et al., 2002; Damiano et al., 2006). Finally, in sporadic ALS patients, fragmented and swollen mitochondria were observed in the soma and proximal axons of motor neurons in the anterior horns (Sasaki and Iwata, 2007).

More recently in MS, which has traditionally been considered an auto-inflammatory neurologic disorder, there is now evidence of neurodegeneration associated with mitochondrial dysfunction. For instance, several past studies have correlated mitochondrial abnormalities with MS pathophysiology, including the presence of oxidative damage to mitochondrial DNA in chronic MS plaques (Lu et al., 2000) and the reduction of mitochondrial respiratory chain complex I and complex III activity as well as

mitochondrial transcripts in MS patient brain (Dutta et al., 2006). In addition, a recent paper utilizing live imaging of transgenic mice with fluorescence-labeled neurons and mitochondria showed that mitochondrial morphology changes preceded demyelination and axonal damage in the murine MS model experimental autoimmune encephalomyelitis (EAE) (Nikic et al., 2011). This particular result was also demonstrated in lesioned tissue from patient brain biopsies, in which quadruple immunostaining of axons, myelin, mitochondria, and cell infiltration revealed changes in mitochondrial morphology even in the absence of demyelination and axonal damage. Overall, the studies described here suggest that mitochondrial dysfunction may be a key component of neurodegenerative pathways in a multitude of neurologic diseases.

A key mediator of mitochondrial dysfunction is the permeability transition pore (PTP). The PTP is a transient pore that opens upon various inducers, including Ca^{2+} and reactive oxygen species (ROS) (Bernardi et al., 2006). Pathologic opening of this pore leads to a series of events including the influx of solutes, matrix expansion, mitochondrial swelling, membrane rupture, and finally release of cytochrome C into the cytoplasm activating caspases and cell death pathways. While the components of the pore have yet to be defined, it has been established that cyclophilin D is a key regulatory component of the PTP (Basso et al., 2005). CyPD inhibition via both genetic and pharmacologic manipulation has demonstrated that this mitochondrial matrix protein plays a significant role in mediating pore opening and cell death. For instance, CyPD-KO mice generated by knocking out the *ppif* gene encoding the protein are viable, and

interestingly, the mitochondria still do undergo permeability transition, but require significantly more Ca^{2+} to induce pore opening (Basso et al., 2005; Forte et al., 2007).

CyPD-KO mice have been used in a variety of *in vitro* and *in vivo* studies, and the results indicate protection associated with CyPD elimination. *In vivo*, CyPD-KO mice have demonstrated significant protection in several animal models mimicking human diseases, including liver damage, ischemic/reperfusion of the heart, and ischemic/traumatic brain injury (Baines et al., 2005; Schinzel et al., 2005). Furthermore, CyPD-KO mice are protected in many neurodegenerative disease models, including Alzheimer's disease and MS. An extensive paper by Du et al. showed that CyPD and Aβ colocalized to mitochondria in both the Alzheimer's disease mouse model mAPP, which overexpresses a mutant form of human amyloid precursor protein (APP), and in Alzheimer's patient brain (Du et al., 2008). In addition, CyPD deficiency by either genetic or pharmacologic inhibition in mAPP mitochondria resulted in a higher buffering capacity of Ca^{2+} and greater resistance to swelling. Interestingly, CyPD-KO mice performed significantly better than WT mice in behavioral tests analyzing spatial learning and memory. In terms of the MS model EAE, CyPD-KO mice were found to have reduced clinical weakness and paralysis, and also showed significant axonal protection in spinal cords without notable alteration of MOG peptide immunoreactivity (Forte et al., 2007). In addition, it was demonstrated that *in vitro* that CyPD-KO neurons were protected from oxidative stressors.

Similarly, alteration of upstream inducers of PTP opening such as mitochondrial ROS can provide axonal protection as indicated by the results described in Section II. Briefly,

the elimination of p66, a redox enzyme that generates mitochondrial ROS, reduced the extent of axonal damage in spinal cords and optic nerves following EAE induction without altering MOG peptide immunoreactivity.

While these results suggest that p66 elimination incurs axonal protection, the nature of the *in vivo* studies limits the ability to analyze its effects in neurons specifically and to observe temporal changes. Therefore, to further investigate how p66 elimination affects neurons and whether it indeed mediates PTP opening downstream to promote mitochondrial dysfunction and cell death, a range of assessments were performed to analyze cellular dynamics, in particular, mitochondria-related dynamics, in p66-KO and WT neurons. More specifically, cell viability and mitochondrial properties, including changes in morphology, transport, and ROS production, were assessed to examine and compare potential differences between the two genotypes.

With regards to the *in vitro* studies, the objective was to develop a controlled experimental environment in which the p66-KO and WT neurons could be subjected to various conditions and subsequently characterized in multiple ways. As previously mentioned, the proposed neurodegenerative pathways in MS involve the pathologic generation of ROS by activated immune cells in an acute inflammatory attack, and by dysfunctional mitochondria during both acute and chronic stages of disease (Su et al., 2009). Therefore, to mimic a state of oxidative stress *in vitro*, the neurons were treated with different concentrations of nitric oxide (NO) and hydrogen peroxide (H_2O_2), and then assessed for general viability as well as specific aspects of mitochondrial structure and function.

In particular, the characterization of mitochondria in the treated p66-KO and WT neurons focused on changes in morphology, ROS production, and transport. The rationale for assessing these parameters was as follows. For one, mitochondrial morphology changes have been shown to correlate with organelle dysfunction in numerous studies. Normally branched and elongated in appearance, mitochondria can undergo severe fragmentation and become short and round in morphology following treatment with stressors and pro-apoptotic stimuli (Barsoum et al., 2006). Such morphologic changes have been shown to occur in both *in vitro* and *in vivo* settings, including the treatment of cultured neurons with the NO donor S-nitrosocysteine, and following middle cerebral artery occlusion and reperfusion in mice. Similarly, in the aforementioned paper by Nikic et al. it was demonstrated that significant changes in mitochondrial morphology occurred prior to perceivable axonal degeneration (Nikic et al., 2011). Specifically, there was a significant presence of dysmorphic mitochondria in axons that were swollen but still intact with preserved myelin, and notably, these morphology changes coincided with mitochondrial dysfunction as determined by simultaneous assessment of mitochondrial membrane potential. Furthermore, treatment of spinal cord axons *in vivo* with oxidative agents H_2O_2 and NO donor spermine NONOate resulted in apparent mitochondrial morphology changes. Mechanistically, the mitochondrial swelling and fragmentation is likely associated with altered fission and fusion dynamics as well as PTP formation, which allows for influx of solutes into the mitochondrial matrix (Perkins et al., 2009; Chen and Chan, 2009). Therefore, given the role of p66 in mitochondrial ROS production and ensuing

pathologic PTP opening, analysis of mitochondrial morphologic changes may show differences between the p66-KO and WT neurons.

In addition, the parameter of mitochondrial ROS production was utilized in the *in vitro* studies to assess and compare mitochondrial function and integrity in p66-KO and WT neurons. Mitochondria are major producers of ROS due to oxidative phosphorylation and the constant transference of electrons along the electron transport chain to reduce O_2. Under normal conditions, mitochondria are able to regulate ROS levels by the presence of enzymes such as superoxide dismutases and catalases, which convert the harmful ROS into less damaging reactants. However, during increased cellular stress, pathologic levels of mitochondrial ROS may be poorly controlled, leading to the disruption of mitochondrial function and the damage of mitochondrial components such as DNA, proteins, and lipids (Dutta et al., 2006). In addition, the elevated ROS levels may activate PTP opening and ensuing cell death pathways (Petronilli et al., 1994). Interestingly, cytoplasmic ROS can serve as a cellular distress signal to mitochondria and mediate the initiation of apoptotic pathways. In a recently published paper, the authors showed that treatment of HeLa cells with selenite, which increases intracellular ROS, resulted in transient mitochondrial membrane potential changes and superoxide flashes that preceded mitochondrial fragmentation and apoptosis (Ma et al., 2011). Furthermore, p66 has been proposed as a signaling molecule that serves as a cellular ROS sensor and targets to mitochondria to amplify mitochondrial ROS and mediate apoptotic pathways via PTP opening (Gertz and Steegborn, 2010). Thus, the comparative analysis of mitochondrial ROS production in

the p66-KO and WT neurons may provide insight into mitochondrial integrity following oxidative stress, and the mechanisms by which p66 elimination is neuroprotective.

The final assessment for characterizing p66 elimination in neurons was the analysis of mitochondrial transport. Due to the unique structure and function of neurons, intact mitochondrial transport is particularly crucial to cell integrity and survival, providing and maintaining ATP sources and ion homeostasis along the extensive processes. While p66 may not be directly associated with mitochondrial transport mechanisms, it is involved in mitochondrial integrity via the regulation of mitochondrial ROS production and downstream PTP activation. As of now, mitochondrial transport has not yet been well characterized, especially with regards to how changes in mitochondrial dynamics alter transport properties. Therefore, the comparative analysis of mitochondrial transport in treated p66-KO and WT neurons may provide intriguing results on the impact of p66 elimination and its downstream effects on mitochondrial transport.

Overall, based on the protective effects shown *in vivo* in the EAE studies, I hypothesized that p66-KO neurons treated with oxidative stressors *in vitro* would be more protected compared to WT neurons. Furthermore, I hypothesized that the p66-KO neurons would show reduced changes in mitochondrial morphology, ROS production, and transport resulting from p66 elimination and associated preservation of mitochondrial integrity.

III. Methods

Animals

p66-KO mice and WT controls were maintained as homozygotes in a C57BL/6 background (Migliaccio et al., 1999). All experimental procedures were conducted following NIH guidelines under an Institutional Animal Care and Use Committee-approved protocol from the Oregon Health & Science University.

Cell viability experiments

For each experiment, hippocampi were obtained from post-natal mouse pups (P0-P2) and incubated for 30-35 minutes at 37°C in a solution of 2 mg/mL papain (Worthington Biochemical Corp., Lakewood, NJ) in B27/Neurobasal A medium (Invitrogen, Carlsbad, CA) with 0.5 mM glutamine (Sigma, St. Louis, MO, USA). The hippocampi were then transferred into 2 mL of culture medium [B27/Neurobasal A medium with 0.5 mM glutamine and 50 mg/L gentamicin (Sigma, St. Louis, MO)] and triturated ten times with a 1000μL pipette tip, followed by ten times with a 200μL pipette tip. Approximately 2 mL of the supernatant was transferred into a new tube, and the remaining tissue was resuspended in another 2 mL of medium and triturated as described above. The cells were counted by hemocytometer and seeded on 6 well plates pre-coated with 10 μg/mL poly-d-lysine (PDL) (Sigma, St. Louis, MO) at a density of 100,000 cells/well. After 24 hr incubation in a humidified incubator at 37°C and 5% CO_2, the medium was replaced with fresh culture medium.

The neuronal cultures were maintained for one week before experimental manipulation. Prior to treatment with either diethylenetriamine/nitric oxide adduct (DETA-NO) or H_2O_2 (Sigma, St. Louis, MO), the cells were washed with Neurobasal A medium/0.5 mM glutamine. Half of the 6 wells were designated control wells and

incubated with Neurobasal A medium/0.5 mM glutamine. The other wells were designated treatment wells and incubated with different concentrations of DETA-NO (100, 250, and 500 µM) or H_2O_2 (100, 250, 500 µM and 1 mM) in Neurobasal A medium/0.5 mM glutamine. The DETA-NO treatments were incubated for 1 hr at room temperature to allow for the generation and release of nitric oxide. Cells treated with H_2O_2 were incubated for 15 minutes at 37 °C, and cells treated with DETA-NO were incubated for 3 hrs at 37 °C. Following the indicated treatment period, the cells were washed twice in Neurobasal A medium/0.5 mM glutamine and returned to the incubator in fresh culture medium. Neuronal viability was assessed 24 hours later by incubating the cells in 1µM Calcein AM (AnaSpec, San Jose, CA) for 30 minutes at 37 °C, and manually counting live neurons based on morphologic appearance and presence of green fluorescent dye at 20X with a fluorescence inverted microscope. Each well was divided and marked into 8 regions, and 3 random areas were counted per region. A total of 72 random areas were counted per treatment or control group per plate. The cell viability percentage was calculated per plate as follows: (live cell count in treatment group)/(live cell count in control group) x 100. All analyses were done blinded to genotype.

Qualitative images of the cell viability studies were taken with either a widefield inverted microscope at 10X or with a Zeiss LSM710 confocal microscope at 5x.

Mitochondrial morphology experiments

Post-natal neurons were dissociated from hippocampal tissue as described above, and 1-2 million cells were pelleted and resuspended in 100 µL of nucleofection solution

with 3 µg each of the mito-GFP plasmid and mCherry–β-actin plasmid (generously provided by Dr. Gary Banker at OHSU). The cell/plasmid solution was electroporated following the Amaxa electroporation system protocol (Amaxa, Lonza, Basel, Switzerland) for post-natal neurons using program O-05. Following electroporation, the cells were counted and plated in culture medium at 100,000 cell/well in 6 well plates, with each well containing a 25 mm glass coverslip coated overnight with 10 µg/mL PDL. After 24 hr incubation in a humidified incubator at 37°C and 5% CO_2, the medium was replaced with fresh culture medium.

Week-old cultures were treated with either the control medium (Neurobasal A medium/0.5 mM glutamine), 25 µM H_2O_2, or 500µM DETA-NO for 1 hr at 37°C. The cells were then washed twice with Neurobasal A medium/0.5 mM glutamine and fixed with 4% paraformaldehyde for 20 minutes at 37°C. Following fixation, the cells were washed twice with 1X PBS, and the coverslips were mounted on slides with Prolong Gold Anti-Fade (Invitrogen, Carlsbad, CA). The slides were imaged with a Zeiss LSM710 confocal microscope using a 63X oil objective. For each randomly chosen neuron, a Z-stack of the axon was imaged (0.38 µm sections; 8-10 sections per neurite). Each z-stack was converted into a 3D image and analyzed by Bitplane Imaris ™ software (BitPlane Inc., Saint Paul, MN). To quantify mitochondrial morphology changes, mitochondria in each image were selected by thresholding and analyzed using the Ellipsoid Axis C parameter (Figure 2D). Mitochondrial length was defined as the Ellipsoid Axis C parameter X 2. All analyses were done blinded to genotype.

Mitochondrial ROS production experiments

Post-natal hippocampal neurons were electroporated with mito-GFP plasmid and plated on 25mm PDL-coated glass coverslips in 6 well plates as described above. Week old cells were treated with either the control medium (Neurobasal A medium/0.5 mM glutamine), 25 µM H_2O_2, or 500µM DETA-NO for 1 hr at 37°C. Afterwards, the cells were washed twice with Neurobasal A medium/0.5 mM glutamine and incubated with 1µM Mitosox Red (Invitrogen, Carlsbad, CA) at 37°C for 10 minutes. The cells were then washed twice with Neurobasal A/0.5 mM glutamine, fixed with 4% paraformaldehyde for 20 minutes at 37°C, and washed twice with 1X PBS. The coverslips were mounted onto slides with Prolong Gold Anti-Fade.

The slides were imaged with a Zeiss LSM710 confocal microscope using a 63X oil objective. Axons of neurons expressing mito-GFP were imaged in both red and green channels to capture mitochondrial GFP expression and corresponding Mitosox Red staining. Images were analyzed using Metamorph software (Molecular Devices, Sunnyvale, CA) to acquire average intensity measurements of randomly selected mitochondria. Between 20-30 axonal mitochondria were analyzed per image.

Mitochondrial transport experiments

Post-natal hippocampal neurons were electroporated with mito-GFP plasmid and plated on 18mm PDL-coated glass coverslips in 6 well plates (2 coverslips/well) as described above. Week old coverslips were used for transport imaging on a Yokogawa CSU-10 spinning disk confocal head mounted on a Nikon TE2000 inverted microscope with PFS attachment for continuous Z-drift compensation during live-cell imaging.

Neurons were imaged with a 40X oil objective heated to ~34°C. Between 5-6 neurons were randomly chosen for recording per coverslip, and a baseline pretreatment recording of transport was carried out for each corresponding axon in imaging buffer. The neurons were then treated with either 25 μM H_2O_2 or 500μM DETA-NO in imaging buffer, and recordings were taken for an entire hour, cycling between the selected axons.

The mitochondrial transport movies were analyzed using Metamorph software. Kymographs were generated using Metamorph journals (developed by Banker lab, OHSU), and anterograde/retrograde movement vectors were marked manually. Movement information per transport movie, including the number of anterograde and retrograde events per 100μm, was acquired by using Metamorph journals and Excel spreadsheets developed by the Banker lab.

Statistics

All statistical comparisons between the p66-KO and WT groups were calculated using the Student's T-test for groups with unequal variance. Statistical significance was defined as $p<0.05$.

IV. Results

p66-KO neurons are more resistant to oxidative challenges compared to WT neurons

Reactive oxygen and nitrogen species generated by activated immune cells have been proposed to induce mitochondrial dysfunction and neurodegeneration in EAE and MS. Therefore, to determine whether p66 elimination protects neurons from the deleterious

effects of oxidative stress, p66-KO and WT neuronal cultures were treated with physiologic and pathologic levels of NO and H_2O_2 and cell viability was assessed 24 hours later (Malinski et al., 1993; Hyslop et al., 1995; Solenski et al., 2003). While similar studies on p66-KO and WT neuronal cultures prepared from adult brain cortices have been previously addressed in Section II of this thesis, these "adult" cultures have not been well characterized and are generally less uniform with a high glial cell percentage. However, given that MS is a neurologic disease usually affecting adults, the utilization of these "adult" cultures for experimentation is intriguing and the results provide compelling evidence of neuroprotection associated with p66 elimination. To confirm these neuroprotective effects in a well-characterized culture system, postnatal hippocampal cultures were utilized for the experiments in this section.

The results showed that p66 elimination promoted significant neuroprotection in the p66-KO postnatal hippocampal cultures following treatment with varying concentrations of either NO or H_2O_2. Specifically, a range of physiologic and pathologic H_2O_2 concentrations was analyzed (100, 250, 500 μM, and 1mM), and p66-KO cultures showed significantly greater cell viability compared to WT cultures (*Figure 1A*). At the lowest concentration of H_2O_2 tested (100 μM), p66-KO cultures demonstrated an average of 89.83±0.60% survival compared to 77.80±1.04% survival in the WT neurons (*p=0.00081*). At the mid-range concentration of 500 μM H_2O_2, p66-KO cultures showed an average of 72.43±0.90% survival compared to 25.90±1.93% in the WT cultures *(p=0.00015*). At the highest tested concentration of 1mM H_2O_2, p66-KO cultures averaged 8.83±0.92% survival compared to 2.07±0.42% in the WT cultures (*p=0.0042*).

Based on the concentration vs. survival percentage curves generated, the H_2O_2-associated EC50 for 50% survival was approximately 280 μM for WT neurons and 680 μM for p66-KO neurons, more than twice the WT concentration.

In addition, p66-KO and WT cell cultures were treated with three different concentrations of NO donor DETA-NO. According to previous studies, 1000 μM DETA-NO equates to approximately 7μM NO by 4 hours of incubation, and this concentration correlates with NO levels measured with brain microdialysis during brain ischemia/reperfusion (1-10μM) (Malinski et al., 1993; Solenski et al., 2003). Therefore, the concentrations of DETA-NO utilized in the cell viability experiments (100-500 μM) are likely in the physiologic to pathologic range. Similar to the H_2O_2 results, p66 elimination was found to be associated with significant neuroprotection following DETA-NO treatment (*Figure 1B*). At the lowest concentration of 100 μM DETA-NO, p66-KO cultures had an average 94.93±0.07% survival compared to 70.60±0.40% survival in the WT neurons (*p=0.00419*). At the mid-range concentration of 250 μM DETA-NO, p66-KO cultures averaged 88.90±0.60% survival compared to 44.70±1.00% in the WT cultures (*p=0.00105*). Finally, at the highest concentration of 500 μM DETA-NO, cell viability averaged 84.00±0.80% in p66-KO cultures and 20.90±2.10% in the WT cultures (*p=0.00475*). The DETA-NO-associated EC50 was approximately 220 μM for WT neurons, and beyond experimental treatment concentrations for the p66-KO neurons.

Overall, the cell viability results indicate that p66 elimination in neurons provides significant protection in response to agents implicated in MS neurodegenerative pathways, and furthermore, support the *in vivo* and *in vitro* data reported in Section II.

p66-KO axonal mitochondria show greater preservation of mitochondrial length following oxidative stress

Mitochondrial morphology has been associated with axonal damage and oxidative stress in both *in vitro* and *in vivo* studies (Pinton et al., 2007; Nikic et al., 2011). In particular, past studies on mouse embryonic fibroblasts (MEFs) treated with H_2O_2 demonstrated that mitochondrial morphology was considerably preserved with p66 elimination. Specifically, mitochondria of treated p66-KO MEFs remained thin and elongated in structure compared to those of WT MEFs, which were considerably rounder and shortened (Pinton et al., 2007).

To assess whether mitochondrial morphology changes occurred in p66-KO neurons, hippocampal cultures electroporated with mito-GFP and mCherry beta-actin plasmids were treated with 25μM H_2O_2, 500μM DETA-NO, or the control medium for an hour, and were subsequently analyzed for changes in mitochondrial structure. Utilizing Imaris software, 3D reconstructions of axons were generated from imaged z-stacks, and mitochondrial length was assessed by the ellipsoid axis C parameter (*Figure 2*). In the control medium-treated neurons, the average mitochondrial length was similar between the WT and p66-KO neurons (WT 2.10±0.11μm, p66-KO 2.08±0.12 μm; *p=0.45638*). Following treatment with either DETA-NO or H_2O_2, both p66-KO and WT neuronal cultures showed decreases in mitochondrial length. In cultures treated with 25 μM H_2O_2, WT mitochondria were shortened by 0.48±0.03 μm compared to 0.19±0.08 μm for the p66-KO mitochondria, and this difference was found to be statistically significant *(p=0.00759).* The resultant WT mitochondria were an average length of 1.62±0.03 μm

compared to 1.89±0.08 μm for the p66-KO mitochondria (*p=0.01006*). Similarly, in cultures treated with 500 μM DETA-NO, WT mitochondria were significantly more shortened by 0.31±0.02 μm compared to 0.06±0.01 μm for the p66-KO mitochondria (*p=0.00014*). The resultant WT mitochondria were an average length of 1.79±0.02 μm compared to 2.02±0.01 μm for the p66-KO mitochondria (*p=0.0002*). Overall, the results demonstrated that mitochondria were significantly more shortened in axons of treated WT neurons compared to p66-KO neurons, suggesting that p66 elimination preserves neurons mechanistically by the maintenance of mitochondrial integrity under oxidative conditions.

p66-KO axonal mitochondria demonstrate less ROS changes following oxidative stress

The role of p66 in cellular mechanisms revolves around the generation of mitochondrial ROS. In the presence of oxidative agents, p66 becomes serine phosphorylated by protein kinase C-Beta (PKCβ) and translocates into the mitochondrial intermembrane space (Giorgio et al., 2005; Pinton et al., 2007). There, p66 mediates the transference of electrons from cytochrome c to oxygen to form ROS (Giorgio et al., 2005), and it is proposed that this source of mitochondrial ROS induces pathologic PTP opening and eventual cell death activation.

To determine whether p66 elimination in neurons impacts mitochondrial ROS generation in the context of EAE and MS, p66-KO and WT cultures were treated with control medium or oxidative agents implicated in neurodegenerative pathways (25μM H_2O_2, 500μM DETA-NO) and then assessed for changes in mitochondrial ROS levels in

axons via Mitosox staining. The results demonstrated that mitochondria of WT cultures had significantly greater increases in Mitosox intensity levels compared to mitochondria of p66-KO neurons following treatment (*Figure 3*). Specifically, mitochondria in WT neurons treated with 25 μM H_2O_2 showed a 1.48±0.12X increase in Mitosox intensity compared to a 1.03±0.03X increase in mitochondria of p66-KO neurons (*p=0.00286*). Similarly, mitochondria in WT neurons treated with 500 μM DETA-NO showed a 1.37±0.12X increase in Mitosox intensity compared to minimal change (0.96±0.04X) in mitochondria of p66-KO neurons (*p=0.00322*). Overall, these results suggest that mitochondrial ROS levels increase significantly more in axons of WT neurons compared to p66-KO neurons following oxidative insults.

p66 elimination does not protect mitochondrial transport in neurons following oxidative stress

The final assessment of mitochondrial properties in p66-KO and WT neurons addressed changes in mitochondrial transport. While mitochondrial transport is not yet well characterized and understood, multiple studies have shown that changes in mitochondrial transport occur in various neurodegenerative disease models (Chang et al., 2006; Baloh et al., 2007; Kim-Han et al., 2011). Therefore, to assess the effects of p66 elimination on mitochondrial transport in the context of EAE and MS, mitochondrial transport was recorded in axons of p66-KO and WT neurons prior to treatment with either 25 μM H_2O_2 or 500 μM DETA-NO, and for 50 minutes following treatment. Changes in mitochondrial transport were assessed by comparing pre-treatment transport with transport at 35-50 minutes post-treatment (*Figure 4*).

Results showed that there were similar decreases in anterograde and retrograde transport for both p66-KO and WT mitochondria following treatment with 500 μM DETA-NO. Specifically, WT mitochondria averaged 4.88±0.67 anterograde movements/100 μm prior to treatment, which significantly decreased to 3.16±0.50 movements/100 μm post-treatment (*p=0.02476*). Similarly, p66-KO mitochondria averaged 5.13±0.67 movements/100 μm prior to treatment, which significantly decreased to 3.44±0.69 movements/100 μm post treatment (*p=0.04553*). Statistically, there were no significant differences between the WT and p66-KO pre-treatment (*p=0.39732*) and post-treatment (*p=0.367*) movement frequencies. In terms of retrograde transport, WT mitochondria averaged 6.56±0.66 movements/100 μm prior to treatment, which significantly decreased to 1.87±0.35 movements/100 μm post-treatment (*p=1.02E-06*). Likewise, p66-KO mitochondria averaged 5.07±0.87 movements/100 μm prior to treatment, which significantly decreased to 1.57±0.44 movements/100 μm post treatment (*p=3.49E-05*). Similar to anterograde transport, there were no significant differences between the WT and p66-KO pre-treatment (*p=0.09249*) and post-treatment (*p=0.30213*) movement frequencies.

In neurons treated with H_2O_2, retrograde mitochondrial transport was decreased in both axons of p66-KO and WT neurons. Average WT transport decreased from 6.74±1.07 to 2.37±0.62 movements/100 μm post-treatment compared to a decrease from 5.14±0.59 to 2.86±0.46 movements/100 μm in the p66-KO neurons. Again, there were no significant differences between the WT and p66-KO pre-treatment (*p=0.10023*) and post-treatment (*p=0.26346*) movement frequencies. Interestingly, p66-KO neurons

treated with 25 μM H_2O_2 showed significantly preserved anterograde mitochondrial transport compared to WT neurons. Specifically, WT mitochondria averaged 5.63±0.84 movements/100 μm prior to treatment, which significantly decreased to 2.50±0.35 movements/100 μm post-treatment. In contrast, p66-KO mitochondria averaged 5.43±0.68 movements/100 μm pre-treatment and 4.12±0.63 movements/100 μm post-treatment (*p=0.0831*). Comparison of p66-KO and WT transport data confirmed that the pre-treatment transport frequencies were similar between the two genotypes (*p=0.42587*) but that the post-treatment frequencies were significantly different (*p=0.01652*). While an intriguing result, further experimentation will be necessary to determine whether p66 elimination has a significant effect on mitochondrial anterograde transport, especially given that anterograde movement was similarly decreased in p66-KO and WT neurons following treatment with the milder stressor DETA-NO. Overall, the results of the mitochondrial transport experiments demonstrate that oxidative insults significantly decrease both anterograde and retrograde movement in neurons, though whether p66 elimination may play a role in preserving some anterograde transport remains to be determined.

V. Discussion

In this report, p66-eliminated neurons were protected in the presence of oxidative stressors implicated in EAE and MS neurodegenerative pathways. Specifically, greater cell viability was demonstrated in p66-KO cultures compared to WT cultures at various treatment concentrations of H_2O_2 and DETA-NO. To further address the underlying mechanisms associated with increased cell viability in the p66-KO neurons, changes in

mitochondrial morphology, ROS production, and transport were characterized following treatment. The results showed that mitochondrial morphology changes were less prominent in the p66-KO neurons compared to the WT neurons, with significantly greater preservation of mitochondrial length. In addition, the p66-KO neurons exhibited less elevated mitochondrial ROS levels compared to WT neurons following oxidative insults. Finally, p66-KO and WT neurons showed similar decreases in retrograde mitochondrial transport following either H_2O_2 or DETA-NO treatment and in anterograde transport following DETA-NO treatment, though anterograde transport was notably protected in H_2O_2-treated p66-KO neurons. Overall, these findings suggest that p66 elimination incurs greater neuronal robustness and preservation of mitochondrial integrity following oxidative insults implicated in EAE- and MS-associated degenerative mechanisms.

Importantly, these findings support our current understanding of p66 and its role in cellular mechanisms. As previously discussed, p66 serves as a ROS sensor and amplifier under conditions of cellular stress by generating mitochondrial ROS via cytochrome c oxidation and oxygen reduction (Giorgio et al., 2005). Subsequently, elevated mitochondrial ROS has been shown to induce PTP opening as demonstrated by mitochondrial swelling, rupture, and release of cytochrome c to activate apoptotic pathways (Petronilli et al., 1994; Vercesi et al., 1997; Yang et al., 2007).

The results reported here correlate with this proposed pathway, as shown by the greater regulation of ROS levels following cellular stress induced by DETA-NO or H_2O_2 treatment. Based on the Mitosox analyses of treated neurons, there were significantly

less increases in mitochondrial ROS levels in the p66-KO neurons compared to WT neurons, suggesting that p66 elimination reduces the amplification of mitochondrial ROS following oxidative insult. This, in turn, provides greater preservation of mitochondrial integrity as visualized by mitochondrial morphology. The studies here demonstrated that mitochondrial length was preserved in the p66-KO neurons compared to the WT neurons. Previous studies have correlated changes in mitochondrial morphology with mitochondrial integrity and activity, including the balance of fission and fusion events and mitophagy of damaged mitochondria. In particular, it has been shown that the dissipation of the mitochondrial membrane potential affects fusion and induces mitochondrial fragmentation (Legros et al., 2002). Furthermore, mitochondrial morphology changes may be correlated to matrix swelling mediated by pathologic opening of the permeability transition, release of cytochrome c and activation of cell death pathways (Scorrano et al., 2002). Assuming that p66 elimination alters the cell crisis signal of elevated mitochondrial ROS, preserves mitochondrial integrity, and subsequently regulates PTP-mediated cell death, this would suggest greater neuronal robustness in p66-KO neurons under conditions of oxidative stress. The results of the cell viability studies support this assumption.

Interestingly, the effects of p66 elimination did not extend to preservation of mitochondrial transport, which in general was similarly decreased in both p66-KO and WT neurons following treatment with DETA-NO or H_2O_2. While mitochondrial motility is likely a reflection of the health of a cell, it is mediated by mechanisms that are currently being defined. The basic mitochondrial transport proteins of Miro and Milton have

been identified, and the importance of Ca^{2+} in transport regulation has been demonstrated as well (Wang and Schwarz, 2009). However, key aspects of mitochondrial transport remain unclear, including why a majority of mitochondria (approximately two-thirds) remain stationary and distributed along the axons, and why the mobile mitochondria display distinct motility patterns including saltatory bidirectional movements in which they frequently stop and start (Ligon and Steward, 2000; MacAskill and Kittler, 2010). Given the limited understanding of mitochondrial transport mechanisms, it is difficult to explain exactly why p66 elimination did not preserve transport frequencies, though one can speculate that mitochondrial transport mechanisms are quite complex and likely mediated by multiple cellular components not directly influenced by p66.

Overall, the characterization of p66 elimination in neurons supports previous studies demonstrating mitochondrial integrity as a key marker of neuronal viability and fate (Nikic et al., 2011). Hence, therapeutics promoting mitochondrial preservation may prove essential to current treatment regimens for neurodegenerative diseases including MS. Mitochondria-targeted drugs are currently being developed, utilizing lipophilic cations or peptides to deliver drug directly to the negatively charged mitochondrial matrix (Sheu et al., 2006; Murphy, 2008). Furthermore, drugs are being developed for specific mitochondrial components such as the PTP via cyclosporin A derivatives targeting the regulatory component CyPD, and ROS via antioxidants such as MitoQ and SS-peptides. The results reported here suggest that pharmacologic inhibition of p66 may also provide neuroprotection by the aforementioned mechanisms, and

correspondingly, the results from the *in vivo* studies of Section II have demonstrated potential physiologic protection associated with p66 elimination in the context of EAE. It will be intriguing to see whether pharmacologic p66 inhibition is neuroprotective in patients with MS and other neurodegenerative diseases.

VI. References:

Baines CP, Kaiser RA, Purcell NH, Blair NS, Osinska H, Hambleton MA, Brunskill EW, Sayen MR, Gottlieb RA, Dorn GW, Robbins J, Molkentin JD (2005) Loss of cyclophilin D reveals a critical role for mitochondrial permeability transition in cell death. Nature 434:658-662.

Baloh RH, Schmidt RE, Pestronk A, Milbrandt J (2007) Altered Axonal Mitochondrial Transport in the Pathogenesis of Charcot-Marie-Tooth Disease from Mitofusin 2 Mutations. The Journal of Neuroscience 27:422-430.

Barsoum MJ, Yuan H, Gerencser AA, Liot G, Kushnareva Y, Graber S, Kovacs I, Lee WD, Waggoner J, Cui J, White AD, Bossy B, Martinou J-C, Youle RJ, Lipton SA, Ellisman MH, Perkins GA, Bossy-Wetzel E (2006) Nitric oxide-induced mitochondrial fission is regulated by dynamin-related GTPases in neurons. EMBO J 25:3900-3911.

Basso E, Fante L, Fowlkes J, Petronilli V, Forte MA, Bernardi P (2005) Properties of the Permeability Transition Pore in Mitochondria Devoid of Cyclophilin D. Journal of Biological Chemistry 280:18558-18561.

Bernardi P, Krauskopf A, Basso E, Petronilli V, Blalchy-Dyson E, Di Lisa F, Forte MA (2006) The mitochondrial permeability transition from in vitro artifact to disease target. FEBS Journal 273:2077-2099.

Bueler H (2009) Impaired mitochondrial dynamics and function in the pathogenesis of Parkinson□s disease. Experimental Neurology 218:235-246.

Chang DTW, Rintoul GL, Pandipati S, Reynolds IJ (2006) Mutant huntingtin aggregates impair mitochondrial movement and trafficking in cortical neurons. Neurobiology of Disease 22:388-400.

Chen H, Chan DC (2009) Mitochondrial dynamics–fusion, fission, movement, and mitophagy–in neurodegenerative diseases. Human Molecular Genetics 18:R169-R176.

Damiano M, Starkov AA, Petri S, Kipiani K, Kiaei M, Mattiazzi M, Flint Beal M, Manfredi G (2006) Neural mitochondrial Ca2+ capacity impairment precedes the onset of motor symptoms in G93A Cu/Zn-superoxide dismutase mutant mice. Journal of Neurochemistry 96:1349-1361.

De Vos KJ, Chapman AL, Tennant ME, Manser C, Tudor EL, Lau K-F, Brownlees J, Ackerley S, Shaw PJ, McLoughlin DM, Shaw CE, Leigh PN, Miller CCJ, Grierson AJ (2007) Familial amyotrophic lateral sclerosis-linked SOD1 mutants perturb fast axonal transport to reduce axonal mitochondria content . Human Molecular Genetics 16:2720-2728.

Du H, Guo L, Fang F, Chen D, A Sosunov A, M McKhann G, Yan Y, Wang C, Zhang H, Molkentin JD, Gunn-Moore FJ, Vonsattel JP, Arancio O, Chen JX, Yan SD (2008) Cyclophilin D deficiency attenuates mitochondrial and neuronal perturbation and ameliorates learning and memory in Alzheimer□s disease. Nat Med 14:1097-1105.

Dutta R, McDonough J, Yin X, Peterson J, Chang A, Torres T, Gudz T, Macklin WB, Lewis DA, Fox RJ, Rudick R, Mirnics K, Trapp BD (2006) Mitochondrial dysfunction as a cause of axonal degeneration in multiple sclerosis patients. Annals of Neurology 59:478-489.

Forte M, Gold BG, Marracci G, Chaudhary P, Basso E, Johnsen D, Yu X, Fowlkes J, Bernardi P, Bourdette D (2007) Cyclophilin D inactivation protects axons in experimental autoimmune encephalomyelitis, an animal model of multiple sclerosis. Proceedings of the National Academy of Sciences 104:7558-7563.

Gertz M, Steegborn C (2010) The Lifespan-Regulator p66Shc in Mitochondria: Redox Enzyme or Redox Sensor? Antioxidants & Redox Signaling 13:1417-1428.

Giorgio M, Migliaccio E, Orsini F, Paolucci D, Moroni M, Contursi C, Pelliccia G, Luzi L, Minucci S, Marcaccio M, Pinton P, Rizzuto R, Bernardi P, Paolucci F, Pelicci PG (2005) Electron Transfer between Cytochrome c and p66Shc Generates Reactive Oxygen Species that Trigger Mitochondrial Apoptosis. Cell 122:221-233.

Hyslop PA, Zhang Z, Pearson DV, Phebus LA (1995) Measurement of striatal H2O2 by microdialysis following global forebrain ischemia and reperfusion in the rat: correlation with the cytotoxic potential of H2O2 in vitro. Brain Research 671:181-186.

Kim-Han JS, Antenor-Dorsey JA, O□Malley KL (2011) The Parkinsonian Mimetic, MPP+, Specifically Impairs Mitochondrial Transport in Dopamine Axons. The Journal of Neuroscience 31:7212-7221.

Legros F, Lombes A, Frachon P, Rojo M (2002) Mitochondrial Fusion in Human Cells Is Efficient, Requires the Inner Membrane Potential, and Is Mediated by Mitofusins. Molecular Biology of the Cell 13:4343-4354.

Ligon LA, Steward O (2000) Movement of mitochondria in the axons and dendrites of cultured hippocampal neurons. The Journal of Comparative Neurology 427:340-350.

Lu F, Selak M, O'Connor J, Croul S, Lorenzana C, Butunoi C, Kalman B (2000) Oxidative damage to mitochondrial DNA and activity of mitochondrial enzymes in chronic active lesions of multiple sclerosis. Journal of the neurological sciences 177:95-103.

Ma Q, Fang H, Shang W, Liu L, Xu Z, Ye T, Wang X, Zheng M, Chen Q, Cheng H (2011) Superoxide flashes: early mitochondrial signals for oxidative stress-induced apoptosis. Journal of Biological Chemistry: Epub ahead of print.

MacAskill AF, Kittler JT (2010) Control of mitochondrial transport and localization in neurons. Trends in cell biology 20:102-112.

Malinski T, Bailey F, Zhang ZG, Chopp M (1993) Nitric Oxide Measured by a Porphyrinic Microsensor in Rat Brain After Transient Middle Cerebral Artery Occlusion. J Cereb Blood Flow Metab 13:355-358.

Mattiazzi M, D□Aurelio M, Gajewski CD, Martushova K, Kiaei M, Beal MF, Manfredi G (2002) Mutated Human SOD1 Causes Dysfunction of Oxidative Phosphorylation in Mitochondria of Transgenic Mice. Journal of Biological Chemistry 277:29626-29633.

Migliaccio E, Giorgio M, Mele S, Pelicci G, Reboldi P, Pandolfi PP, Lanfrancone L, Pelicci PG (1999) The p66shc adaptor protein controls oxidative stress response and life span in mammals. Nature 402:309-313.

Murphy MP (2008) Targeting Antioxidants to Mitochondria by Conjugation to Lipophilic Cations In Drug-Induced Mitochondrial Dysfunction John Wiley & Sons, Inc., p. 575-587.

Narendra DP, Jin SM, Tanaka A, Suen D-F, Gautier CA, Shen J, Cookson MR, Youle RJ (2010) PINK1 Is Selectively Stabilized on Impaired Mitochondria to Activate Parkin. PLoS Biol 8:e1000298.

Nikic I, Merkler D, Sorbara C, Brinkoetter M, Kreutzfeldt M, Bareyre FM, Bruck W, Bishop D, Misgeld T, Kerschensteiner M (2011) A reversible form of axon damage in experimental autoimmune encephalomyelitis and multiple sclerosis. Nat Med 17:495-499.

Perkins G, Bossy-Wetzel E, Ellisman MH (2009) New insights into mitochondrial structure during cell death. Experimental Neurology 218:183-192.

Petronilli V, Nicolli A, Costantini P, Colonna R, Bernardi P (1994) Regulation of the permeability transition pore, a voltage-dependent mitochondrial channel inhibited by cyclosporin A. Biochimica et Biophysica Acta (BBA) - Bioenergetics 1187:255-259.

Pinton P, Rimessi A, Marchi S, Orsini F, Migliaccio E, Giorgio M, Contursi C, Minucci S, Mantovani F, Wieckowski MR, Del Sal G, Pelicci PG, Rizzuto R (2007) Protein Kinase C ß and Prolyl Isomerase 1 Regulate Mitochondrial Effects of the Life-Span Determinant p66Shc. Science 315:659-663.

Rui Y, Tiwari P, Xie Z, Zheng JQ (2006) Acute Impairment of Mitochondrial Trafficking by β-Amyloid Peptides in Hippocampal Neurons. The Journal of Neuroscience 26:10480-10487.

Sasaki S, Iwata M (2007) Mitochondrial Alterations in the Spinal Cord of Patients With Sporadic Amyotrophic Lateral Sclerosis. Journal of Neuropathology & Experimental Neurology 66:10-16.

Schinzel AC, Takeuchi O, Huang Z, Fisher JK, Zhou Z, Rubens J, Hetz C, Danial NN, Moskowitz MA, Korsmeyer SJ (2005) Cyclophilin D is a component of mitochondrial permeability transition and mediates neuronal cell death after focal cerebral ischemia. Proceedings of the National Academy of Sciences of the United States of America 102:12005-12010.

Scorrano L, Ashiya M, Buttle K, Weiler S, Oakes SA, Mannella CA, Korsmeyer SJ (2002) A Distinct Pathway Remodels Mitochondrial Cristae and Mobilizes Cytochrome c during Apoptosis. Developmental Cell 2:55-67.

Sheu S-S, Nauduri D, Anders MW (2006) Targeting antioxidants to mitochondria: A new therapeutic direction. Biochimica et Biophysica Acta (BBA) - Molecular Basis of Disease 1762:256-265.

Silver I, Erecińska M (1998) Oxygen and ion concentrations in normoxic and hypoxic brain cells. Adv Exp Med Biol 454:7-16.

Solenski NJ, Kostecki VK, Dovey S, Periasamy A (2003) Nitric-oxide-induced depolarization of neuronal mitochondria: implications for neuronal cell death. Molecular and Cellular Neuroscience 24:1151-1169.

Su K, Banker G, Bourdette D, Forte M (2009) Axonal degeneration in multiple sclerosis: The mitochondrial hypothesis. Current Neurology and Neuroscience Reports 9:411-417.

Vercesi AE, Kowaltowski AJ, Grijalba MT, Meinicke AR, Castilho RF (1997) The Role of Reactive Oxygen Species in Mitochondrial Permeability Transition. Bioscience Reports 17:43-52.

Wang X, Su B, Lee H-gon, Li X, Perry G, Smith MA, Zhu X (2009) Impaired Balance of Mitochondrial Fission and Fusion in Alzheimer□s Disease. The Journal of Neuroscience 29:9090-9103.

Wang X, Schwarz TL (2009) The Mechanism of Ca2+-Dependent Regulation of Kinesin-Mediated Mitochondrial Motility. Cell 136:163-174.

Yang J, Wu L-jun, Tashino S-ichi, Onodera S, Ikejima T (2007) Critical roles of reactive oxygen species in mitochondrial permeability transition in mediating evodiamine-induced human melanoma A375-S2 cell apoptosis. Free Radical Research 41:1099-11083.

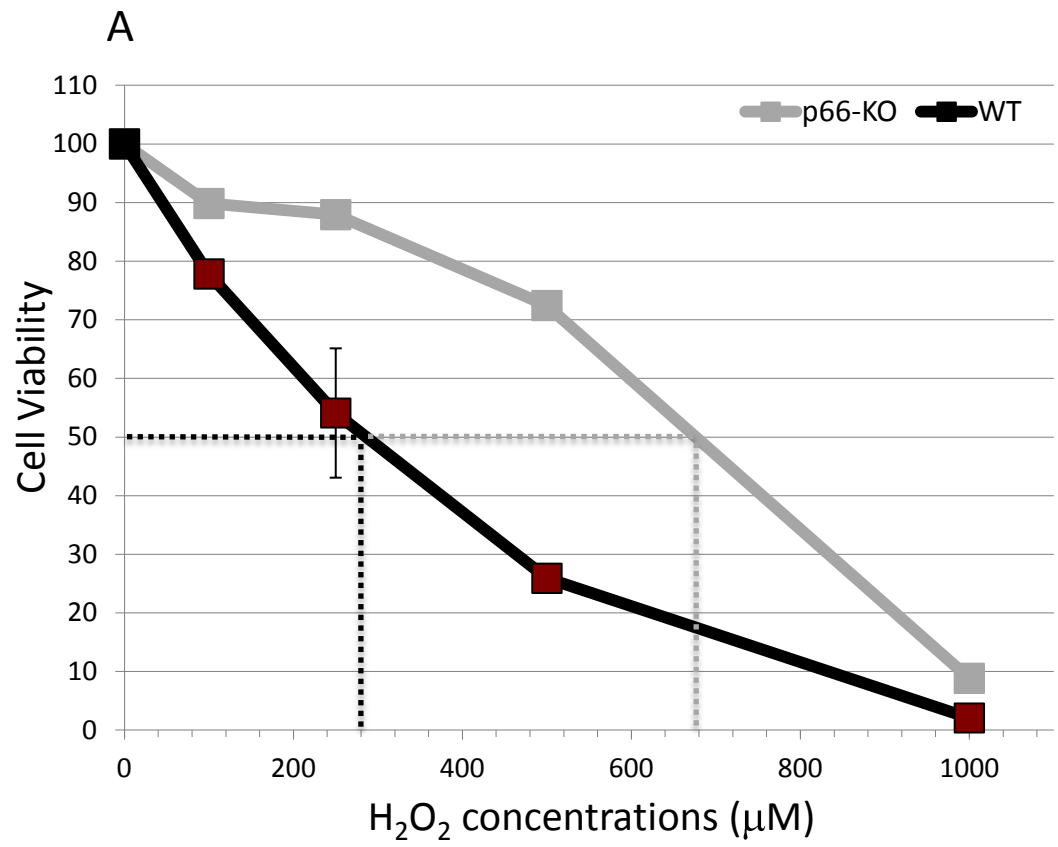
A
p66-KO
WT
Cell Viability
110
100
90
80
70
60
50
40
30
20
10
0
0
200
400
600
800
1000
H2O2 concentrations (μM)

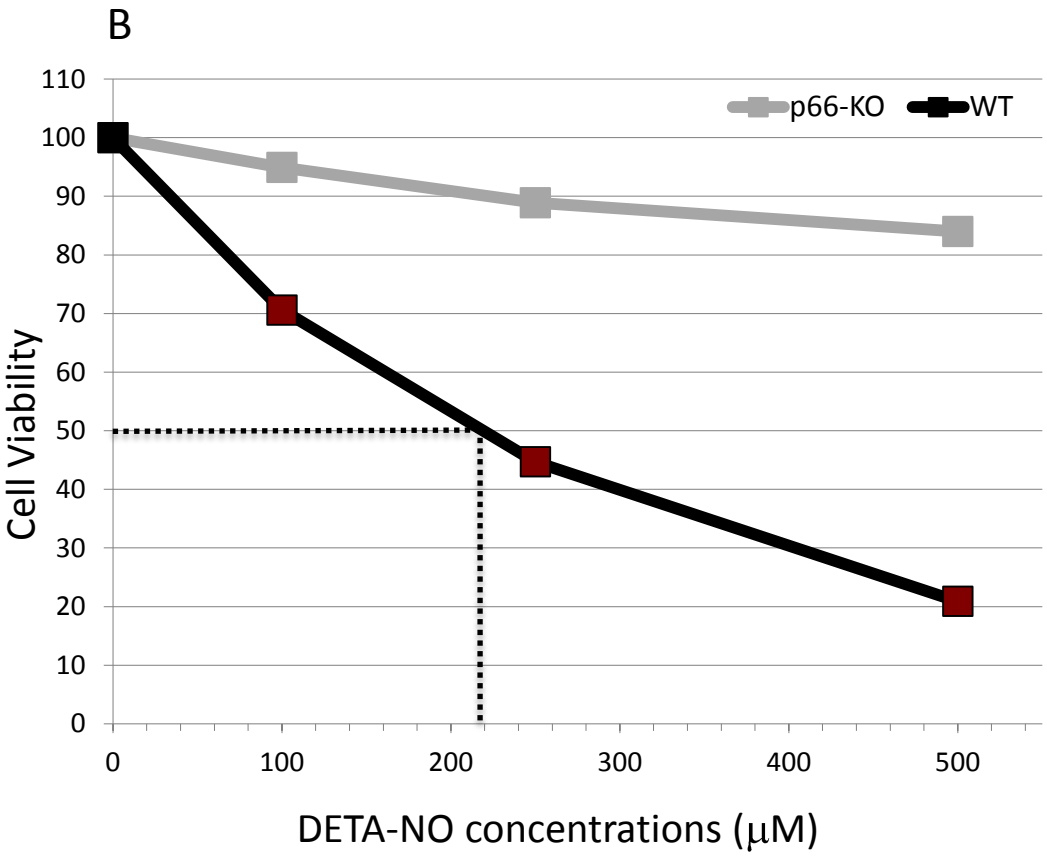
B
p66-KO
WT
Cell Viability
110
100
90
80
70
60
50
40
30
20
10
0
0
100
200
300
400
500
DETA-NO concentrations (μM)

C

Control media

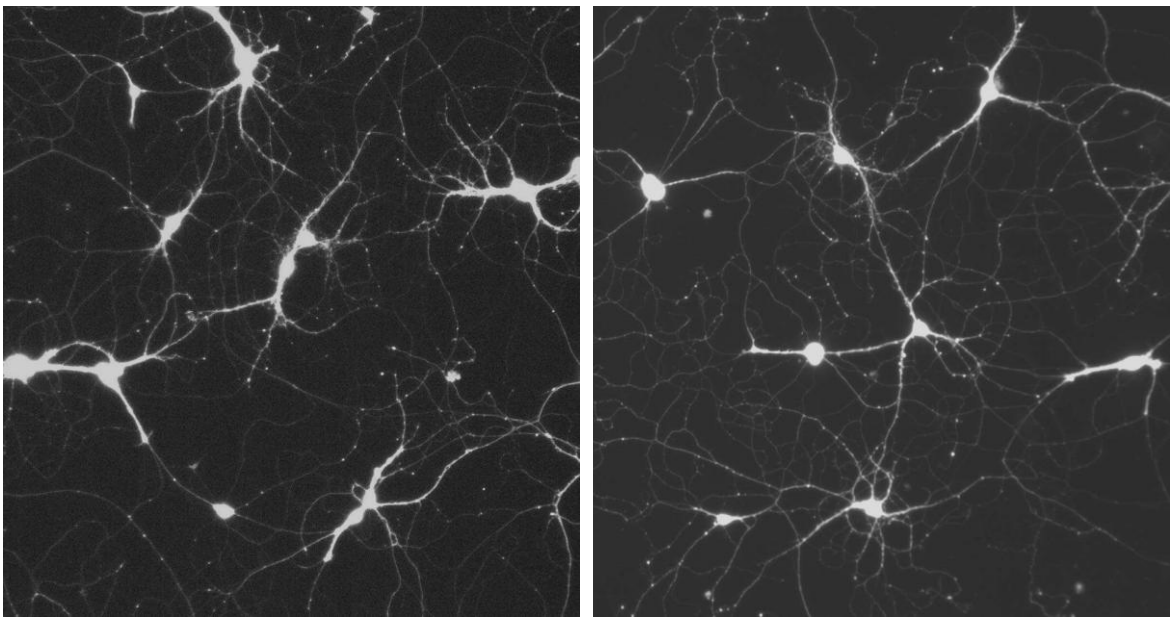

WT p66-KO

D

500 μM H_2O_2

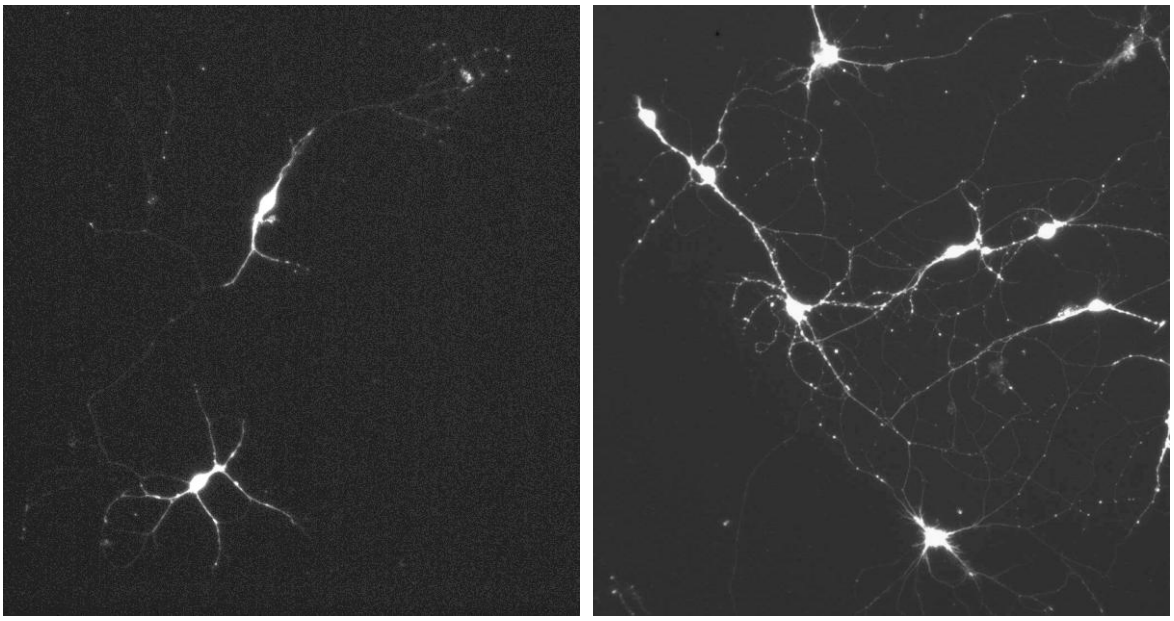

WT p66-KO

E

Control media

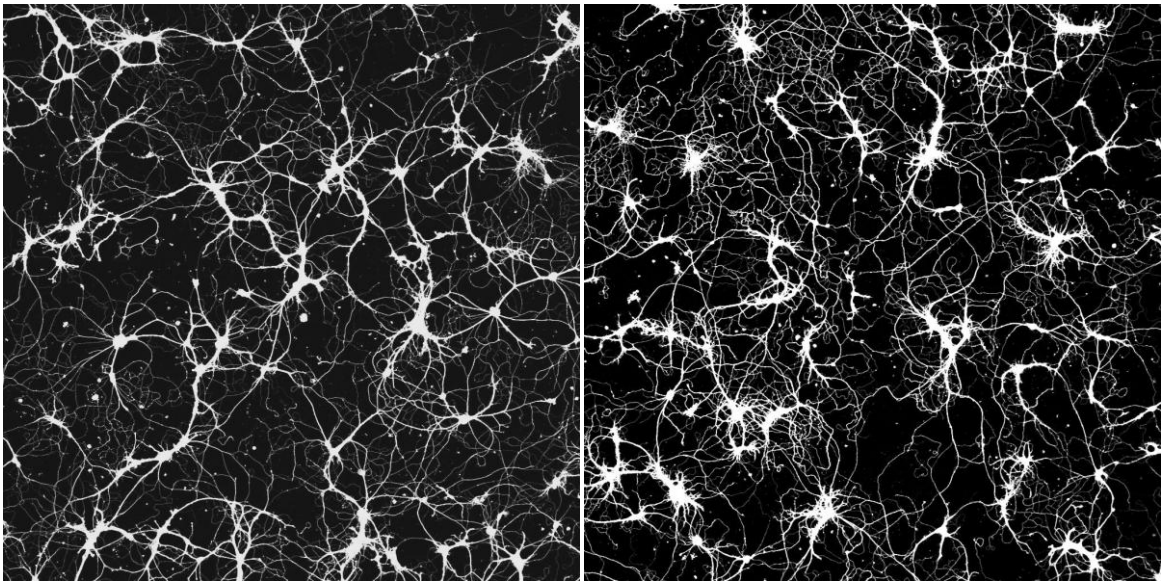

WT p66-KO

F

500 μM DETA-NO

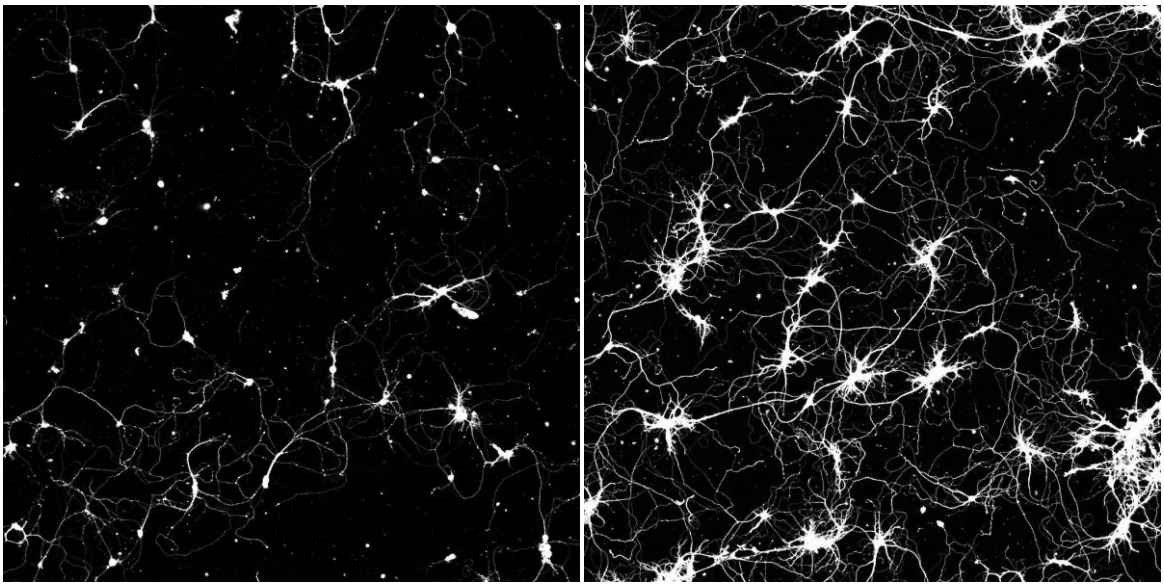

WT p66-KO

Figure 1. p66-KO post-natal hippocampal neurons showed greater protection following treatment with oxidative insults implicated in EAE and MS neurodegenerative pathways. p66-KO neurons had a significantly greater cell viability percentage compared to WT neurons when treated with various concentrations of DETA-NO (A) and H_2O_2 (B). Cell counts were obtained 24 hours post treatment. Red data points indicate significant differences between p66-KO and WT cultures at the corresponding treatment concentration (*$p<0.05$*). Dotted lines indicate approximate EC_{50} concentrations. (n per treatment/genotype = 3 cultures/; 4 plates/culture) Representative images of treated cultures taken with either a widefield inverted fluorescence microscope at 10X (C,D) or a laser scanning confocal microscope at 5X (E,F). Note the higher percentage of viable neurons in the p66-KO cultures.

A

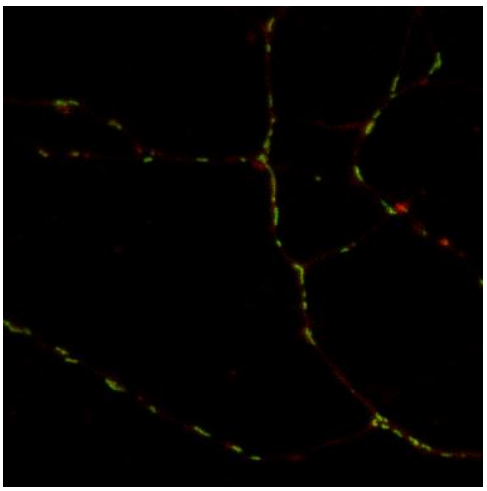

WT
Control medium

B

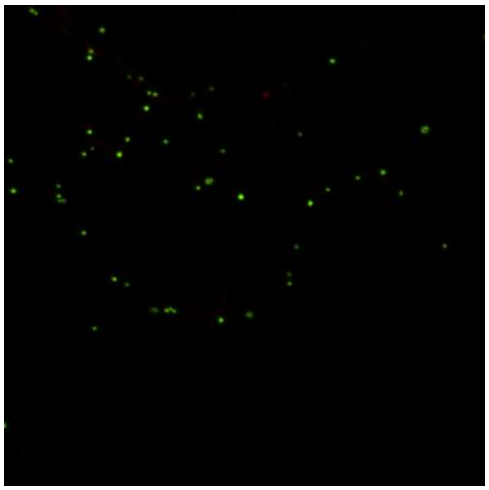

WT
25μM H_2O_2

C

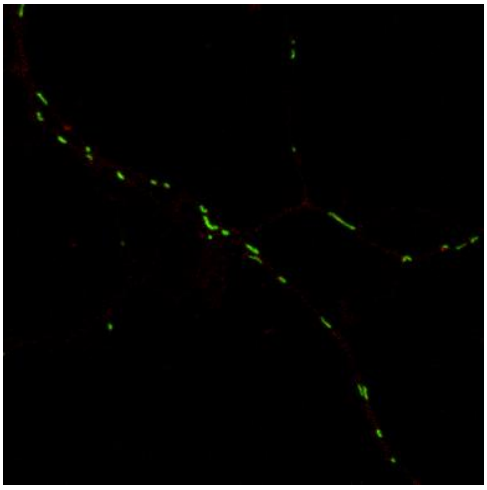

p66-KO
25μM H_2O_2

D

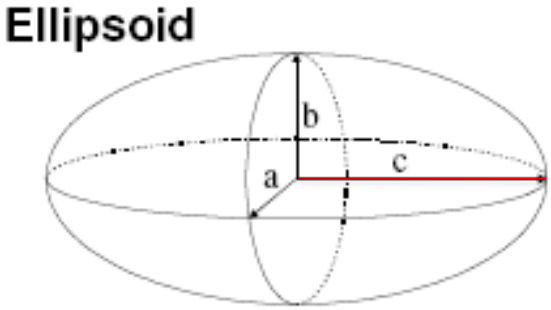

E

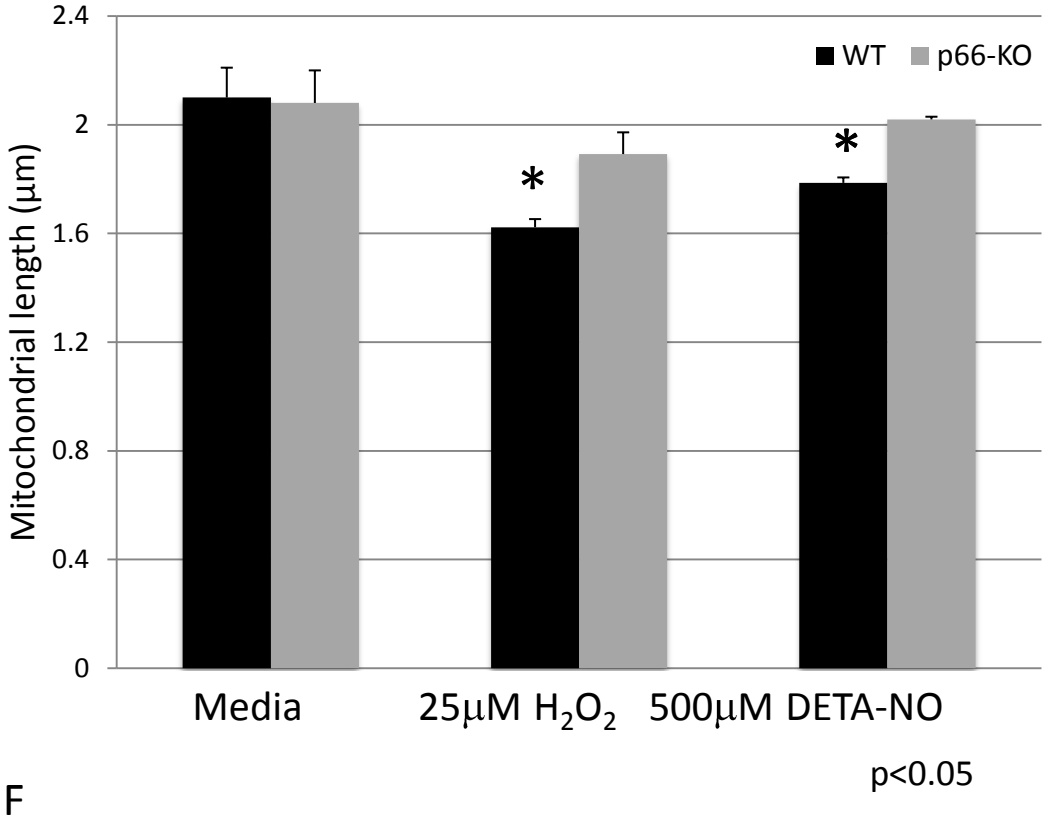
2.4
2
1.6
1.2
0.8
0.4
0
Mitochondrial length (µm)
WT
p66-KO
*
*
Media
25µM H_2O_2
500µM DETA-NO

p<0.05

F

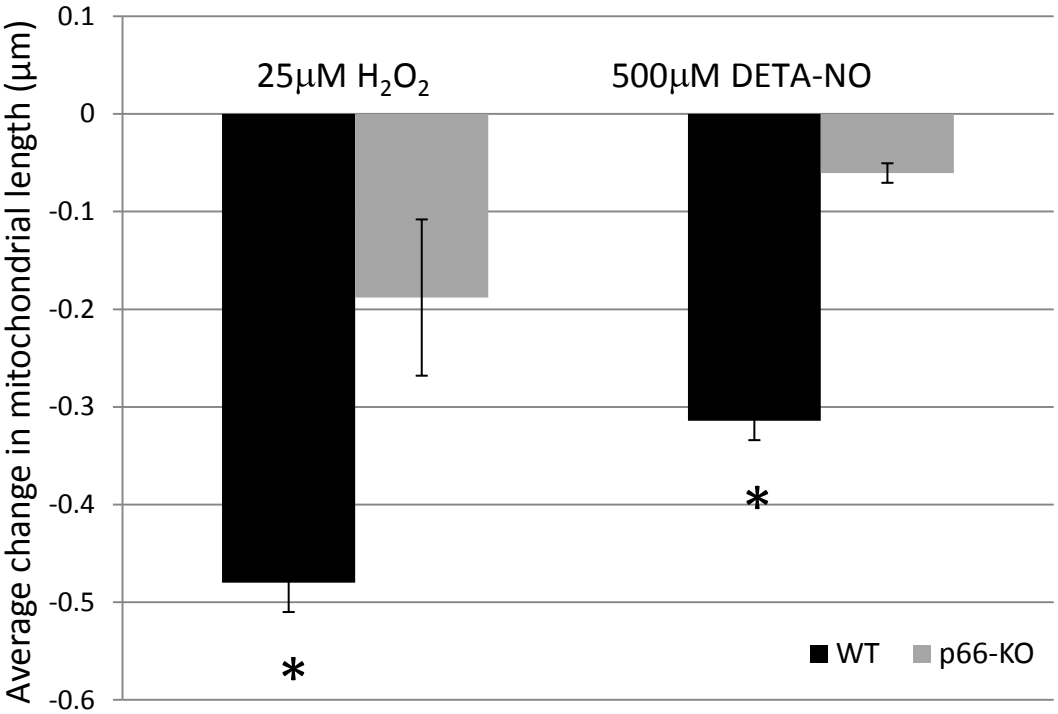
0.1
0
-0.1
-0.2
-0.3
-0.4
-0.5
-0.6
Average change in mitochondrial length (µm)
25µM H_2O_2
500µM DETA-NO
*
*
WT
p66-KO

p<0.05

Figure 2. Greater preservation of mitochondrial morphology in axons of p66-KO neurons compared to WT neurons following oxidative insults. Analysis of mitochondrial morphology changes demonstrated less significant decreases in mitochondrial length of p66-KO neurons compared to WT neurons. A-C) Representative images of mitochondria labeled with mito-GFP plasmid and mCherry beta-tubulin. A) Mitochondria of control medium treated neurons are thin and elongated in structure. Beta-actin expression indicates that axons are intact. Following treatment with either DETA-NO or H_2O_2, changes in mitochondrial morphology are apparent. B) Mitochondria of WT neurons treated with H_2O_2 are round and fragmented in appearance. C) Mitochondria of p66-KO neurons have more preserved mitochondrial morphology. D) To quantify the observed changes in mitochondrial morphology, Imaris software was utilized to assess changes in ellipsoid length c, which was doubled to determine mitochondrial length. E, F) Quantification of mitochondrial morphology changes showed significantly greater decreases in mitochondrial length of WT neurons compared to p66-KO neurons following treatment with either DETA-NO to H_2O_2. (n = 10 images/treatment/genotype)

Control medium

A

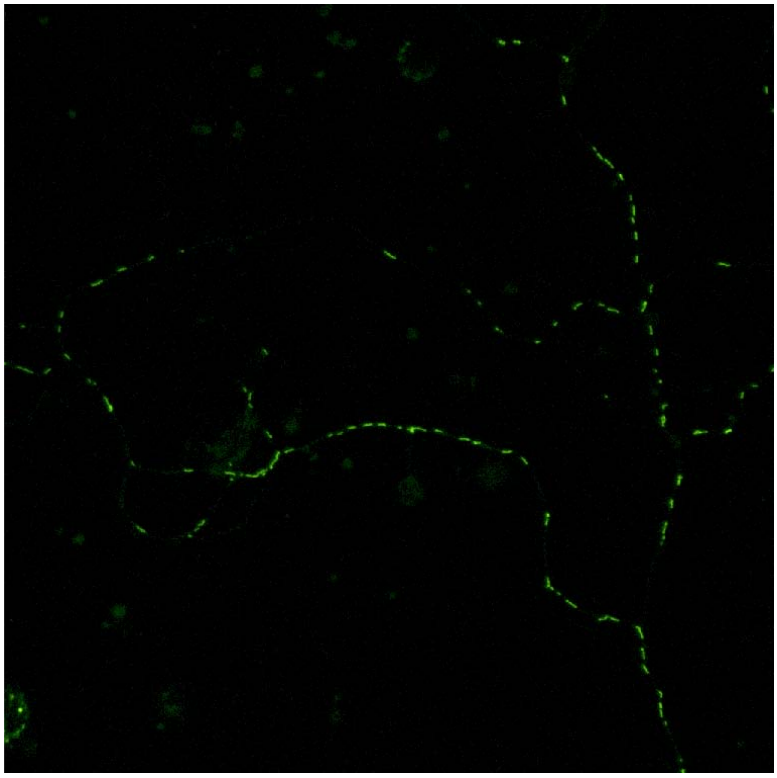

Mito-GFP

B

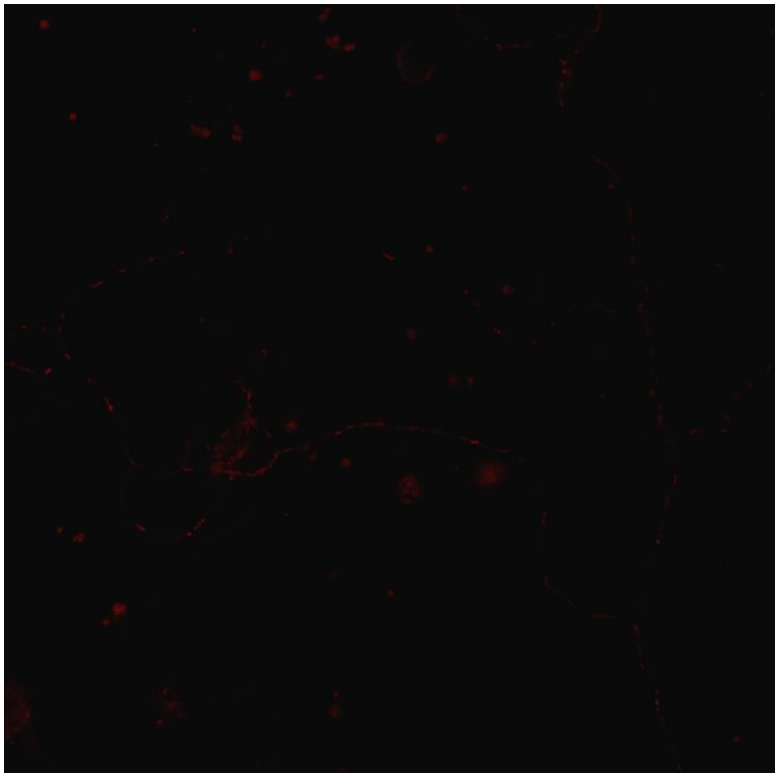

Mitosox

25μM H_2O_2

C

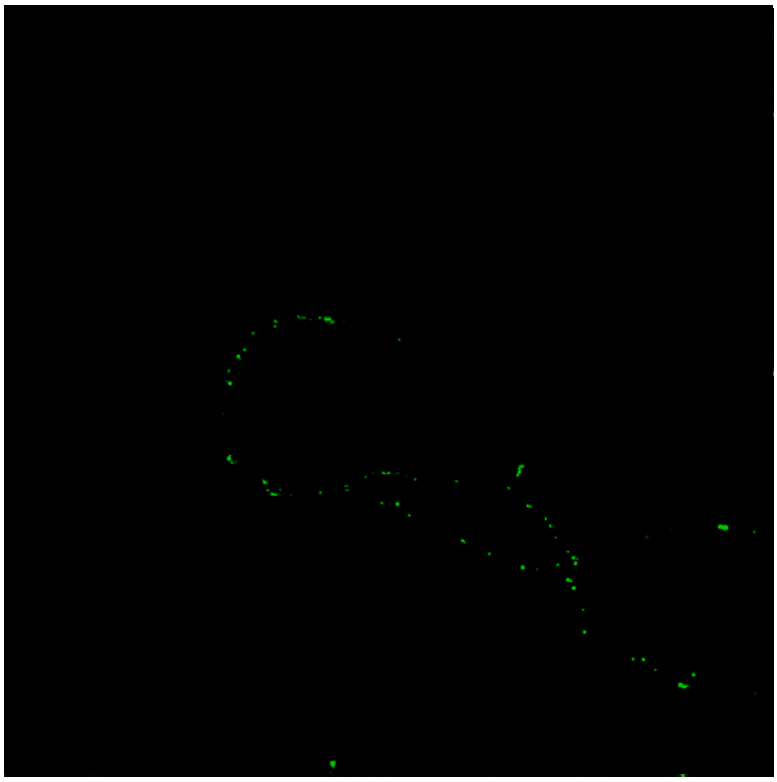

Mito-GFP

D

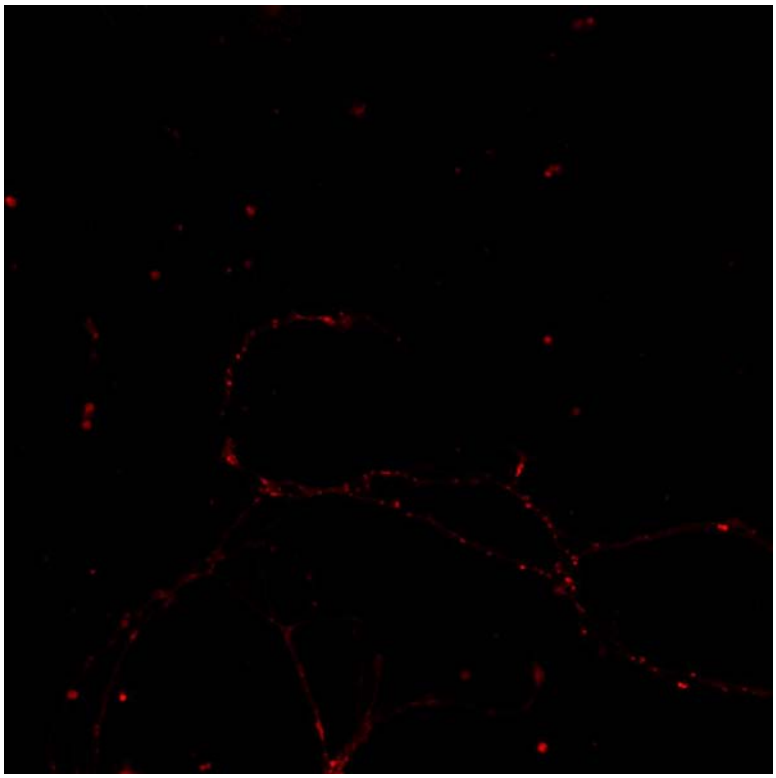

Mitosox

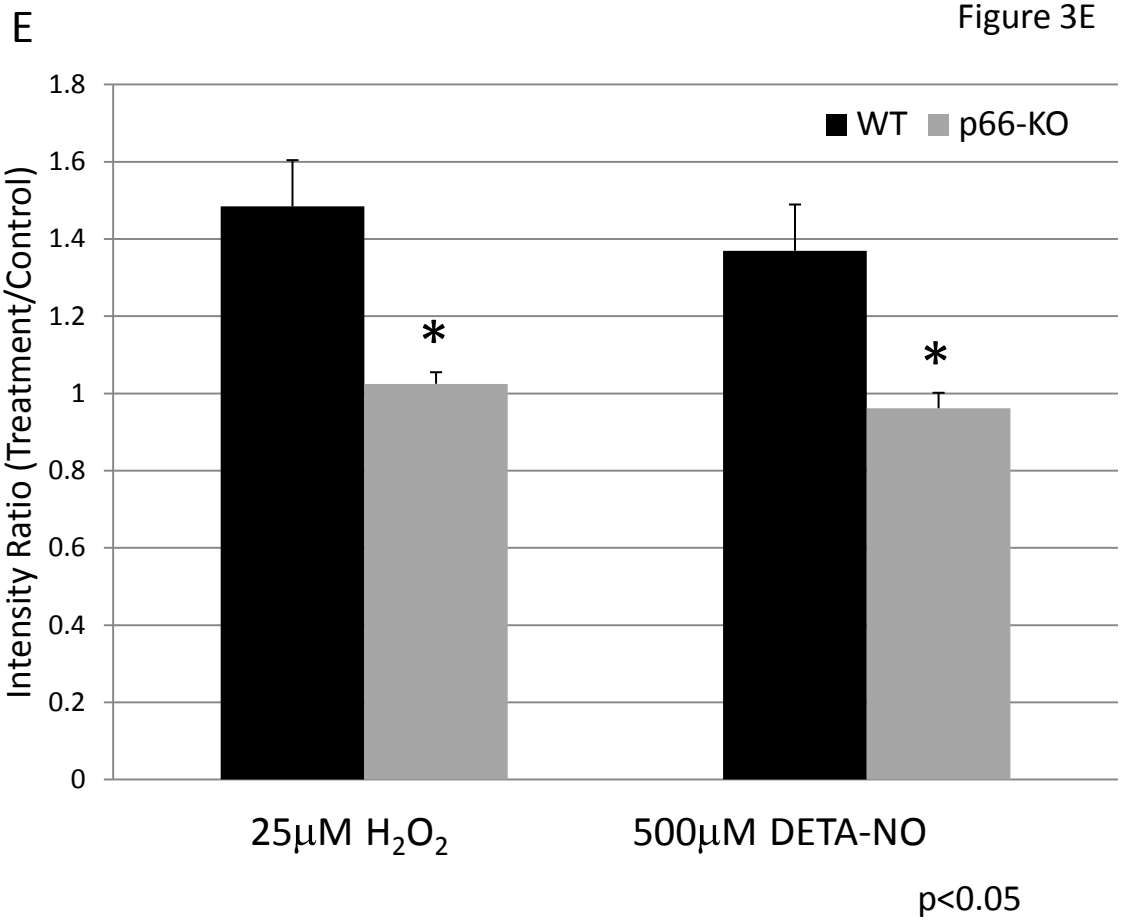

Figure 3. Significantly less mitochondrial ROS increases in axons of p66-KO neurons compared to WT neurons following oxidative insults.

A-D) Representative images of mito-GFP labeled mitochondria and corresponding Mitosox staining in neurons. A) Mito-GFP and B) Mitosox labeling of control medium treated neurons. C) Mito-GFP and D) Mitosox labeling of H_2O_2 treated neurons. E) Quantification of Mitosox intensity showed significant differences between axonal mitochondria of p66-KO and WT neurons following DETA-NO or H_2O_2 treatment. (n = 10 images/treatment/genotype)

A

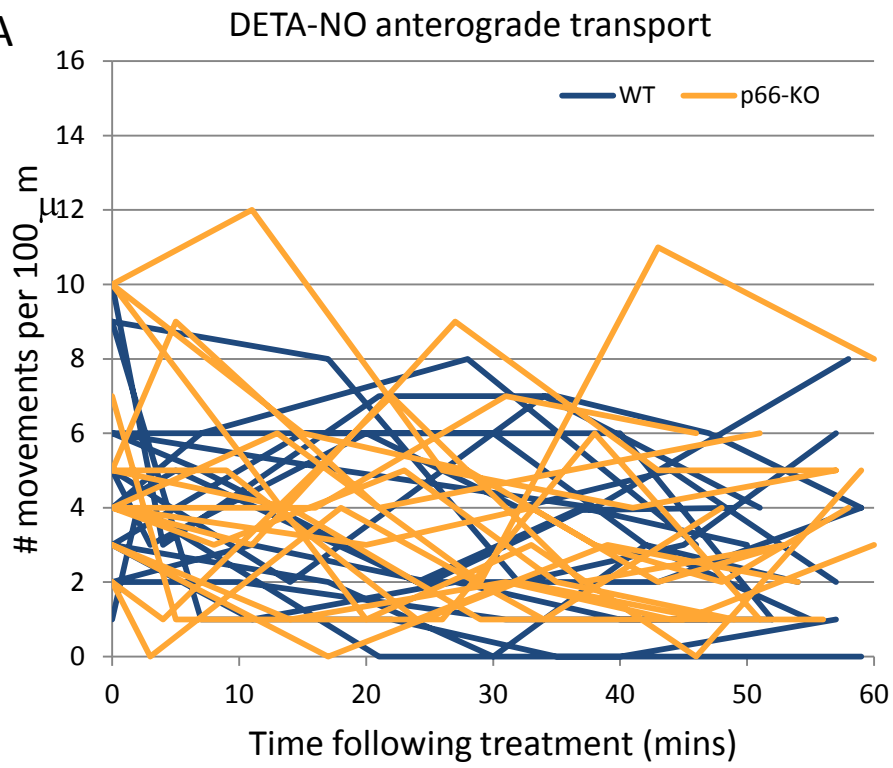
DETA-NO anterograde transport
WT
p66-KO
movements per 100 µm
0
2
4
6
8
10
12
14
16
0
10
20
30
40
50
60
Time following treatment (mins)

B

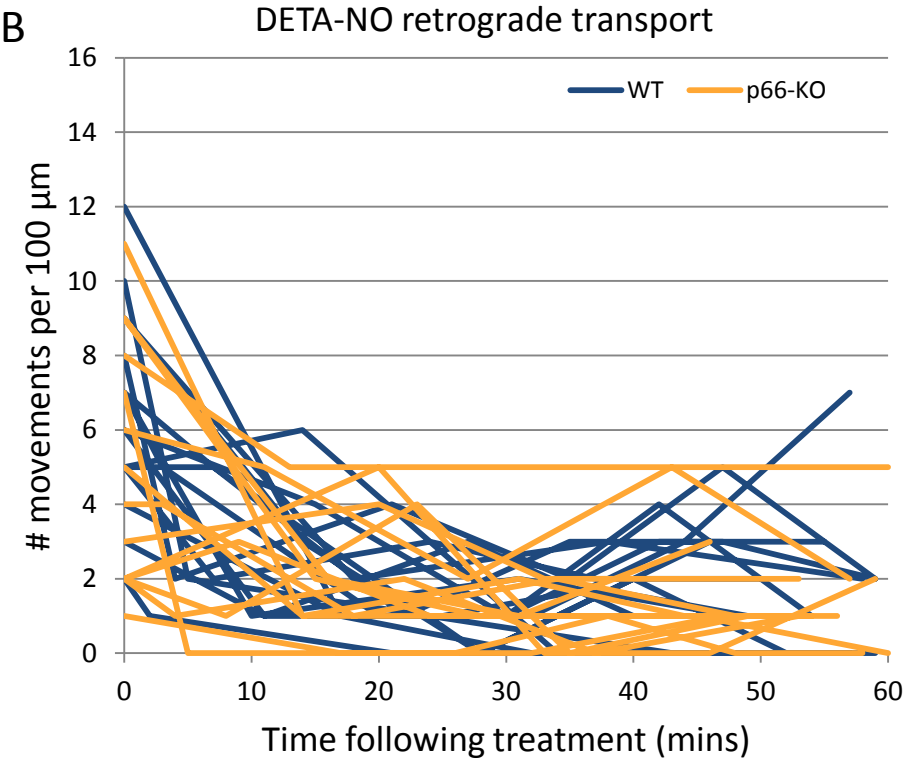
DETA-NO retrograde transport
WT
p66-KO
movements per 100 µm
0
2
4
6
8
10
12
14
16
0
10
20
30
40
50
60
Time following treatment (mins)

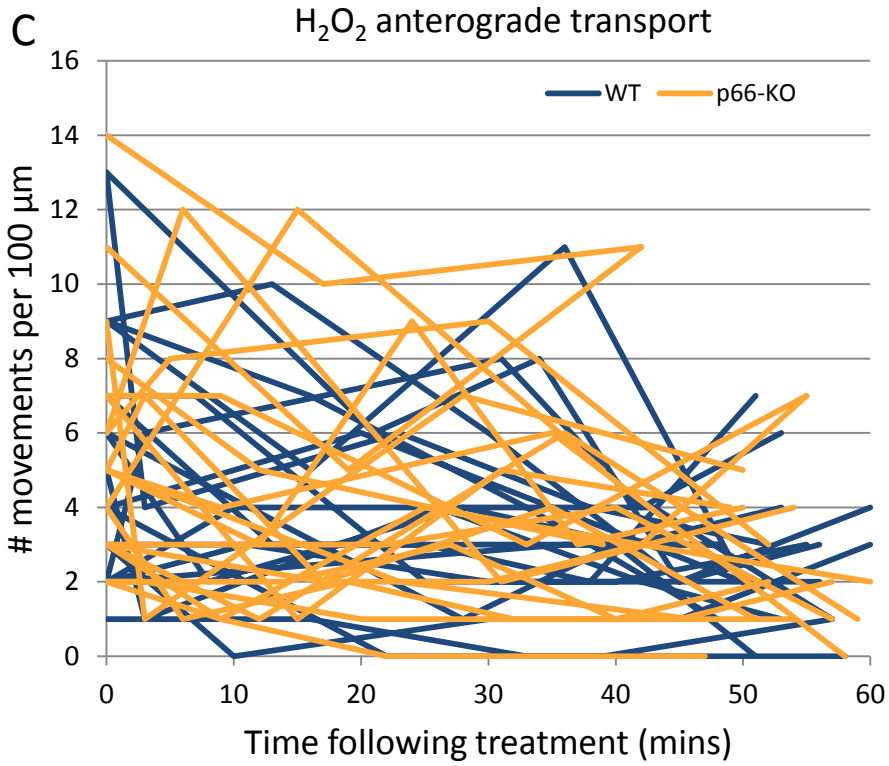
C
H_2O_2 anterograde transport
WT
p66-KO
movements per 100 µm
0
2
4
6
8
10
12
14
16
0
10
20
30
40
50
60
Time following treatment (mins)

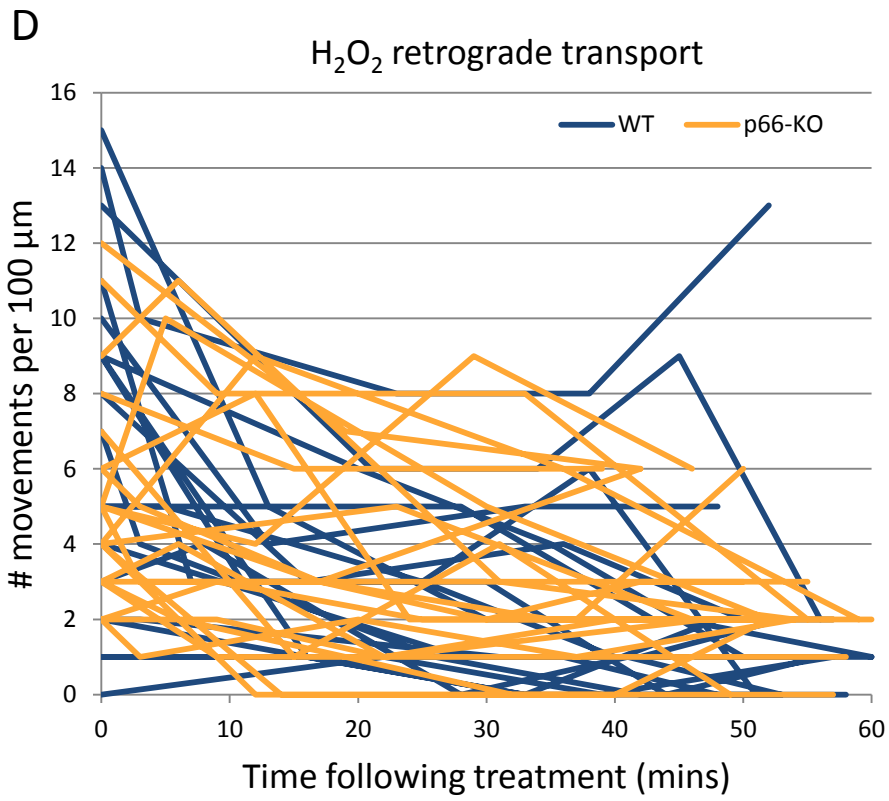
D
H_2O_2 retrograde transport
WT
p66-KO
movements per 100 µm
0
2
4
6
8
10
12
14
16
0
10
20
30
40
50
60
Time following treatment (mins)

E

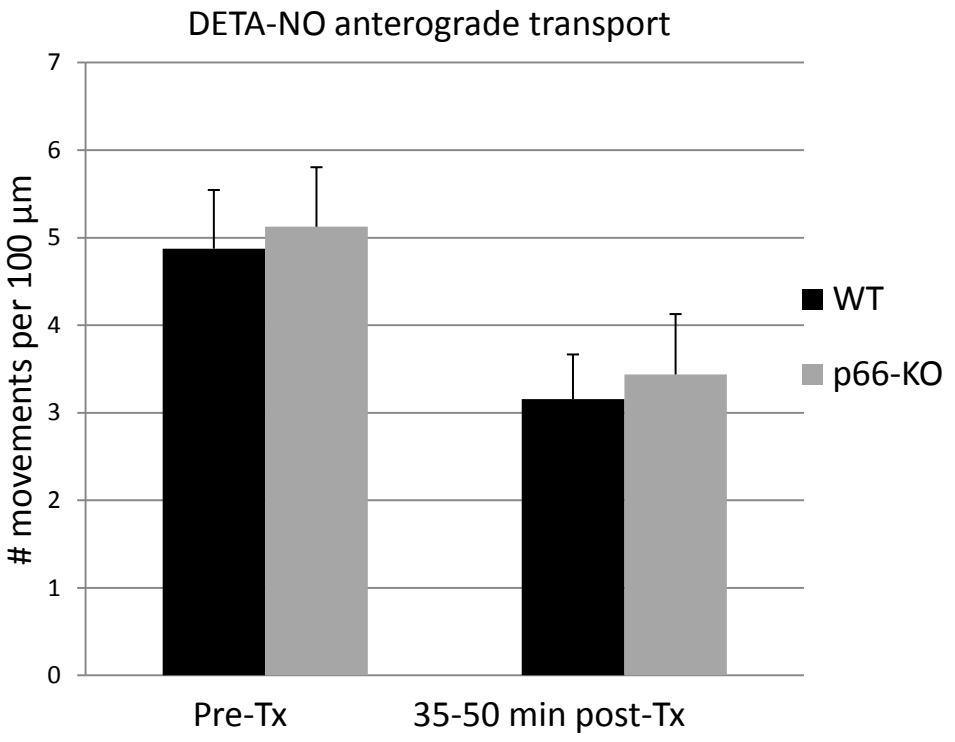
DETA-NO anterograde transport
movements per 100 µm
0
1
2
3
4
5
6
7
Pre-Tx
35-50 min post-Tx
WT
p66-KO

F

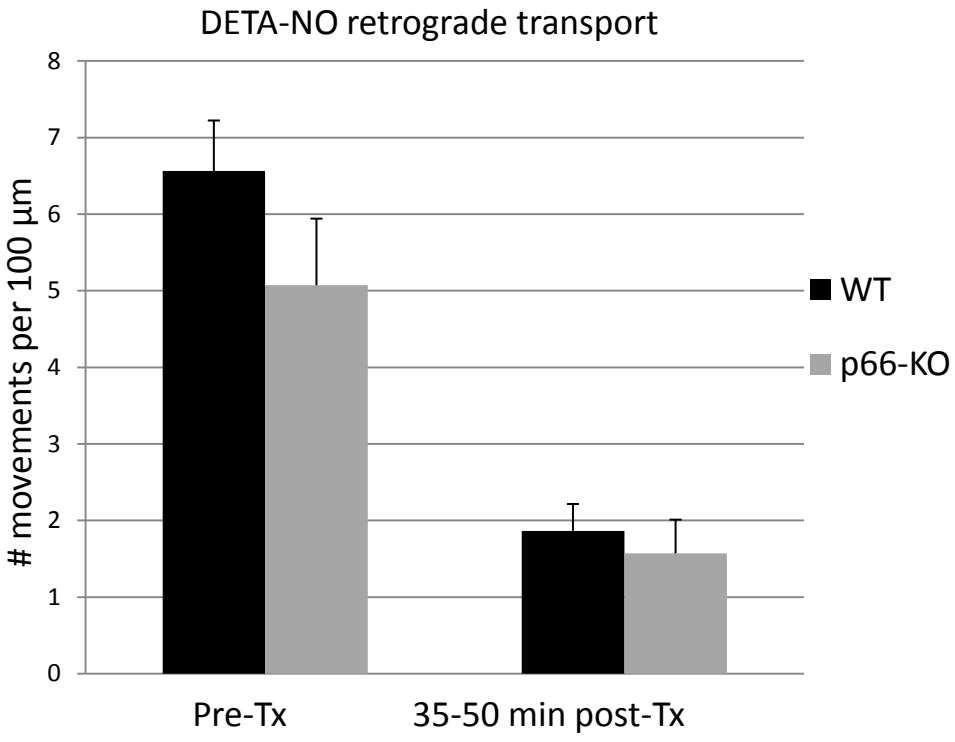
DETA-NO retrograde transport
movements per 100 µm
0
1
2
3
4
5
6
7
8
Pre-Tx
35-50 min post-Tx
WT
p66-KO

G

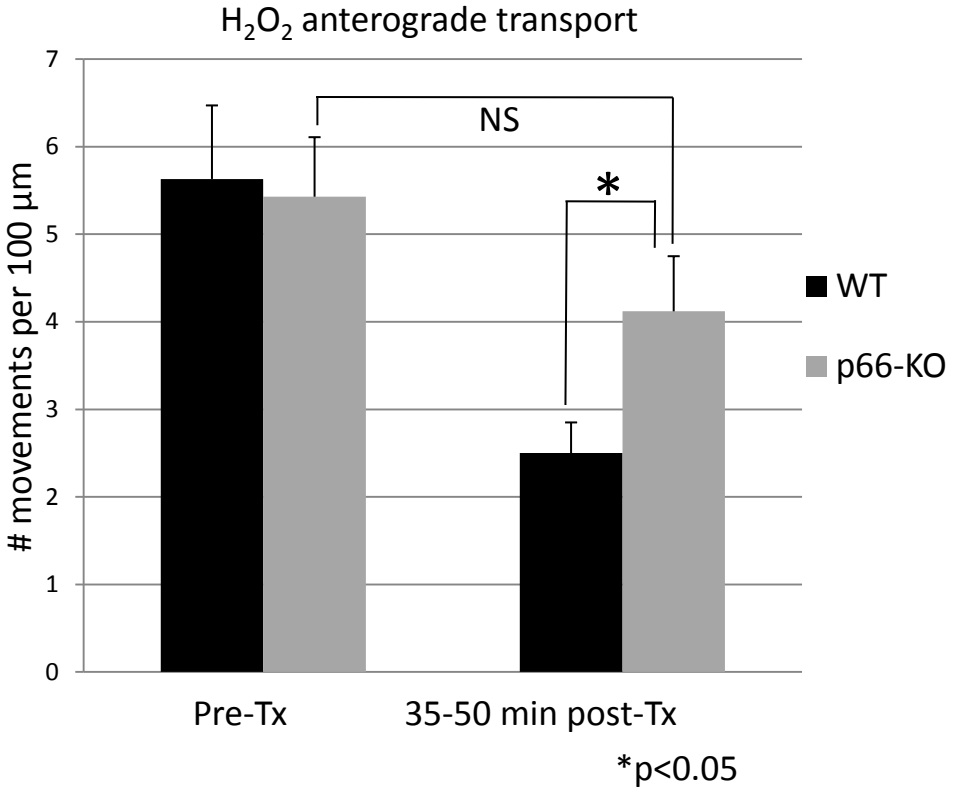
H_2O_2 anterograde transport
movements per 100 µm
0
1
2
3
4
5
6
7
NS
*
WT
p66-KO
Pre-Tx
35-50 min post-Tx
*p<0.05

H

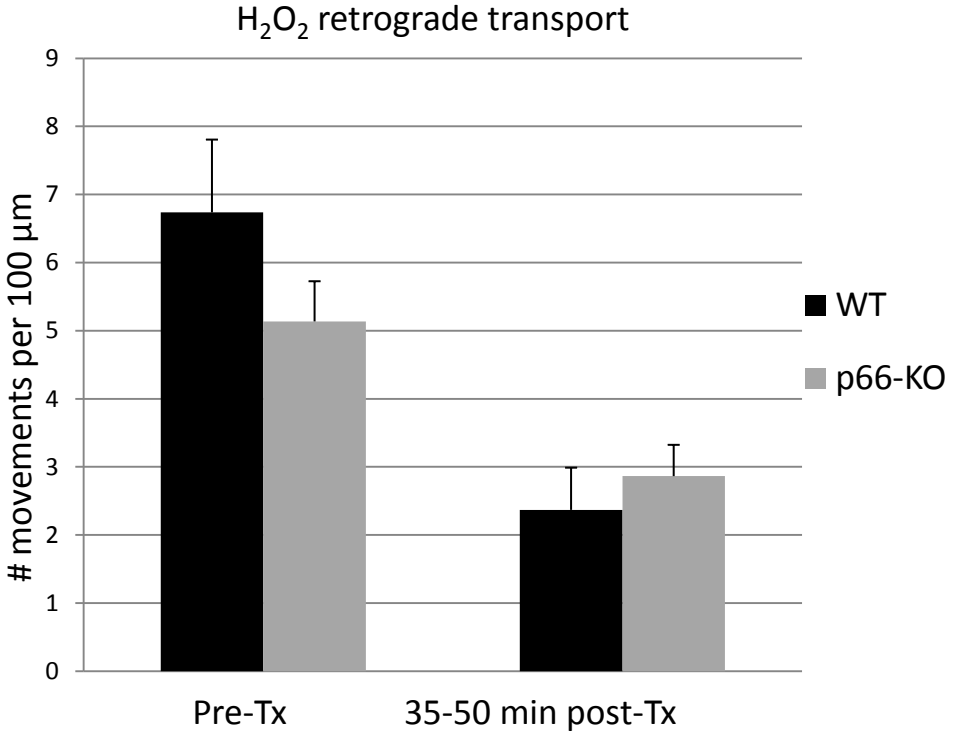
H_2O_2 retrograde transport
movements per 100 µm
0
1
2
3
4
5
6
7
8
9
WT
p66-KO
Pre-Tx
35-50 min post-Tx

Figure 4. p66 elimination does not preserve mitochondrial transport in axons of p66-KO neurons. Comparison of mitochondrial transport in p66-KO and WT neurons following treatment with either 500 μM DETA-NO or 25 μM H_2O_2 showed no significant differences in general. A-D) Graphs of anterograde and retrograde mitochondrial transport for each axon recorded over time in cultures treated with DETA-NO (A, B) or H_2O_2 (C, D) showed no observable differences between the p66-KO and WT genotypes. (E-H) Quantitative analysis of mitochondrial transport at pre-treatment and at 35-50 minutes post-treatment. E, F) No significant differences were found between mitochondrial transport of p66-KO and WT neurons following treatment with DETA-NO (n = 3 cultures; WT = 16 neurons; p66-KO = 14 neurons). G) Anterograde mitochondrial transport was significantly preserved in p66-KO neurons compared to WT neurons following treatment with H_2O_2 (n = 3 cultures; WT = 19 neurons; p66-KO = 21 neurons) H) No significant differences were found in retrograde mitochondrial transport between p66-KO and WT neurons following treatment with H_2O_2.

CHAPTER V:

Summary and conclusions

Multiple sclerosis (MS) has traditionally been considered an auto-inflammatory disorder mediated by the attack and destruction of myelin, leading to signs and symptoms of weakness, fatigue, visual problems, and eventual neurologic decline. However, advancements in imaging and experimental techniques have now convincingly shown that axonal injury and loss plays a significant role in MS pathophysiology throughout the disease course, from the early relapsing-remitting stages to the progressive stages of MS. Such evidence highlights the need to investigate mechanisms associated with MS degeneration in order to develop neuroprotective treatments noticeably lacking in the MS therapy toolbox.

Therefore, the underlying objective of this thesis project was to examine mechanisms associated with the mitochondrial hypothesis of MS degeneration. This hypothesis points to mitochondrial dysfunction as the key component of neurodegenerative processes, occurring in both acute and chronic stages of MS. Furthermore, this hypothesis suggests that pathologic opening of the permeability transition pore (PTP) is the common endpoint that leads to eventual mitochondrial dysfunction and cell death. Known inducers of pathologic PTP opening include Ca^{2+} and reactive oxygen species (ROS), and this project focused on investigating how the latter contributed to MS-associated neurodegeneration.

The project was designed to examine the effects of altered mitochondrial ROS production in both *in vivo* and in vitro settings. Mice with genetically eliminated p66ShcA (p66), a mitochondria-targeted redox enzyme, were utilized. The studies of Aim 1 provided an initiation point for analyzing the effects of altered mitochondrial ROS in the context of a disease model for MS. In contrast, Aim 2 provided a more focused and directed analysis of mitochondrial ROS in neurons, which was not feasible in the Aim 1 *in vivo* studies. The goal of characterizing the p66-KO neurons *in vitro* was to confirm whether p66 elimination was indeed neuroprotective in the context of agents implicated in EAE and MS neurodegenerative pathways, and if so, to define the differences between the p66-KO and WT neurons.

The results of this thesis project confirmed that p66 elimination was neuroprotective in both the *in vivo* EAE model and the *in vitro* neuronal cultures. Specifically, in the context of EAE, p66-KO spinal cords and optic nerves showed significantly less tissue and axonal damage. Furthermore, this protection was not attributable to significant changes in MOG peptide immunoreactivity as confirmed by various techniques including immune cell infiltration via immunohistochemistry, proliferation studies, and cytokine studies. The results from Aim 2 of this project further supported the protective effects indicated in Aim 1, with greater viability demonstrated in p66-KO neuronal cultures compared to WT cultures following treatment with oxidative agents implicated in MS neurodegenerative mechanisms. Hence, the results from both project aims suggest that altered mitochondrial ROS production via p66 elimination may be neuroprotective in the context of EAE, and by extension, MS.

Furthermore, Aim 2 was designed to characterize the neuroprotective mechanisms associated with p66 elimination. The results showed that the mitochondria in p66-KO neurons had less significant changes in mitochondrial morphology under conditions of oxidative stress. In particular, mitochondrial length was more preserved in p66-KO neurons, which may be explained by the reduction of ROS-induced pathologic PTP opening and ensuing mitochondrial matrix swelling and bursting. In addition, mitochondrial ROS levels were less altered in p66-KO neurons compared to WT neurons following treatment with either H_2O_2 or DETA-NO, possibly due to the elimination of p66 and the consequent reduction in mitochondrial ROS amplification. Finally, analysis of mitochondrial transport indicated that p66 elimination generally had no notable effect on preserving anterograde and retrograde transport. However, given that anterograde transport was significantly preserved in p66-KO neurons treated with H_2O_2 but not DETA-NO suggests that mechanisms mediating transport are likely complex and therefore warrant further examination. Nevertheless, the overall results of Aim 2 demonstrate that p66 elimination enhances neuronal robustness and preservation of mitochondrial integrity under conditions of oxidative stress.

There are, of course, several potential limitations to these experiments. For one, no animal model perfectly mimics human disease, and EAE is no exception. However, it is important to note that a majority of the MS therapies currently used were developed from EAE, which emphasizes the benefits of utilizing this model for research. In addition, another potential limitation of this project is the use of universal p66-KO mice in the EAE experiments instead of neuron-specific knockout mice. Given that p66 is

universally eliminated, it is conceivable that the protective effects may be due to p66 inactivation in other cell types within the CNS such as oligodendrocytes, microglia, or astrocytes. While the *in vitro* cell viability studies address this limitation within the means of this project, the generation and experimentation of neuron-specific p66-KO mice is likely more ideal.

Another potential limitation to this project is our current understanding of p66 and the PTP. The discovery of the p66 ShcA isoform is relatively recent, and it is reasonable to assume that p66 may have other cellular functions yet to be defined that could indirectly contribute to the findings demonstrated in this project. Likewise, the structural components of the PTP are also poorly understood, and the ongoing search for proteins forming the PTP will undoubtedly help define other players that may be important in p66-dependent activation of the PTP. In this project, the attempt to define the relationship between p66 and the PTP was limited to utilizing double knockout p66/CyPD mice as indicated in Chapter II and Chapter III of this thesis. While the results of the double knockout experiments suggest that p66 may be upstream of the PTP, further studies are likely necessary to establish the relationship given the complexity of mammalian systems. Such studies may include the creation of transgenic lines in which p66 and CyPD are overexpressed, resulting in "gain-of-function" (GOF) phenotypes in neurons (e.g., p66-GOF phenotypes would be suppressed in CyPD-KO animals whereas CyPD-GOF phenotypes would be unaffected in p66-KO animals).

Finally, the nature of *in vitro* studies can be limiting due to oversimplification of the dynamic *in vivo* setting. Neurons are not isolated in the nervous system of MS patients,

and it is certain that neurodegenerative processes are due to the combinatory effects of immune system cells and supporting cells such as astrocytes and oligodendrocytes. However, beyond such concerns, *in vitro* studies are an ideal complement to the *in vivo* EAE studies, as they offer a closer examination of knockout and WT neurons, and a controlled experimental setting to compare neuronal responses to induced stressors. These advantages are key to understanding the effects of p66 elimination and the mechanisms behind neurodegenerative pathways in EAE and MS.

Despite the limitations discussed above, this project has provided intriguing results and future directions. Regarding the EAE experiments of Aim 1, future experiments may involve utilizing Thy1-mito-CFP/YFP transgenic mice that have fluorescently labeled mitochondria and neurons. By crossing these transgenic mice with p66-KO mice, this will allows for live imaging of mitochondrial and neuronal changes in EAE-induced animals, as well as subsequent analysis of neuronal and mitochondrial morphologic changes in tissue. In terms of Aim 2, additional experiments to compare p66-KO and WT neurons may include further assessment of mitochondrial integrity beyond mitochondrial morphology and transport changes. Given the role of mitochondria in energy production, Ca^{2+} homeostasis, and apoptosis via the PTP and cytochrome c release, it would be intriguing to analyze and compare changes in mitochondrial ATP levels, membrane potential, Ca^{2+} dynamics, and cytochrome c localization between stressed p66-KO and WT neurons.

In conclusion, the novel experiments and results of this thesis project have provided evidence to strengthen the mitochondrial hypothesis of MS neurodegeneration and to

highlight mitochondrial ROS and p66 as potential targets for neuroprotective therapies. Once simply known as the cellular "powerhouses", the role of mitochondria in physiologic and pathologic conditions has expanded significantly, and mitochondria are now recognized as key components of neurodegenerative mechanisms not only in MS, but also in a multitude of prominent disorders including Alzheimer's disease, Parkinson's disease, Huntington's disease, and amyotrophic lateral sclerosis (ALS). Therefore, as our understanding of such mechanisms progresses with further investigation, undoubtedly so will the development of essential neuroprotective treatments targeting mitochondria.

CHAPTER VI:

Final reflections: Mitochondria-targeted neuroprotective treatments in store for patients?

In 1868, Dr. Jean-Martin Charcot described his examination of a young woman with a particular tremor he had never seen before. He noted that she had other apparent

neurological problems including slurred speech and abnormal eye movements. After her death, a brain autopsy was performed, and plaques or scleroses were noted upon examination. Charcot termed the disease sclerose en plaques, and this was the first clinical description of MS (Lublin, 2005).

We have come a long way in our understanding of MS since Charcot first penned his description of the disease nearly 150 years ago. We now know that there is a definite immunologic component that leads to destruction of myelin by activated immune cells and ensuing manifestation of characteristic MS symptoms. This understanding has led to an extensive effort to develop immunomodulatory and immunosuppressant drugs to treat MS. Inclusive in this group of drugs are interferon beta 1-a and 1-b, glatiramer acetate, mitoxanthrone, natalizumab, and the recently FDA-approved oral drug fingolimod (Lublin, 2005; Cohen et al., 2010). Mechanistically, all of these drugs work at some level to combat the pernicious autoimmune attack on the CNS, prevent the breakdown of the protective blood brain barrier, and suppress the infiltration of activated immune cells targeting myelin. Unfortunately, these drugs, while more or less adequate in treating relapsing-remitting MS, are unable to treat the progressive, debilitating decline in function that plagues a significant number of patients.

Obviously, the MS therapy toolbox needs to be expanded. In light of the recent progress and advancements in MS research, this may be possible in the near future. Importantly, it is now recognized that MS is not simply a demyelinating, autoimmune disease, but rather one of greater complexity. Charcot, himself, noted axonal loss in

demyelinated lesions of MS patients, and this pathology has been convincingly confirmed with the aid of today's impressive technological tools.

The study of neurodegenerative pathways in MS has been in full force in the recent decades. While still a fairly young area of research, there has been considerable effort to understand the mechanisms involved and define potential pharmacologic targets. As mentioned throughout this paper, the mitochondrion has been identified as one such target, a key convergence point for multiple pathways leading to axonal damage and loss.

Mitochondria-directed therapies are still in their infancy, largely limited to in vitro and in vivo animal studies to test their properties and efficacy, though a few are now being investigated in human clinical trials. They span a wide range of mitochondria-specific targets including the electron transport chain, ATP synthase, mitochondrial ROS, and the PTP (Camara et al., 2009). Some noteworthy drugs that may potentially be neuroprotective in the context of MS degenerative mechanisms include the Szeto–Schiller peptides, mitoquinone (MitoQ), and non-immunosuppressive cyclosporin A derivatives. Both Szeto-Schiller (SS) peptides and MitoQ, for instance, target to mitochondria, and have ROS scavenging capabilities. SS peptides, unlike MitoQ, do not require mitochondrial membrane potential for uptake, which may be beneficial when dealing with diseased mitochondria with reduced mitochondrial membrane potentials (Szeto, 2008). Both are currently being tested in a variety of disease models, including Parkinson's disease, ischemia-reperfusion injury, and amyotrophic lateral sclerosis, showing potential benefits. Cyclosporin A and its non-immunosuppressant derivatives,

in comparison, directly inhibit the PTP regulator CyPD, and have been shown to provide significant protection for cultured neurons induced with hypoglycemic, oxidative, and ischemic damage, as well as in several kidney, liver, and heart disease models (Camara et al., 2009).

The effectiveness of these mitochondria-targeted drugs in treating MS will depend on multiple factors. For one, a common issue of drugs tested in vitro and in animal models is that there is that undeniable gap between a petri dish and experimental animal (i.e., mouse, rat) and a human. In addition, animal models of human diseases are imperfect. While both may present with similar phenotypes, the etiology behind the manifested signs and symptoms may be different. This discrepancy likely contributes to the failure of clinical trials in which the drug had significant effects in tested animal models, but discouraging results in humans. Furthermore, there is another level of complexity when it comes to the treatment of CNS disorders, namely restricted drug delivery. Unlike many other organ systems, it can be difficult to achieve therapeutic drug levels due to inability of the drug to cross the protective blood brain barrier. Cyclosporin A and its non-immunosuppressant derivatives, for instance, represent one such class of drugs. While highly effective in blocking the PTP, they penetrate the CNS poorly, limiting their effectiveness as neuroprotectants. Therefore, drug modification and utilization of barrier-permeable delivery vehicles may need to be taken into consideration. Finally, drug accumulation within the mitochondria will be crucial to drug design and potential effectiveness. As mentioned above, SS peptides can localize to abnormal mitochondria with affected membrane potentials, and hence may make them more suitable than

similar compounds like MitoQ for treating MS in which mitochondria are likely altered by degenerative disease pathways.

Obviously, there is a lot of work ahead, and it will not be easy. But considering the fast pace at which research is being carried out, we are definitely steps closer to developing mitochondria-targeted neuroprotective drugs for MS patients. With better understanding of MS degenerative mechanisms, continued discovery of novel pharmacologic targets such as p66, refined development of mitochondria-targeted drugs, and eventual translation from the bench to the bedside, neuroprotective treatments will undoubtedly be part of standard MS therapy in the near future.

References:

Camara AKS, Lesnefsky EJ, Stowe DF (2009) Potential Therapeutic Benefits of Strategies Directed to Mitochondria. Antioxidants & Redox Signaling 13:279-347.

Cohen JA, Barkhof F, Comi G, Hartung H-P, Khatri BO, Montalban X, Pelletier J, Capra R, Gallo P, Izquierdo G, Tiel-Wilck K, Vera A de, Jin J, Stites T, Wu S, Aradhye S, Kappos L (2010) Oral Fingolimod or Intramuscular Interferon for Relapsing Multiple Sclerosis. New England Journal of Medicine 362:402-415.

Lublin F (2005) History of modern multiple sclerosis therapy. Journal of Neurology 252:iii3-iii9.

Szeto HH (2008) Development of Mitochondria-targeted Aromatic-cationic Peptides for Neurodegenerative Diseases. Annals of the New York Academy of Sciences 1147:112-121.